STABILITY OF PROTEINS WITHIN BIODEGRADABLE MICROSPHERES

by

KAREN FU

BS, Chemical Engineering (1990), MIT
MA, Comparative Biochemistry (1991), UC Berkeley
MS, Chemical Engineering School of Practice (1993), MIT

Submitted to the Harvard-MIT Division of Health Sciences and Technology
in Partial Fulfillment of the Requirements for the Degree of

DOCTOR OF PHILOSOPHY
IN MEDICAL ENGINEERING AND MEDICAL PHYSICS

at the
MASSACHUSETTS INSTUTUTE OF TECHNOLOGY
June, 2000
[September, 2000]

Signature of Author _____
Division of Health Sciences and Technology
June 15, 2000

Certified by _____
Robert S. Langer, Sc.D.
Germeshausen Professor of Chemical and Biomedical Engineering
Massachusetts Institute of Technology
Thesis Supervisor

Certified by _____
Alexander M. Klibanov, Ph.D.
Professor of Chemistry
Massachusetts Institute of Technology
Thesis Supervisor

Accepted by _____
Martha L. Gray, Ph.D.
Edward Hood Taplin Professor of Medical and Electrical Engineering
Co-Direcor, Harvard-MIT Division of Health Sciences and Technology

STABILITY OF PROTEINS WITHIN BIODEGRADABLE MICROSPHERES

Abstract

In the past decade, biodegradable polymers have become the materials of choice for a variety of biomaterials applications. In particular, poly(lactic-*co*-glycolic acid) (PLGA) microspheres have been extensively studied for controlled-release protein delivery. However, significant issues arise in formulating such delivery systems since few proteins have been successfully encapsulated and released from these microspheres. Here, methods are developed to determine the causes of protein instability and solutions are provided for overcoming these problems.

A commonly used technique for protein encapsulation in PLGA microspheres is the double-emulsion method. The harsh processing associated with this method can cause denaturation of the encapsulated protein. Herein, we have used Fourier transform infrared (FTIR) spectroscopy to determine the secondary structures of two model proteins, bovine serum albumin (BSA) and chicken egg-white lysozyme, within PLGA microspheres. This is a novel technique for *in situ* evaluation of proteins within microspheres and potentially a powerful and quick method for assessment of formulations. Results for both proteins indicate changes in structure upon entrapment within the microspheres. However, addition of the stabilizing excipient trehalose prevents the denaturing effects incurred during processing. In addition, BSA released from microspheres is improved by incorporation of trehalose.

With microspheres made by double emulsion, there is often a large, initial burst of drug release upon injection. This results in inefficient use of therapy. To prevent this loss, a modified spontaneous emulsification method was explored. With this procedure both protein and polymer are soluble in a single solvent system thus avoiding creation of a water/solvent interface. The process was optimized for microsphere size and protein loading. Addition of a charged surfactant served to improve protein solubility and thus increase protein loading. *In vitro* and *in vivo* release kinetics showed a minimal burst, lower than that found with double emulsion microspheres, followed by sustained release.

Upon injection of the microspheres *in vivo*, the PLGA microspheres begin to degrade. Degradation of the polymer generates acidic monomers, and acidification of the inner polymer environment is a central issue in the development of these devices for drug delivery. To quantitatively determine the intraparticle acidity, pH-sensitive fluorescent dyes were entrapped within the microspheres and imaged with confocal fluorescence microscopy. The technique allows visualization of the spatial and temporal distribution of pH within the degrading microspheres. The data indicate the formation of a very acidic environment within the particles with the minimum pH as low as 1.5. The images show a pH gradient, with the most acidic environment at the center of the spheres and higher pH near the edges, which is characteristic of diffusion-controlled release of the acidic degradation products. Strategies to avoid the accumulation of acidic monomers involve decreasing the diffusion distance of the degradation products by either decreasing the overall diameter of the microspheres or creating porous particles.

Thesis advisors: Robert Langer
Germeshausen Professor of Chemical and Biomedical Engineering

Alexander M. Klibanov
Professor of Chemistry

I dedicate my thesis to my Mom and Dad.

Acknowledgments

I want to say a tremendous THANK YOU to all those who affected my tenure at MIT and HST. Through this experience I have learned much about drug delivery, medicine, and academic life.

Thank you to my advisors Robert Langer and Alexander Klibanov for the opportunity to learn and work in their labs.

Next, I thank Dan Pack and Dave Putnam. Without their help and advice, I would still be in the lab.

Many friends have helped me to get through this time and in many ways if it were not for them, I would also still be in the lab. Thank you Mark Powers, Joe Seidel, Shane Williams, Sachiko Hirosue, Betty Yu, Jennifer Elisseeff, Hongming Chen, Jeff Hrkach, Justin Hanes, and Tommy Thomas.

I would like to acknowledge Noah Lotan, Maria Figuerido, Mike Frongillo, Matthew Dyer, Michael Lipp, Nenad Bursac, Matthew Lazzara, and Mike O'Boyle for their time and assistance.

Finally, thank you to my parents and brother for their constant support, and thank you to Will Somers for giving me incentive to graduate.

Table of Contents

List of Figures

List of Tables

1. Introduction

1.1. Motivation

The potential of protein therapies is vast as proteins with their complex three dimensional structures have specific actions within the body. In many cases, it is difficult to mimic the interaction between a protein and its receptor or target with a small molecule. Furthermore, as research from genomics and proteomics come to fruition, the number of protein products on the market will expand as new targets are identified.

Recombinant protein therapies have emerged within the last 20 years and changed the face of modern medicine. With the ability to mass produce and even redesign proteins for adequate therapy, treatments that were once purified from human or animal organs are no longer needed. More importantly, these manufactured products are safe from blood borne pathogens, and have low toxicity, are non-carcinogenic and non-teratogenic as compared to other drugs. For many disease states, it is now possible to replace the missing molecule. Other strategies of protein therapeutics include modulation of the immune system (interferons and interleukins), immunization (hepatitis B vaccine), and more recently immunotherapy where antibodies are used for removal of overproduced "antigens". The first recombinant product was insulin for treatment of diabetes made by Genentech and marketed by Eli Lilly in 1982. Protein therapeutics on the market today span a wide spectrum, from endocrine replacement such as human growth hormone and insulin, to hematopoetic factors such as erythropoietin and factor VIII, to vaccines such as diphtheria toxoid and tetanus toxoid (see Table 1-1).

Table 1-1. Approved recombinant proteins (Buckel, 1996)

Product	Company	First indication	Approved in US
Human insulin	Eli Lilly	Diabetes	1982
Human growth hormone	Genentech	Growth hormone deficiency in children	1985
Interferon α-2b	Schering-Plough	Hairy cell leukemia	1986
Interferon α -2a	Hoffmann-LaRoche	Hairy cell leukemia	1986
Hepatitis B vaccine	Merck	Hepatitis B prevention	1986
Human growth hormone	Eli Lilly	Growth hormone deficiency in children	1987
Tissue plasminogen activator	Genentech	Acute myocardial infarction	1987
Erythropoietin	Amgen	Renal anemia	1989
Hepatitis B vaccine	SmithKline Beecham	Hepatitis B prevention	1989
Interferon α -n3	Interferon Sciences	Genital warts	1989
Interferon γ-1b	Amgen	Chronic granulomatosis	1990
G-CSF	Amgen	Chemotherapy-induced neutropenia	1991
GM-CSF	Immunex	Autologous bone marrow transplantation	1991
Interleukin-2	Chiron	Renal cell carcinoma	1992
Antihemophilic factor	Genetics Institute	Hemophilia A	1992
Factor VIII	Miles	Hemophilia A	1993
Interferon β-1b	Chiron	Multiple sclerosis	1993
DNase	Genentech	Cystic fibrosis due to chronic renal insufficiency	1993
Glucocerebrosidase	Genzyme	Gaucher's disease	1994

Current delivery forms of these drugs are as injectables where patients either administer the injections themselves or receive the injections from a health care provider. As these therapeutics are directly introduced into the systemic circulation, they have short half-lives due to proteolysis and rapid clearance from the bloodstream (Pitt, 1990). Thus, patients often require daily injections. In some cases, the short half-life prevents use of the protein as a drug. Encapsulation of proteins within biodegradable polymers has been shown to enhance the half-life *in vitro* (Cohen, Yoshioka *et al.,* 1991; Tabata, Gutta *et al.,* 1993). This system has many advantages, including 1) the ability to release a constant level of therapeutic with the potential to reduce side effects due to the normal "peak and valley" concentrations seen in multiple dosing methods of drug administration, 2) efficient use of therapeutic resulting in lower doses, 3) localized drug delivery, for example, to the brain or blood vessels, which can potentially create new therapeutic modalities by delivering a drug directly to its target, and 4) a need for fewer administrations of the therapeutic.

Of the biodegradable polymers, the most widely investigated polymers in regard to available toxicological and clinical data are the aliphatic polyesters based on lactic and glycolic acids (Figure 1-1) or PLGA. Physical characteristics of the polymer include strength and hydrophobicity (Couvreur, Blanco-Prieto *et al.,* 1997). Advantages of this polymer include biocompatibility, predictability of biodegradation kinetics, and ease of fabrication (Lewis, 1990). The copolymer is known to be nonimmunogenic, and the degradation products are eliminated from the body (Couvreur, Blanco-Prieto *et al.,* 1997). Many different delivery modes can be formulated including tablets, films, rods, microspheres and nanospheres by solvent casting, compression molding, or solvent evaporation techniques (Gombotz and Pettit, 1995).

Degradation occurs by hydrolysis of the ester linkages, and the rate is controlled by factors including the polymer crystallinity, copolymer ratio, temperature, and pH (Couvreur, Blanco-Prieto *et al.,* 1997); this reaction is accelerated by the presence of acid or base (Gombotz and Pettit, 1995). During bulk degradation, an almost immediate and rapid decrease in molecular weight occurs as susceptible bonds in the polymer chain are cleaved. As a result, smaller polymer fragments are produced. This initial molecular weight decrease precedes any polymer mass loss. When the small fragments begin to obtain a critical molecular weight, they become soluble in the aqueous degradation media, causing mass loss (Hausberger and DeLuca, 1995).

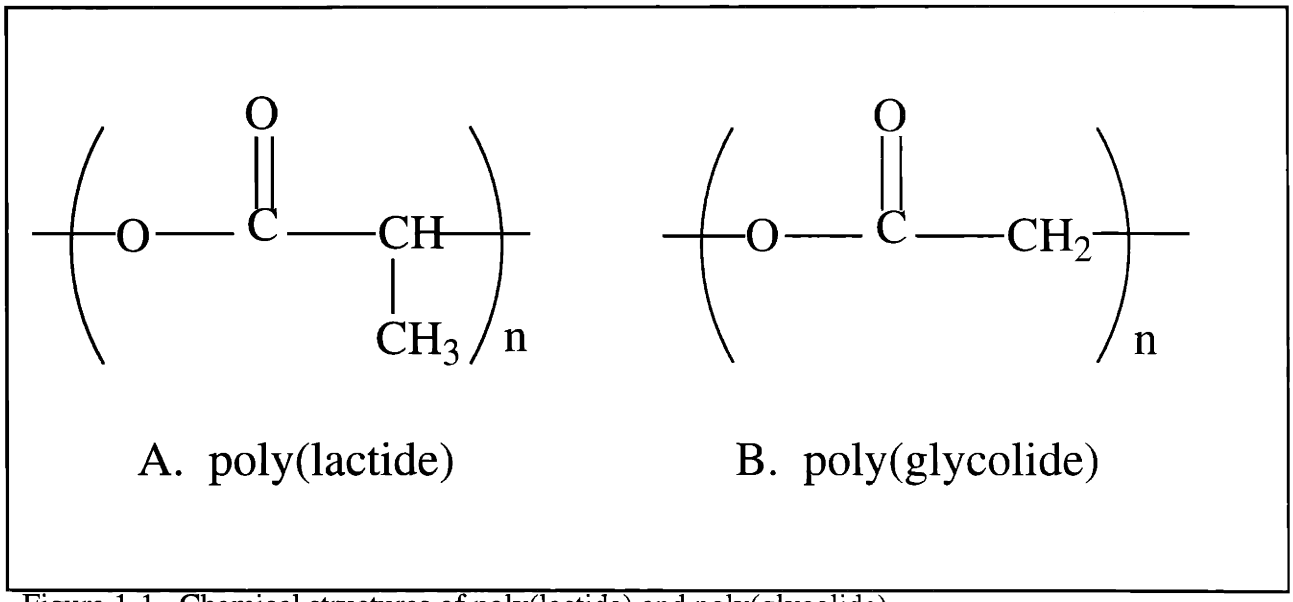

Figure 1-1. Chemical structures of poly(lactide) and poly(glycolide).

The problem of entrapping a hydrophilic molecule within a hydrophobic one is difficult. Thus far the most common method of formulating microspheres is the double emulsion technique which relies on physical mixing of the two components to bring them within close proximity of each other. Emulsion techniques expose the protein to a water/organic interface which causes

proteins to unfold and lose activity (Tabata, Gutta *et al.,* 1993; O'Donnell and McGinity, 1997; Iwata, Tanaka *et al.,* 1998). Proteins at this interface may also undergo aggregation (Alonso, Gupta *et al.,* 1994; Lu and Park, 1995, Sah, 1999).

To stabilize proteins during emulsification, many approaches have been tried. Surfactants have been included in the emulsion to decrease the concentration of protein at the water/organic interface (O'Donnell and McGinity, 1997). Others have used lyoprotectants such as trehalose and mannitol to stabilize proteins within the emulsions (Cleland and Jones, 1996). Carrier proteins such as gelatin and albumin have also been used within formulations (O'Donnell and McGinity, 1997).

Griebenow and Klibanov showed that proteins lose secondary structure when exposed to water/organic mixtures but not pure organic solvents (Griebenow and Klibanov, 1996). To take advantage of this, protein particles are dispersed in a polymer solution and then microspheres are formed with either an oil-in-oil emulsion or an oil-in-water emulsion (Wang, Schmitt *et al.,* 1991). By co-mixing lyophilized proteins and polymer in an organic solvent, the primary emulsion step is eliminated thus giving a single emulsion technique. By encapsulating lyophilized proteins with this method where protein is not exposed to a water/oil interface, the protein is entrapped under conditions of limited mobility and thus cannot unfold or aggregate.

A completely anhydrous system, the spray freeze-drying process, has been used successfully to entrap and completely release human growth hormone from PLGA microspheres (Johnson, Cleland *et al.,* 1996). Here micronized protein particles suspended in the polymer solution are atomized into droplets that are frozen in liquid nitrogen. Ethanol is then used to extract the organic solvent.

Once microspheres are formed, they are typically washed and freeze-dried for storage. Prior to injection, the particles are resuspended in injection vehicle, and upon administered microencapsulated proteins become hydrated and incubate at elevated temperature and high concentration within the polymer device before release. Deleterious reactions may occur in solid protein systems exposed to moisture, and these modifications may be divided into chemical instability pathways and covalent modification pathways.

Chemical inactivation results generally from modification of side chains by deamidation, oxidation, or hydrolysis of the peptide backbone. Deamidation occurs most often at neutral to alkaline conditions at asparagine and glutamine residues. Examples of deamidation have been shown in solid protein and peptide systems upon exposure to moisture and elevated temperatures (Hageman, Bauer *et al.,* 1992; Oliyai, Patel *et al.,* 1994; Schwendeman, Costantino *et al.,* 1995). Oxidation typically occurs at amino acids methionine, tryptophan, cysteine, histidine, and tyrosine. In a protein/polymer system, methionine and cysteine are more likely to undergo oxidation. For examples, oxidation of methionine in a solid protein has been observed for human growth hormone (Pearlman and Nguyen, 1992). Under acidic conditions, the peptide backbone may be hydrolyzed. Hydrolysis occurs more frequently near aspartate residues, especially when aspartate is adjacent to proline. Recombinant bovine growth hormone has been shown to undergo hydrolysis in the solid state (Hageman, Bauer *et al.,* 1992).

Covalent reactions involve β-elimination at disulfide bonds or cysteines and incorrect or non-native formation of disulfide bonds between intramolecular or intermolecular disulfides. Products of β-elimination are unstable, and Costantino, *et al.* (Costantino, Langer *et al.,* 1994) have directly followed the solid state β-elimination of insulin at elevated temperatures and

moistures. Incorrect disulfide formation occurs in solid-state proteins such as albumin (Liu, Langer *et al.,* 1991) and tetanus toxoid (Schwendeman, Lee *et al.,* 1994).

Although encapsulation of several proteins in a variety of polymer systems has been studied (Pitt, 1990; Okada and Toguchi, 1995), to date only one such formulation has been approved by the FDA for therapeutic use. Alkermes and Genentech received approval in 1999 for a sustained release formulation of recombinant human growth hormone within biodegradable PLGA microspheres. In spite of this example, introduction of a hydrophilic protein into a hydrophobic polymer device is a challenge which has not been completely resolved. Proteins have several levels of structure and many different interactions determine the final, active, three-dimensional structure of a protein. This balance of interactions must be maintained during formulation of the delivery device as well as during delivery. However, known and perhaps other complex protein-protein and protein-polymer interactions result in protein denaturation and aggregation. Thus for many proteins, complete release of active protein from a biodegradable device has not been achieved (Cleland, 1997). This incomplete delivery wastes expensive materials as an excessive loading of the therapeutic agent is needed to achieve an equivalent therapeutic effect. Furthermore, undesirable release kinetics and immunologic reactions may occur as a consequence of protein denaturation. Because this loss of protein and activity is not well understood, difficulties arise in rationally formulating an efficient delivery system. So far, these hurdles have been overcome in only a few specific cases (Johnson, Cleland *et al.,* 1996) and have made the use of controlled delivery difficult for many proteins. Thus, the motivation of this thesis is to identify important paradigms in achieving a pharmaceutically efficient, safe, biodegradable, delivery system capable of releasing biologically active protein.

1.2. Project scope

The processes during which protein stability is of concern include encapsulation, storage of the delivery device, and release of the protein from the delivery device *in vivo*. During manufacture, the protein is often exposed to hydrophobic interfaces, high energy forces, and lyophilization. Under storage conditions, deleterious reactions such as aggregation can occur due to hydration of the protein (Arakawa, Prestrelski *et al.,* 1993). Finally, during polymer degradation, acidic products are formed acidifying the local environment within the device (Mader, Gallez *et al.,* 1995; Burke, 1996). Under these conditions, proteins may aggregate, undergo hydrolytic degradation, and/or chemical modification (Couvreur, Blanco-Prieto *et al.,* 1997). Proteins may also adsorb reversibly or irreversibly to the polymers causing denaturation or aggregation (Couvreur, Blanco-Prieto *et al.,* 1997; Crotts, Sah *et al.,* 1997). By understanding these effects, improved formulations and methods of production to protect the protein can be designed. Here, we develop new methods to characterize and improve protein microsphere systems.

1.2.1 *In situ* protein characterization

The most widely used technique for protein encapsulation in microspheres is the double-emulsion method (Cohen, Yoshioka *et al.,* 1991). As it is difficult to entrap a hydrophilic molecule within a hydrophobic polymer, this technique takes advantage of high energy mixing to accomplish this goal. An initial water-in-oil (w/o) emulsion of protein and polymer is formed, and then a second emulsion, (w/o)/w, is formed by dispersion of the first emulsion in an aqueous

phase (See Figure 1-2). The organic solvent used to dissolve the polymer is then removed from the microparticles.

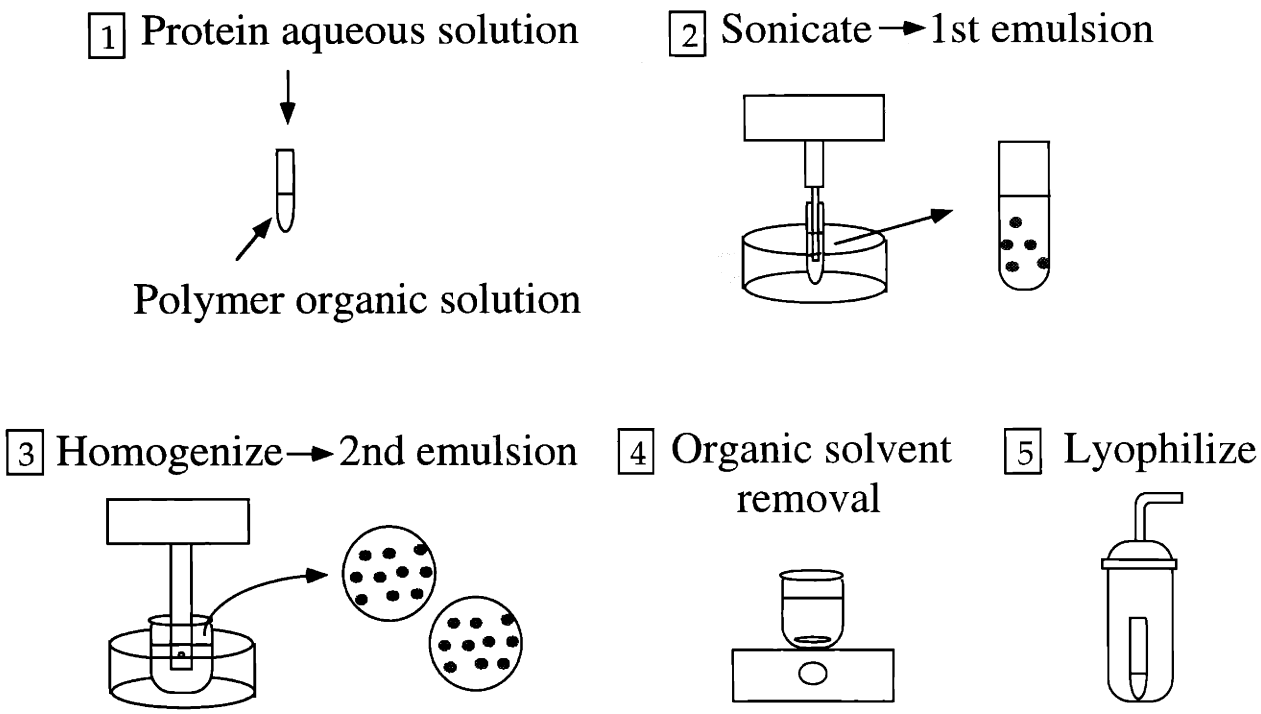

Figure 1-2. Schematic representation of the double emulsion technique: 1) addition of protein solution to polymer dissolved in organic solvent, 2) the first emulsion is formed via sonication; round particles in test tube represent protein droplets suspended in polymer solution, 3) the first emulsion is added to a larger aqueous volume and the mixture is homogenized to form the second emulsion; protein droplets are now suspended within polymer droplets, 4) the organic solvent is allowed to evaporate and the particles harden, 5) the mixture is then lyophilized to remove water and microspheres are recovered.

During formation of the first emulsion, the aqueous protein is exposed to high energy forces and to organic solvent. It is at this aqueous/organic interface that proteins become denatured (Tabata, Gutta *et al.,* 1993; Lu and Park, 1995; Schwendeman, Costantino *et al.,* 1996; Cleland and Jones, 1996; Sah, 1999; Krishnamurthy, 1997). To characterize the changes to the protein due to encapsulation, an analytical method was developed to determine the protein structure within the polymer. This is essential as protein structure determines protein activity. There have been no studies published that examine the structure of the protein within a polymer microsphere or other formulation. With application of Fourier self-deconvolution and Gaussian curve-fitting techniques, protein secondary structure can be quantitatively determined using Fourier transform infrared (FTIR) spectroscopy (Byler and Susi, 1986). This novel technique can provide detailed information regarding protein conformation in a noninvasive manner, that is without alteration or degradation of the controlled-release system. The success of this technique will have beneficial repercussions in the biotechnology industry. The ability to quickly and simply determine the protein structure within a delivery device will greatly aid in assessing different processing steps, final formulations, and determining product quality.

1.2.2 Strategy to minimize initial burst

The release kinetics of proteins from double emulsion microspheres often exhibit a large burst of release. The hypothesis is that ion-paired protein/surfactant complexes formulated into microspheres via spontaneous emulsion will minimize this initial burst. The protein/surfactant complex readily dissolves in organic solvent and thus a homogeneous distribution of protein is achieved throughout the polymer solution. In addition, this process avoids exposure of protein to

a water/organic interface and may increase protein stability. Specifically, the spontaneous emulsification process will be optimized and key factors that affect the loading within and size of the microspheres will be identified. The effect of different charged surfactants on protein solubility in organic solvents will be examined. Following optimization of the microsphere formulation, the amount and activity of the protein released from the microspheres will be quantified.

1.2.3 Characterization of microsphere environment

Upon injection of microspheres into the body, water enters the polymer and hydrates the protein. Polymer degradation yields acidic monomers and low molecular weight chains. Thus, the pH within a microsphere during polymer degradation directly influences encapsulated protein stability. The hypothesis is that the pH within degrading microspheres is at an extreme and damages the encapsulated protein. To test this, the pH changes within microspheres will be quantified as a function of degradation time, microsphere diameter, and microsphere porosity using pH-sensitive, fluorescent dyes and confocal light microscopy.

1.3. References

Alonso, M.J., R.K. Gupta, C. Min, G.R. Siber and R. Langer, (1994). Biodegradable microspheres as controlled-release tetanus toxoid delivery systems. *Vaccine* **12(4)**: 299-306.

Arakawa, T., S. J. Prestrelski, W. C. Kenney and J. F. Carpenter, (1993). Factors affecting short-term and long-term stabilities of proteins. *Adv. Drug Del. Rev.* **10**: 1-28.

Buckel, P. (1996). Recombinant proteins for therapy. *TiPS* **17**: 450-456.

Burke, P.A. (1996). Determination of internal pH in PLGA microspheres using 31P NMR spectroscopy. Intern. Symp. Control. Rel. Bioact. Mater., Controlled Release Society.

Byler, D. M. and H. Susi, (1986). Examination of the secondary structure of proteins by deconvolved FTIR spectra. *Biopolymers* **25**: 469-487.

Cleland, J. L. (1997). Protein delivery from biodegradable microspheres. Protein Delivery: Physical Systems. S. A. Hendren. New York, Plenum Press: 1-43.

Cleland, J. L. and A. J. S. Jones, (1996). Stable formulations of recombinant human growth hormone and interferon-gamma for microencapsulation in biodegradable microspheres. *Pharm. Res.* **13**: 1464-1474.

Cohen, S., T. Yoshioka and R. Langer, (1991). Controlled delivery systems for proteins based on poly(lactic/glycolic acid) microspheres. *Pharm. Res.* **8(6)**: 713-720.

Costantino, H.R., R. Langer and A.M. Klibanov, (1994). Moisture-induced aggregation of lyophilized insulin. *Pharm. Res.* **11**: 21-29.

Couvreur, P., M. J. Blanco-Prieto, F. Puisieux, B. Roques and E. Fattal, (1997). Multiple emulsion technology for the design of microspheres containing peptides and oligopeptides. *Adv. Drug Del. Rev.* **28**: 85-96.

Crotts, G., H. Sah and T. G. Park, (1997). Adsorption determines in-vitro protein release rate from biodegradable microspheres: quantitative analysis of surface area during degradation. *J. Cont. Rel.* **47**: 101-111.

Gombotz, W. R. and D. K. Pettit, (1995). Biodegradable polymers for protein and peptide drug delivery. *Bioconj. Chem.* **6**: 332-351.

Griebenow, K. and A.M. Klibanov, (1996). On protein denaturation in aqueous but not non-aqueous organic solvents. *J. Am. Chem. Soc.* **118(47)**: 11695-11700.

Hageman, M.J., J.M. Bauer, P.L. Possert and R.T. Darrington, (1992). Preformulation studies oriented toward sustained delivery of recombinant somatotropins. *J. Agric. Food Chem.* **40**: 348-355.

Hausberger, A.G. and P.P. DeLuca, (1995). Characterization of biodegradable poly(D,L-lactide-*co*-glycolide) polymers and microspheres. *J. of Pharm. Biomed. Anal.* **13(6)**: 747-760.

Iwata, M., T. Tanaka, Y. Nakamura and J.W. McGinity, (1998). Selection of the solvent system for the preparation of poly(D,L-lactic-co-glycolic acid) microspheres containing tumor necrosis factor-alpha (TNF-α). *Int. J. Pharm.* **160**: 145-156.

Johnson, O. L., J. L. Cleland, H. J. Lee, M. Charnis, E. Duesnas, W. Jaworowicz, D. Shepard, A. Shahzamani, A. J. Jones and S. D. Putney, (1996). A month-long effect from a single injection of microencapsulated human growth hormone. *Nat. Med.* **7(July 2)**: 795-799.

Krishnamurthy, R., (1997). Denaturation of lysozyme during microencapsulation. Chemical and Biochemical Engineering. Baltimore, University of Baltimore County**:** 126.

Lewis, D. H. (1990). Controlled release of bioactive agents from lactide/glycolide polymers. Drugs and the Pharmaceutical Sciences. M. Chasin and R. Langer. New York, Marcel Dekker, Inc. **45**: 1-41.

Liu, R., R. Langer and A.M. Klibanov, (1991). Moisture-induced aggregation of lyophilized proteins in the solid state. *Biotechnol. Bioeng.* **37**: 177-184.

Lu, W. and T. G. Park, (1995). Protein release from poly(lactic-co-glycolic acid) microspheres: protein stability problems. *J. Pharm. Sci. Technol.* **49**: 13-19.

Mader, K., B. Gallez, K. J. Liu and H. M. Swartz, (1995). Non-invasive *in vivo* characterization of release processes in biodegradable polymers by low-frequency electron paramagnetic resonance spectroscopy. *Biomaterials* **16(3)**: 1-5.

New, R.R.C. and C.J. Kirby, (1997). Solubilisation of hydrophilic drugs in oily formulations. *Adv. Drug Del. Rev.* **25**: 59-69.

O'Donnell, P.B. and J.W. McGinity, (1997). Preparation of microspheres by the solvent evaporation technique. *Adv. Drug Del. Rev.* **28**: 25-42.

Okada, H. and H. Toguchi, (1995). Biodegradable microspheres in drug delivery. *Crit. Rev. Therap. Drug Carrier Sys.* **12(1)**: 1-99.

Oliyai, C., J.P. Patel, L. Carr and R.T. Borchardt, (1994). Solid state chemical instability of an asparaginyl residue in a model hexapeptide. *J. Pharm. Sci. Technol.* **48**: 167-173.

Pearlman, R. and T. Nguyen, (1992). Pharmaceutics of protein drugs. *J. Pharm. Pharmacol.* **44**: 179-185.

Pitt, C. G., (1990). The controlled parenteral delivery of polypeptides and proteins. *Int. J. Pharm.* **59**: 173-196.

Sah, H, (1999). Protein behavior at the water/methylene chloride interface. *J. Pharm. Sci.* **88(12)**: 1320-1325.

Schwendeman, S.P., H.R. Costantino, R. K. Gupta, A.M. Klibanov and R. Langer, (1995). Controlled release of proteins and peptides from polymeric systems. Controlled Drug Delivery. The Next Generation. K. Park. Washington, DC, ACS Books.

Schwendeman, S. P., H. R. Costantino, R. K. Gupta, M. Tobio, A. C. Chang, M. J. Alonso, G. R. Siber and R. Langer, (1996). Strategies for stabilizing tetanus toxoids toward the development of a single-dose tetanus vaccine. *Dev. Biol. Stand.* **87**: 293-306.

Schwendeman, S.P., J.H. Lee, R. K. Gupta, H.R. Costantino, G.R. Siber and R. Langer, (1994). Inhibition of moisture-induced aggregation of tetanus toxoid by protecting thiol groups. *Proceed. Intern. Symp. Control. Rel. Biact. Mater.* **21**: 54-55.

Tabata, Y., S. Gutta and R. Langer, (1993). Controlled delivery systems for proteins using polyanhydride microspheres. *Pharm. Res.* **10(4)**: 487-496.

Wang, H.T., E. Schmitt, D.R. Flanagan and R.J. Linhardt, (1991). Influence of formulation methods on the in vitro controlled release of protein from poly(ester) microspheres. *J. Cont. Rel.* **17**: 23-32.

2. Determination of protein structure within a delivery device*

2.1 Introduction

Proteins have been shown to not survive the double emulsion process. Indirect evidence of protein instability due to exposure to organic solvent and shearing has been shown for several proteins (Tabata, Gutta *et al.*, 1993; Schwendeman, Costantino *et al.*, 1996; Cleland and Jones, 1996; Sah, 1999). However, there is no direct method to assess the stability of the protein within the device and thus results of protein recovered from microspheres is always confounded with the extraction or release of the protein from the device.

Current methods of protein structure characterization within polymers involve dissolving the polymer away from the protein with an organic solvent to retrieve the protein (Johnson, Cleland *et al.*, 1996) for analysis of structural integrity or activity. Thus far, there are no published studies on the structure of proteins within a microsphere or other formulation. However, Fourier self-deconvolution and Gaussian curve-fitting techniques are used to quantitatively assess protein secondary structure by FTIR spectroscopy. We developed this approach to be applied to microsphere systems to provide detailed information regarding protein conformation non-invasively, i.e., without alteration or degradation of the controlled-release system. The ability to quickly and non-invasively determine the protein structure within a delivery device could greatly aid assessment of different processing steps and final formulations, as well as determination of product quality.

* Published in part in Fu, K., K. Griebenow, L. Hsieh, A. M. Klibanov, R. Langer, (1999). FTIR characterization of the secondary structure of proteins encapsulated within PLGA microspheres. *J. Cont. Rel.* **58:** 357-366.

Such a method can be applied to the specific example of assessing the role of excipients in improving protein stability. Various excipients have been used to protect lyophilized proteins from deterioration during long-term storage (Arakawa, Prestrelski *et al.*, 1993; Fagain, 1995; Carpenter and Crowe, 1988). FTIR spectroscopy has been employed to examine the effect of the sugar excipients trehalose, sucrose, and lactose on the structure of freeze-dried proteins (Carpenter and Crowe, 1989; Carpenter, Prestrelski *et al.*, 1994; Prestrelski, Arakawa *et al.*, 1993; Prestrelski, Tedeschi *et al.*, 1993). Improved stability of both recombinant human growth hormone and interferon-γ within PLGA microspheres by incorporation of trehalose and mannitol has been reported (Cleland and Jones, 1996). Here, we examine the effect of sugars on protein structure and focus on the effects of trehalose on protein structure within the microspheres and on protein release.

2.2. Quantifying protein secondary structure with FTIR spectroscopy

There are many techniques used to determine protein structure including X-ray crystallography, nuclear magnetic resonance (NMR), circular dichroism (CD), Raman spectroscopy, and FTIR spectroscopy. Of these techniques X-ray crystallography provides the most direct measure of protein structure. However, there are practical limitations, namely the need for high-quality crystals and the time required to calculate the structure. Two-dimensional NMR is a dynamic technique often used but is limited to low-molecular-weight proteins (MW < 10,000) (Surewicz and Mantsch, 1988). With the remaining techniques, only the secondary structure of a protein can be characterized. Raman spectroscopy and infrared spectroscopy are similar as both

probe the vibrational energy levels of a molecule, and Raman data is often used to complement IR data (Freifelder, 1982). In addition, the techniques are capable of determining protein secondary structure from both solution and solid state samples.

Spectroscopic techniques rely on the basic principle that molecules absorb energy and the efficiency of absorption is dependent on both the structure and environment of the molecule. Infrared spectroscopy measures characteristic motions of a molecule due to the absorption of light in the infrared region (IR): 10^3 nm to 10^5 nm. Absorption of energy results in transitions between vibrational levels of the ground state of the molecule. The vibrational levels are generated by characteristic motions (bond stretching and bond bending) of different functional groups on the molecule such as methyl, carbonyl, and amide (Freifelder, 1982).

The advantages of infrared spectroscopy include: 1) non-invasive technique--chemical groups which other absorption techniques cannot access can be examined with little perturbation to the sample, 2) sensitivity--small changes in chemical structure, conformation, and environment can be detected, 3) quantitative--protein secondary structure can be quantified using mathematical techniques. Disadvantages of this technique include the need for high protein concentrations (~40 mg/mL) to assess protein secondary structure in the solution state and also the difficult Gaussian curve-fitting procedure due to overlapping bands.

Use of FTIR spectroscopy to quantify protein secondary structure in both the solution state and the solid state has been well established (Arrondo, Muga *et al.,* 1993; Prestrelski, Arakawa *et al.,* 1993; Prestrelski, Tedeschi *et al.,* 1993; Griebenow and Klibanov, 1995). In the solution state, secondary structure determinations correlate well with X-ray crystallography data (Arrondo, Muga *et al.,* 1993). Protein secondary structure determination relies on quantifying the signal due

to chemical bonds absorbing at a certain frequency. The amide group of a peptide bond has many vibrational modes designated amide I, amide II, amide III, etc. For amide I- and more recently amide III-region spectra, this secondary structure can be quantified; the characteristic shape of the band is determined by the configuration of the peptide bonds. Each region may have α-helix, β-sheet, or random coil character, or a combination of the three. Information regarding structure can be elucidated by Fourier self-deconvolution and Gaussian curve-fitting techniques (Byler and Susi, 1986). The wave numbers corresponding to the structure groups are listed in Table 2-1.

Table 2-1. Wavenumbers for secondary structures in amide I and amide III regions

Secondary structure	Amide I (cm^{-1}) (Freifelder, 1982)	Amide III (cm^{-1}) (Griebenow and Klibanov, 1995)
α-helix	1650	1293-1328
β-sheet	1632, 1685	1218-1250
random coil	1658	1257-1288

It is now established that the secondary structure of proteins differs in the aqueous and lyophilized states (Griebenow and Klibanov, 1995). In general, lyophilization of proteins causes a decrease in the α-helix, and increase in the β-sheet, content. The rise in the β-sheet content is likely due to protein-protein interactions leading to the formation of intermolecular β-sheets when the bulk solvent water is removed. Consequently, the β-sheet content of a lyophilized protein does not reflect its actual intramolecular structural content. Therefore, the α-helix content is a preferred indicator of the protein structural integrity (Griebenow and Klibanov, 1996).

2.3. Materials and Methods

2.3.1 Materials

BSA (98% purity, fatty acid content of approximately 0.005%), chicken egg-white lysozyme (95% purity), and D(+)-trehalose were purchased from Sigma (St. Louis, MO). PLGA 50:50 (RG503, lot 34033) was purchased from Boehringer Ingelheim (Montvale, NJ) and had a number average molecular weight of 25,000 Da. Poly(vinyl alcohol) (88% hydrolyzed, 25,000 Da) was obtained from Polysciences (Warrington, PA). The Lowry protein assay kit was purchased from Bio-Rad Laboratories (Hercules, CA), and the BCA kit from Pierce (Rockford, IL). Polyacrylamide gels (4-20%) and Daiichi Silver Stain kits were purchased from Integrated Separation Systems (Natick, MA). All other chemicals were of reagent grade.

2.3.2 Preparation of microspheres

Protein microspheres were prepared by a double-emulsion technique (Cohen, Yoshioka *et al.*, 1991). To 200 μL of aqueous protein solution (100 μL of 100 mg/mL protein adjusted to pH 7.4 and 100 μL of either water or trehalose solution) was added a 1-mL solution of 200 mg/mL PLGA in methylene chloride, and the mixture was sonicated for 6 pulses with a Vibracell (Danbury, CT) sonicator using a microtip probe with an output of 3 and 50% duty. This primary emulsion was then added to a 100-mL aqueous solution of 1% (w/v) poly(vinyl alcohol). The second emulsion was formed by homogenization for 1 min at 3,000 rpm on a Silverson (East Longmeadow, MA) homogenizer using a 5/8" micro-mixing assembly with a general-purpose disintegrating head. The resultant water-in-oil-in-water (w/o)/w emulsion was stirred continuously

for 3 h to achieve solvent evaporation. The hardened microspheres were centrifuged, washed 3 times with water, freeze-dried, and stored under dessicant at -20°C.

2.3.3 Lyophilization

All materials to be lyophilized were frozen in liquid nitrogen and applied to a Labconco (Kansas City, MO) model 8 freeze-drier at a pressure of approximately 10 μm of Hg and a condenser temperature of -50°C for 48 h. Concentrations of proteins were 1 mg/mL in distilled water adjusted to pH 7.4.

2.3.4 Protein loading

Ten mg of dried microspheres were dissolved in 0.1N NaOH/0.5% SDS (3 mL) overnight at 37°C. Protein content was then determined using a Lowry assay.

2.3.5 Protein release studies

Ten mg of dried microspheres were suspended, in triplicate, in round-bottom, 1.8-mL cryovials containing 1 mL of phosphate buffered saline (PBS) at pH 7.4. Sample tubes were incubated at 37°C with continuous shaking on an orbital shaker at 100 rpm. To sample the released protein, tubes were centrifuged and the supernatant was removed and frozen at -20°C. The sample tubes were replenished with PBS, vortexed to resuspend the microspheres, and placed back in the incubator. Time points were taken on days 1, 2, 4, 10, 15, 20, 30.

2.3.6 Sodium dodecyl sulfate-polyacrylamide gel electrophoresis (SDS-PAGE)

SDS-PAGE gels were run in a Daiichi gel box system with a constant current of 25 mA/gel under reduced and non-reduced conditions and then stained with silver. Protein markers from Bio-Rad were used as low molecular weight standards. Following staining, images of the gels were taken with a digital camera, and densitometry data analyzed with NIH Image 1.61 (developed at the U.S. National Institutes of Health and available on the internet at http://rsb.info.nih.gov/nih-image/) to quantitate the amount of protein within each band. A standard densitometry curve was generated by analyzing bands with known amounts of BSA.

2.3.7 Carbohydrate analysis

High-pressure anion exchange chromatography, followed by pulsed amperometric detection, was used to determine the trehalose concentration in the release samples. A Dionex (Sunnyvale, CA) liquid chromatography system was used with a 4 x 250 mm Dionex Carbopac MA1 guard and column. A sample (25 μL) was injected onto the column and eluted with 480 mM NaOH at a flow rate of 0.4 mL/min.

2.3.8 FTIR spectroscopy

FTIR spectroscopy was conducted with a Nicolet Magna-IR 550 spectrophotometer (Madison, WI) equipped with a MCT-B liquid N_2-cooled detector, germanium beamsplitter on KBr substrate (7400-350 cm^{-1}), and a high intensity air-cooled mid-IR Ever-Glo source (9600-50

cm^{-1}). Control of the instrument, as well as collection and primary analysis of data, was accomplished using Omnic 2.1 software. During data acquisition, the optical bench was purged with dry N_2 to reduce interference from water vapor IR absorption. The system was aligned before data collection, and for each run a total of 256 scans, at a resolution of 2 cm^{-1} using Happ-Genzel apodization, were averaged.

Most powder spectra were measured with 2 mg samples in 200 mg of KBr as a pellet pressed with a Spectra-Tech Macro-Micro KBr Die Kit and a Carver Laboratory (Wabash, IN) 12-ton hydraulic press. Alternatively, samples were suspended in the mineral oil Nujol (2 mg sample in approximately 150 μL of Nujol) and placed between two CaF_2 windows with a 15-μm spacer. Solution spectra of 40 mg/mL protein in water were obtained using a 15-μm spacer in a liquid cell equipped with CaF_2 windows.

All samples were measured at least six times. Each spectrum was corrected for the background in an interactive manner to obtain the sample vibrational spectrum. Subtractions of a water background for aqueous solutions and a blank (no protein) microsphere spectrum from protein-containing microsphere spectrum were performed using Omnic 2.1 software. The criterion used for subtraction was a straight baseline in the region of 1800 - 2500 cm^{-1} (Griebenow and Klibanov, 1995).

Background-corrected spectra were analyzed by second derivatization in the amide I and/or amide III band regions for their component compositions and peak frequencies (Griebenow and Klibanov, 1995; Byler and Susi, 1986) using Omnic 2.1 software. Second derivative spectra were smoothed with an 11-point smoothing function (10.6 cm^{-1}). For amide I band regions, Fourier

self-deconvolution was performed using Omnic 2.1 software at a bandwidth of 17 cm^{-1} and an enhancement factor of 2 (Griebenow and Klibanov, 1996; Griebenow and Klibanov, 1997). Gaussian curve-fitting, using GRAMS/386, was then performed on the original (non-smoothed) amide III band region or the Fourier self-deconvoluted amide I band region. The number of components and their peak positions, determined by second derivatization, were used as starting parameters. In all cases, a linear baseline was fitted. The secondary structure content was calculated from the areas of the individual assigned bands and their fraction of the total area in the amide I or III region. The determined areas were averaged, and standard deviations were calculated. Tables 2-2 and 2-3 summarize our results of the component analysis by second derivatization and the secondary structure quantification by Gaussian curve-fitting in the amide I and amide III regions for BSA and lysozyme.

Table 2-2. Infrared band positions of lysozyme and band assignments

Sample	Band Position (cm^{-1})[a]		Area (%)[a]	Assignment[b]
	Second Derivative	Gaussian Curve Fit		
Lyophilized powder				
Amide I	1695 ± 2	1697 ± 2	6 ± 0	β-sheet
	1683 ± 2	1686 ± 1	14 ± 2	unordered
	1672 ± 2	1672 ± 2	25 ± 3	unordered
	1657 ± 1	1656 ± 2	27 ± 3	α-helix
	1647 ± 1	1646 ± 2	13 ± 2	unordered
	1639 ± 1	1638 ± 2	12 ± 3	β-sheet
	1627 ± 1	1629 ± 3	5 ± 3	β-sheet
Amide III	1324 ± 8	1322 ± 3	3 ± 0	α-helix
	1310 ± 1	1310 ± 1	11 ± 1	α-helix
	1289 ± 1	1291 ± 1	12 ± 1	α-helix
	1280 ± 2	1274 ± 0	13 ± 1	unordered
	1262 ± 1	1260 ± 1	17 ± 1	unordered
	1248 ± 1	1249 ± 1	12 ± 3	unordered
	1233 ± 1	1236 ± 1	26 ± 1	β-sheet
In PLGA microspheres				
Amide I	1698 ± 5	1697 ± 3	9 ± 2	β-sheet
	1689 ± 3	1687 ± 2	14 ± 2	β-sheet
	1679 ± 2	1676 ± 3	15 ± 2	unordered
	1669 ± 1	1665 ± 4	14 ± 2	unordered
	1657 ± 2	1655 ± 3	18 ± 2	α-helix
	1648 ± 2	1647 ± 3	10 ± 1	unordered
	1638 ± 3	1638 ± 3	11 ± 2	β-sheet
	1629 ± 1	1628 ± 2	5 ± 1	β-sheet

[a]The ± values are standard deviations calculated by analyzing 3 to 6 individual spectra in each case.
[b](Byler, Susi, 1986; Mishra, Griebenow, *et al.*, 1996)

Table 2-3. Infrared band positions of BSA and band assignments

Sample	Band Position (cm^{-1})[a]		Area (%)[a]	Assignment[b]
	Second Derivative	Gaussian Curve Fit		
Lyophilized powder				
Amide I	1693 ± 2	1695 ± 1	7 ± 1	β-sheet
	1684 ± 4	1687 ± 3	12 ± 2	unordered
	1671 ± 3	1677 ± 4	12 ± 1	unordered
	1665 ± 3	1668 ± 2	8 ± 2	unordered
	1658 ± 1	1657 ± 1	31 ± 1	α-helix
	1648 ± 1	1647 ± 1	7 ± 1	unordered
	1638 ± 2	1639 ± 1	15 ± 4	β-sheet
	1628 ± 1	1628 ± 2	8 ± 3	β-sheet
Amide III	1304 ± 2	1307 ± 2	18 ± 4	α-helix
	1286 ± 2	1286 ± 2	13 ± 3	α-helix
	1274 ± 3	1271 ± 3	17 ± 1	unordered
	1261 ± 1	1259 ± 1	14 ± 4	unordered
	1248 ± 1	1250 ± 1	8 ± 2	unordered
	1239 ± 1	1241 ± 2	18 ± 3	β-sheet
	1228 ± 1	1229 ± 3	13 ± 2	β-sheet
In PLGA microspheres				
Amide I	1694 ± 1	1695 ± 2	4 ± 2	β-sheet
	1688 ± 2	1689 ± 1	9 ± 1	unordered
	1678 ± 0	1678 ± 1	19 ± 2	unordered
	1669 ± 1	1668 ± 1	17 ± 2	unordered
	1657 ± 1	1659 ± 2	21 ± 2	α-helix
	1648 ± 1	1649 ± 1	14 ± 0	unordered
	1637 ± 3	1641 ± 1	9 ± 2	β-sheet
	1627 ± 3	1630 ± 1	6 ± 1	β-sheet

[a]The ± values are standard deviations calculated by analyzing 3 to 6 individual spectra in each case.

[b](Byler and Susi, 1986; Griebenow and Klibanov, 1995)

2.4. Results and Discussion

2.4.1 Secondary structure analysis by FTIR spectroscopy

Chicken egg-white lysozyme and BSA, used as model proteins, were incorporated into PLGA microspheres. These two proteins were chosen as they differ in many aspects including size, stability, and structure. Lysozyme (14,400 Da) is made up of 129 amino acid residues with 4 disulfide bonds (Creighton, 1984). Both the amide I and amide III region spectral data were analyzed to validate the band assignments by employment of two different spectral regions (Griebenow and Klibanov, 1996). In aqueous solution at pH 7.3, the α-helix content of lysozyme is 37 ± 5% by analysis of the amide I region (Table 2-4) and 34 ± 1% in the amide III region. Analysis of lysozyme powder lyophilized from a pH 5.1 solution revealed the secondary structure to be 24% α-helix, 43% β-sheet, and 33% unordered structure (Costantino, Griebenow *et al.*, 1995), as determined by Gaussian curve-fitting the amide III region of the FTIR spectrum. The α-helix content of lysozyme powder lyophilized from pH 7.0 is 27 ± 3% in the amide I region (Table 2-4) and 26 ± 1% in the amide III region. BSA (67,000 Da) is much larger than lysozyme with 583 amino acid residues, 17 disulfide bonds, and one free cysteine. FTIR spectral analysis of BSA in aqueous solution at pH 7.4 revealed a higher α-helix content than lysozyme with 54 ± 6% by analysis of the amide I region (Table 2-5) and 48 ± 3% by analysis of the amide III region. BSA lyophilized from pH 7.0 had an α-helix content of 31 ± 1% by analysis of the amide I region (Table 2-5) and 31 ± 2% by analysis of the amide III region. These data indicate for both lysozyme and BSA that in the solution and solid states, the amide I and amide III region analyses were in agreement.

Table 2-4. Secondary structure of lysozyme under various conditions[a]

Conditions	α-Helix Content, Amide I[b]
aqueous solution, pH 7.3	37 ± 5%
lyophilized powder[c]	27 ± 3%
powder mixed with blank PLGA microspheres	26± 2%
in PLGA microspheres[c]	18 ± 2%
in PLGA microspheres suspended in Nujol	18 ± 2%
lyophilized powder, 1:10 ratio with trehalose[c]	30 ± 2%
in PLGA microspheres, 1:10 ratio with trehalose[c]	22 ± 2%

[a]Determined by Gaussian curve-fitting of the FTIR spectra (see 2.3 Materials and Methods).

[b]For band assignments, positions, and areas of individual Gaussian bands, see Table 2-2. The ± values are standard deviations calculated by analyzing 6 to 9 individual spectra.

[c]Measured as KBr pellet (see 2.3 Materials and Methods). All ratios are by weight.

Table 2-5. Secondary structure of BSA under various conditions[a]

Conditions	α-Helix Content, Amide I[b]
aqueous solution, pH 7.4	54 ± 6%
lyophilized powder[c]	31 ± 1%
lyophilized powder in Nujol	34 ± 1%
in PLGA microspheres[c]	21 ± 2%
lyophilized powder, 1:10 ratio with trehalose[c]	39 ± 1%
in PLGA microspheres, 1:10 ratio with trehalose[c]	30 ± 3%
lyophilized powder, 1:5 ratio with trehalose[c]	39 ± 1%
in PLGA microspheres, 1:5 ratio with trehalose[c]	28 ± 5%
lyophilized powder, 1:2 ratio with trehalose[c]	34 ± 2%
in PLGA microspheres, 1:2.5 ratio with trehalose[c]	22 ± 1%

[a]Determined by Gaussian curve-fitting of the FTIR spectra (see 2.3 Materials and Methods).

[b]For band assignments, positions, and areas of individual Gaussian bands, see Table 2-3. The ± values are standard deviations calculated by analyzing 6 to 9 individual spectra.

[c]Measured as KBr pellet (see 2.3 Materials and Methods). All ratios are by weight.

2.4.2 Determination of protein structure inside delivery device

To determine the structure of a protein encapsulated within a polymer matrix, three sets of FTIR spectra were collected: the protein/polymer device, the solid protein, and the blank polymer device (not containing protein). By subtracting the polymer device spectrum (Figure 2-1a, bottom spectrum) from the protein/polymer composition one (Figure 2-1a, top spectrum), the spectrum of the encapsulated protein (Figure 2-1b, top spectrum) was obtained and analyzed for secondary structure components. We used amide I region data for this study because the polymer does not have a strong signal in this region and thus does not interfere with the protein IR absorption (no sufficient background subtraction could be obtained in the amide III region). As shown in Figure 2-1, the C=O stretching vibration (ca. 1750 cm^{-1}) of the polymer is well separated from the amide I vibration (1600 - 1700 cm^{-1}) of the protein. The results obtained were then compared with those of the lyophilized proteins.

As mentioned, the secondary structure of proteins differs in the aqueous and lyophilized states (Griebenow and Klibanov, 1995). Lyophilization of proteins causes a decrease in the α-helix, and increase in the β-sheet, content, where the rise in β-sheet content is likely due to the formation of intermolecular β-sheets. Because of this, the α-helix content is a preferred indicator of the protein structural integrity (Griebenow and Klibanov, 1996).

Using FTIR spectroscopy, we determined the secondary structure of the model proteins lysozyme and BSA encapsulated within PLGA microspheres. Tables 2-4 and 2-5 report the α-helix contents of the entrapped proteins in the solid state. One can see an additional one-third loss in α-helix content of both encapsulated proteins as compared to that of the freeze-dried proteins alone. (The IR spectra and the Gaussian curve-fitting of lysozyme in the solid state and within the

microspheres are shown in Figure 2-2a and b, and those of BSA are shown in Figure 2-2d and e.) Several controls were run to ensure that the results were not an artifact of the sample preparation technique. First, blank microspheres containing no protein were mixed with lyophilized lysozyme, pressed into a KBr pellet, and analyzed by FTIR spectroscopy. The polymer signal was subtracted from the spectrum, and the α-helix content of the protein mixed with polymer was found to be the same as that of lyophilized lysozyme. Therefore, physical mixing of the protein and PLGA did not cause a change in protein structure, and thus this subtraction of the polymer FTIR spectral bands did not cause artifacts. Second, the microspheres were prepared in two different media to ensure that the sampling technique did not affect the protein structure. One method was to press the microspheres into a KBr pellet and the other to suspend the microspheres in mineral oil (see 2.3 Materials and Methods). The two procedures produced identical results. To ensure that artifacts were not introduced due to subtraction of the background polymer spectra, we analyzed the spectra of BSA encapsulated within PLGA microspheres without any subtraction of the PLGA microsphere background. The α-helix content within these samples (21 ± 2%) was identical to those in which the polymer background had been subtracted (21 ± 2%). We also did not observe any new peak-like features for both lysozyme and BSA when comparing spectra in the freeze-dried state to spectra within PLGA microspheres. In addition, the peaks in the spectra of protein encapsulated within polymer were located at wavenumbers similar to those in the spectra of freeze-dried protein. For BSA, the number of components was the same and the peak frequencies were similar. From this, we concluded that the subtraction of PLGA did not create any spectral artifacts. For lysozyme, this was also the case with the exception of an observed band splitting. Instead of one band at 1672 cm^{-1}, two bands were found for the encapsulated protein at 1679 and 1669 cm^{-1}.

Again, subtraction of PLGA did not create artifacts. The observed splitting of the unordered band into components at 1679 and 1669 cm^{-1} is not due to a subtraction artifact. It is common for proteins to have unordered components at those wavenumbers, see BSA (See Table 2-3).

The additional losses in protein structure, mentioned above, occur during the formation of the microspheres. Others have shown that processing steps, such as interaction with organic solvents (Tabata, Gutta *et al.*, 1993; Schwendeman, Costantino *et al.*, 1996; Cleland and Jones, 1996; Sah, 1999) and sonication (Tabata, Gutta *et al.*, 1993; Cleland and Jones, 1996, Sah; 1999) are damaging to protein activity.

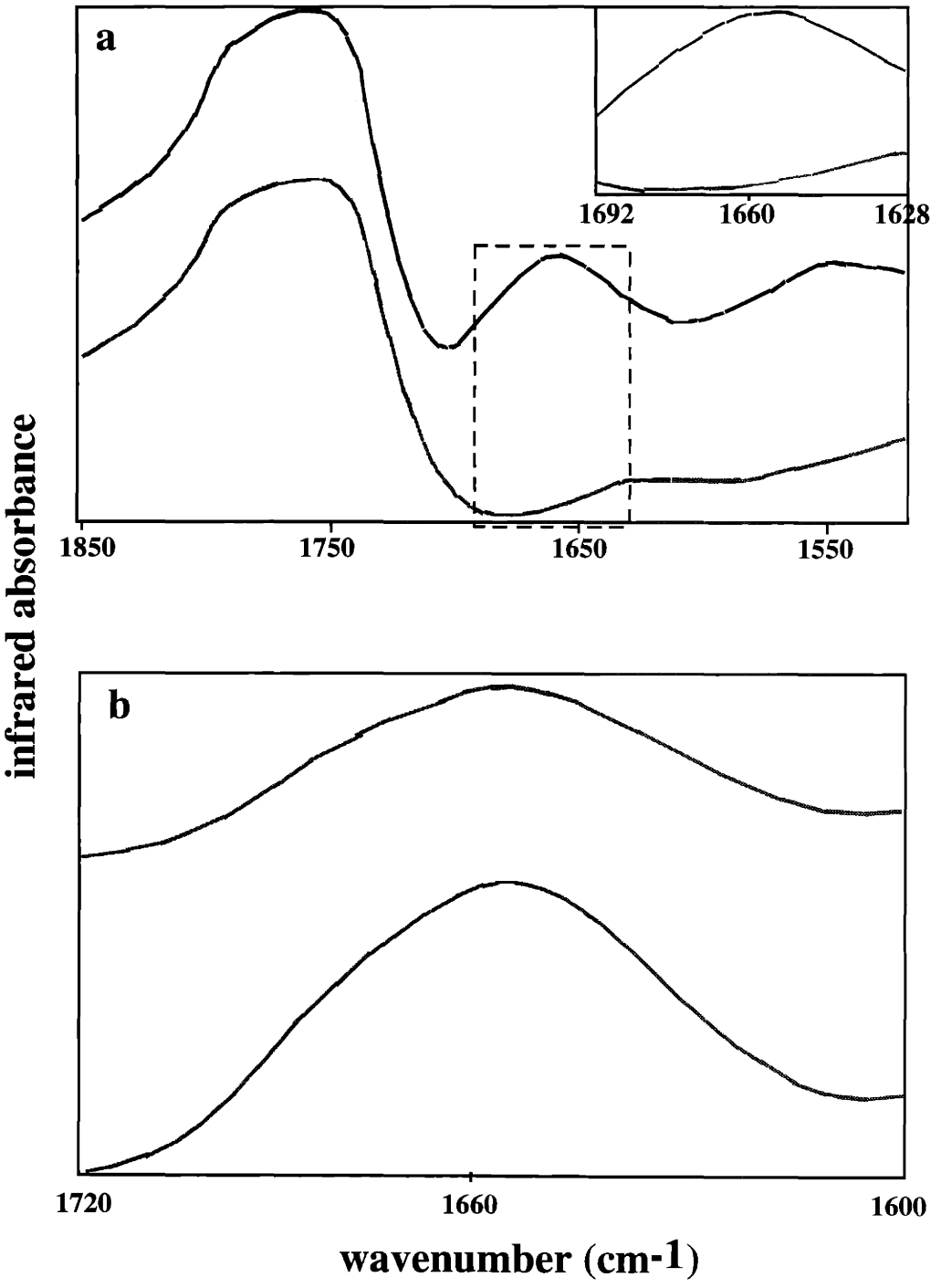

Figure 2-1. (a) Infrared spectra of BSA within PLGA microspheres (top) and blank PLGA microsphere containing no protein (bottom). Inset is an enlargement of the amide I region as shown by the dotted-line box. (b) Subtracted spectra (amide I region) of BSA (PLGA spectra subtracted from BSA within microsphere spectra) (top) compared with spectra of freeze-dried BSA (bottom).

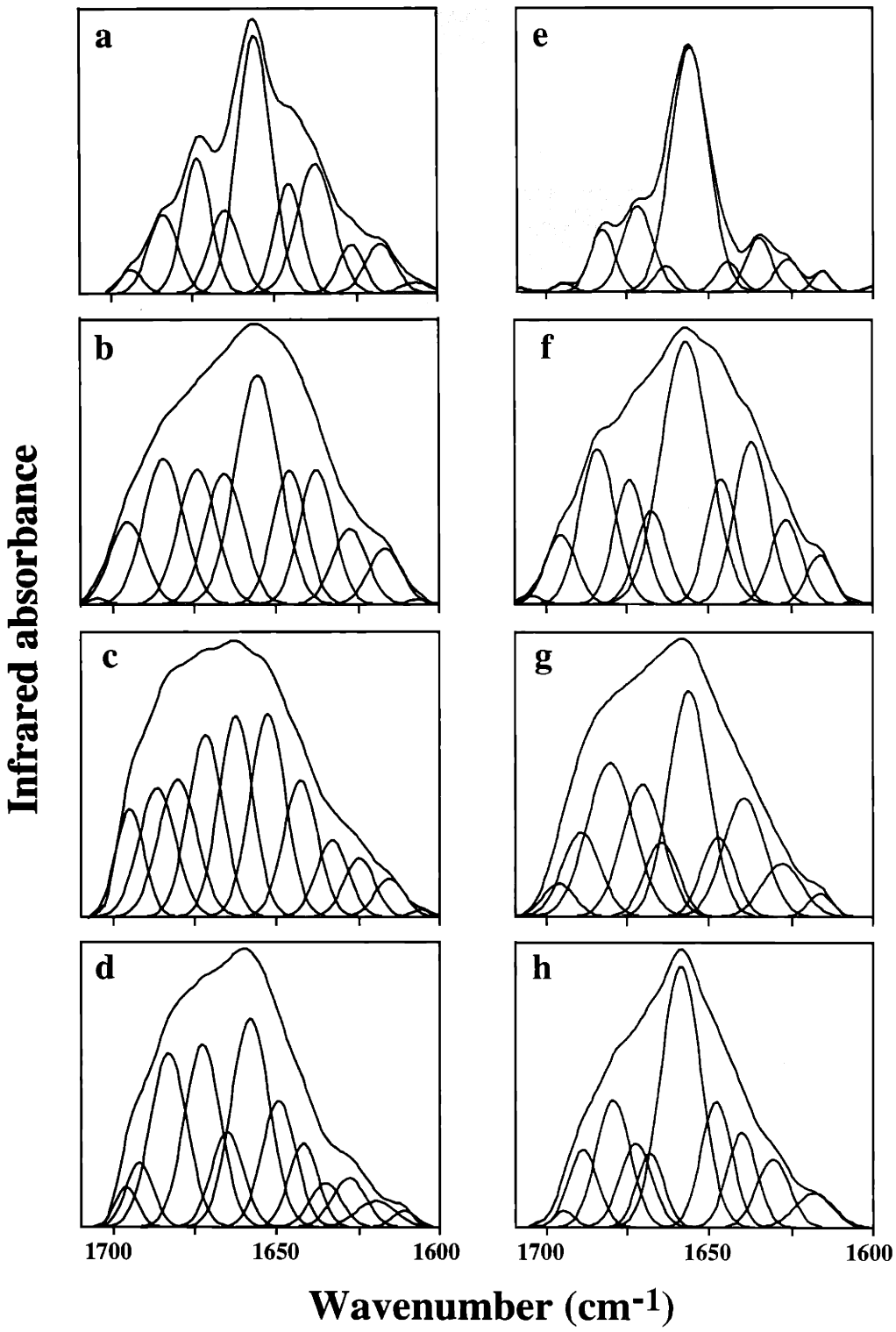

Figure 2-2. Infrared spectra of lysozyme and BSA in the amide I region and their Gaussian curve-fitting (the individual Gaussian bands are shown as symmetrical peaks underneath the IR spectra). Note that spectra are shown on a relative scale and not on an absolute scale. (a) Lysozyme in solution, pH 7.3; (b) Lysozyme powder; (c) lysozyme within PLGA microspheres; (d) lysozyme and trehalose within PLGA microspheres (1:10 lysozyme:trehalose ratio by weight); (e) BSA in solution, pH 7.4; (f) BSA powder; (g) BSA within PLGA microspheres; (h) BSA and trehalose within PLGA microspheres (1:10 BSA:trehalose ratio by weight).

2.4.3 Role of excipient in protein stability

While the observed loss of protein structure may be reversible or irreversible, the goal is to prevent the destabilizing changes from occurring. In the literature, sugars are commonly used as lyoprotectants (Carpenter and Crowe, 1988; Carpenter and Crowe, 1989) and it is thought that the sugars serve to form hydrogen bonds with the protein; the sugars actually replace water in forming the bonds. The formation of the hydrogen bonds keeps the protein in a state that is more native-like thus maintaining a higher α-helix content. In regards to the microsphere formulations, the hypothesis is that the sugars protect the protein not only from lyophilization induced changes but also from changes due to encapsulation. Here, BSA was freeze-dried with several different sugars and analyzed for α-helix content (Figure 2-3). The sugars included disaccharides - trehalose, cellobiose, sucrose, lactose, and maltose - and monosaccharides - glucose and mannose. The results showed improvement of BSA α-helix content in all cases with statistical significance by t-test as compared to the control of freeze-dried BSA alone (95% confidence in all cases except mannose, 88% confidence). As observed, trehalose showed the most change in structure towards native protein, and therefore further studies focused on the use of trehalose for stabilization.

In the solid state, trehalose prevents the loss in α-helix content of BSA, as seen in Table 2-5. At a 1:10 weight ratio of BSA:trehalose, the α-helix content of BSA is increased from 30% (BSA alone) to almost 40% (with trehalose), i.e., much closer to the α-helix content of native BSA (54%). On the other hand, formulations of lysozyme with trehalose at equivalent protein to sugar weight ratios did not show significant improvement (Table 2-4). A hypothesis may be that when compared on a molar ratio, a 1:10 weight ratio for lysozyme to trehalose is equivalent to approximately a 1:2.5 weight ratio for BSA to trehalose since the molecular weight of BSA is

almost 5 times that of lysozyme. At this low a weight ratio, there is little improvement seen with BSA as well. Unfortunately due to detection limitations, it was not possible to examine lysozyme formulations with higher amounts of trehalose as the signal from lysozyme was too low. A future study may be to examine a protein with an intermediate molecular weight between that of lysozyme and BSA.

The ability of non-reducing sugars to increase protein stability within microspheres has been studied, and trehalose and mannitol have been shown to improve the recovery of the native protein after encapsulation and to increase the amount of native protein released from the microspheres (Cleland and Jones, 1996). It is hypothesized that the excipients preferentially solvate the protein and prevent denaturation from occurring at the water/organic solvent interface (Cleland and Jones, 1996). Here, we directly quantify the effect of trehalose on the secondary structure of BSA and lysozyme encapsulated within microspheres. (The IR spectrum and the Gaussian curve-fitting of lysozyme and trehalose within the microsphere are shown in Figure 2-2c, and those of BSA in Figure 2-2f.) Trehalose was added directly to the aqueous protein phase during microsphere preparation. Since there was a concern that trehalose would leach out of the microspheres during processing, a control was performed where the primary emulsion was added to a 1% PVA solution saturated with trehalose. The secondary structure results from the two different procedures were equivalent indicating that trehalose had not leached out.

Incorporation of trehalose into the microspheres improved the stability of BSA considerably (Table 2-5). Trehalose (at a 1:10 ratio of protein:sugar by weight) is able to fully restore the α-helix content of the encapsulated BSA to that of freeze-dried BSA in the absence of sugar. With lysozyme, there was no significant change in the α-helix content with trehalose

included in the formulation at a weight ratio of 1:10 (protein:sugar). Again, since the molecular weight of BSA is some five times that of lysozyme, the equivalent molar ratios of sugar to protein used for BSA could not be examined with lysozyme due to sensitivity limitations of the FTIR instrument.

The quality of the proteins was evaluated by analyzing the protein released from the microspheres under physiologic conditions. Spheres containing BSA and trehalose (loading of 2.7%) and spheres containing BSA and sodium chloride (loading of 3.0%) were studied. Sodium chloride was used as a control excipient in order to compare the effect of trehalose with spheres of approximately equal loading.

To ensure that trehalose was indeed incorporated within the microspheres, release samples were analyzed for the presence of trehalose (Figure 2-4). Over the course of 30 days, trehalose is continuously released. This not only confirms the presence of trehalose but also helps to demonstrate the efficacy of small molecule delivery using PLGA microspheres.

BSA in PLGA microspheres has been shown to be released in part in the form of dimers and higher order multimers rather than just monomers (Crotts and Park, 1997). (Lysozyme has not been reported in the literature to undergo these changes and thus was not studied.) Crotts and Park suggested that the formation of dimers and multimers of BSA occurred due to thiol-disulfide exchange and showed that the ratio of monomeric BSA to dimeric actually increased during incubation of the protein in PBS over 50 days. However when examining BSA released from PLGA microspheres, the opposite occurred and the ratio of monomeric to dimeric protein decreased. For human serum albumin, dimerization has been shown to occur during the emulsification step when the protein is exposed to a water/organic solvent interface (Sah, 1999).

Here, we analyzed the released protein for the relative amount of monomeric vs. dimeric protein. By these analyses, higher order molecular aggregates and non-covalent aggregates were not visualized. These dimers were shown to be covalent in nature as when the samples were reduced, there was no dimer detected by silver stain. Our results reveal that microspheres containing trehalose release more monomeric BSA than those without trehalose. Over 30 days, trehalose-containing microspheres released 70 ± 2 μg of monomeric BSA, while equally-loaded microspheres not containing trehalose (but containing sodium chloride) released only 59 ± 1 μg of monomeric BSA. These translated to 74% and 71% monomeric protein released when compared to total protein released over the course of 30 days. However, there was an improvement in the individual ratios of monomeric protein to dimeric protein released over the latter portion of the 30 days. Between days 10 and 30, the average percentage of monomeric form to total protein released was 95 ± 2% from trehalose-containing microspheres compared to 89 ± 2% from the control microspheres. These data show that addition of trehalose has a beneficial effect on the quality of BSA release and the results are statistically significant with 95% confidence as determined by two-tailed T-tests.

Crotts and Park have shown that the relative amounts of dimers and multimers do not change during processing and formation of the microspheres, and that the presence of the polymer is integral to BSA aggregation during release (Crotts and Park, 1997). Here, we add that the presence of trehalose may slow the formation of BSA dimers.

A possible mechanism by which trehalose prevents BSA dimerization may be dilution of the protein; at a high enough ratio of sugar to protein, trehalose may shield the BSA molecules from each other and reduce dimerization.

Following presentation of this work, both Yang *et al.* and Carrasquillo *et al.* used FTIR spectroscopy to determine the secondary structure of recombinant human growth hormone (rhGH) within PLGA devices (Yang, Dong *et al.*, 1999; Carrasquillo, Costantino *et al.*, 1999). As with BSA and lysozyme, the α-helix content of rhGH decreased upon entrapment within the PLGA device. Both trehalose and zinc were used as excipients within the formulations and were found to improve the α-helix content. In addition, there was a positive correlation between the α-helix content of the protein and the percent of monomeric protein released. These data correlate well with those presented here.

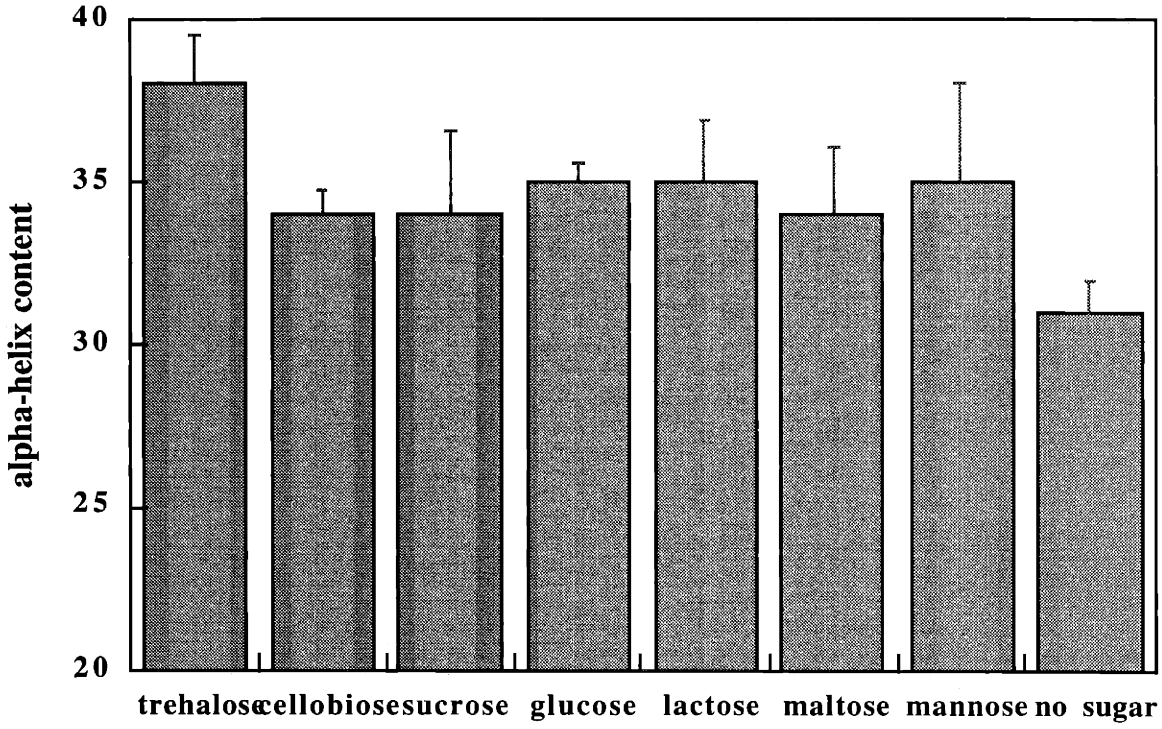

Figure 2-3. The α-helix content of BSA freeze-dried with different sugars compared to the α-helix content of freeze-dried BSA alone (no sugar). The BSA:sugar ratio is 1:10 by weight in each case and the BSA concentration is 2 mg/mL.

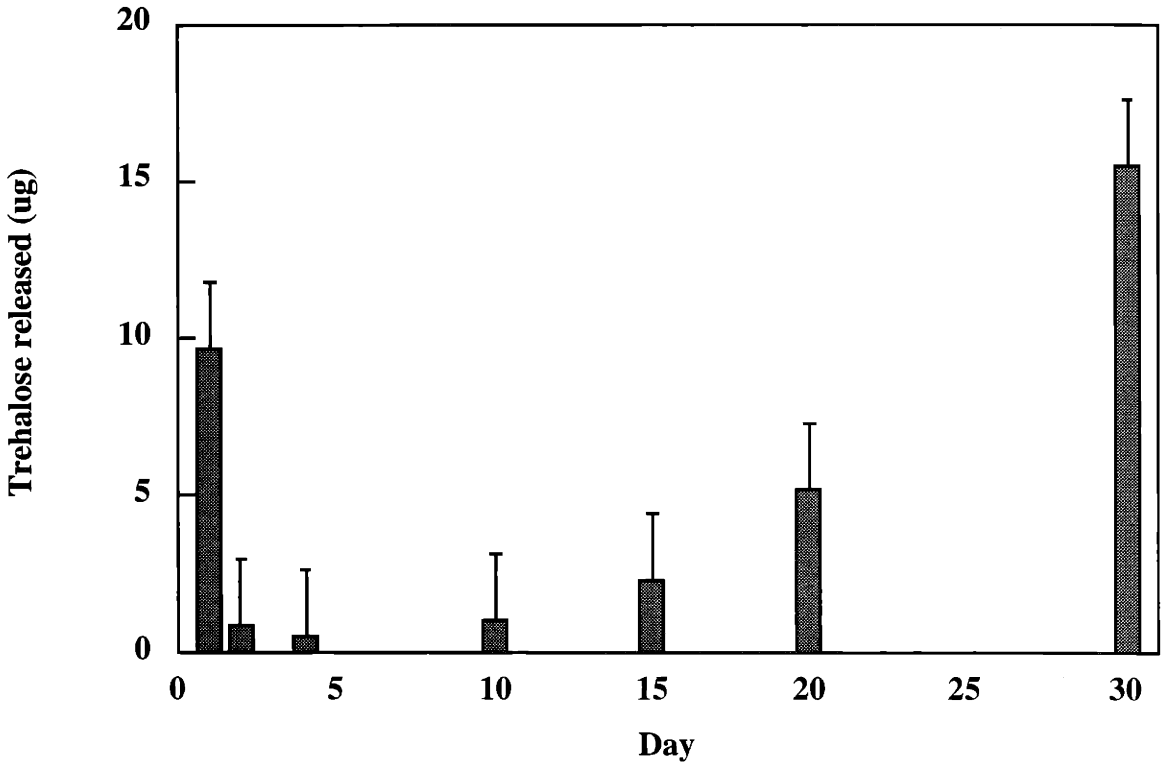

Figure 2-4. Release of trehalose from PLGA microspheres containing BSA:trehalose 1:10 by weight.

2.5. Conclusions

By means of FTIR spectroscopy we have determined the solid-state secondary structure of lysozyme and BSA entrapped within PLGA microspheres. This method is straightforward and, most importantly, non-invasive. Unlike other common methods used to examine proteins encapsulated within polymer devices, the state of the protein delivery device is not altered in order to determine the secondary structure. Thus, this method is optimal for examining microsphere formulations to assess effects on protein structure and also to assess protein microsphere shelf-life. In addition to the lyophilization-induced changes in the native secondary structure, we find about a one-third loss in the α-helix content upon encapsulation of the proteins. This loss of structure can be reduced by incorporating trehalose within the microsphere at a 1:10 weight ratio of BSA:trehalose. The results using lysozyme as a model protein are equivocal; this is likely due to the low molar ratio of sugar to protein used. At equivalently low molar ratios, there is no improvement in the α-helix content of BSA compared to freeze-dried protein alone. Trehalose also helps to improve the quality of BSA released, and the mechanism by which this occurs may be protein dilution. Other works using similar techniques confirm our findings.

2.6. References

Arakawa, T., S. J. Prestrelski, W. C. Kenney and J. F. Carpenter, (1993). Factors affecting short-term and long-term stabilities of proteins. *Adv. Drug Del. Rev.* **10**: 1-28.

Arrondo, J.L R., A. Muga, J. Castresana and F. Goni, (1993). Quantitative studies of the structure of proteins in solution by Fourier-transform infrared spectroscopy. *Prog. Biophys. Molec. Biol.* **59**: 23-56.

Burke, P. A., (1996). Determination of internal pH in PLGA microspheres using 31P NMR spectroscopy. *Intern. Symp. Control. Rel. Bioact. Mater.* **23**: 133-134.

Byler, D. M. and H. Susi, (1986). Examination of the secondary structure of proteins by deconvolved FTIR spectra. *Biopolymers* **25**: 469-487.

Carpenter, J. F. and J. H. Crowe, (1988). The mechanism of cryoprotection of proteins by solutes. *Cryobiology* **25**: 244-255.

Carpenter, J. F. and J. H. Crowe, (1989). An infrared spectroscopic study of the interactions of carbohydrates with dried proteins. *Biochem.* **28:** 3916-3922.

Carpenter, J. F., S. J. Prestrelski, T. J. Anchordoguy, and T. Arakawa, in: J. L. Cleland, R. Langer (Eds.), Formulation and Delivery of Proteins and Peptides, American Chemical Society, Washington, D.C., 1994, pp. 134-147.

Carrasquillo, K.G., H.R. Costantino, R.A. Cordero, C.C. Hsu, K. Griebenow, (1999). On the structural preservation of recombinant human growth hormone in a dried film of a synthetic biodegradable polymer. *J. Pharm. Sci.* **88(2)**: 166-173.

Cleland, J. L. (1997). Protein delivery from biodegradable microspheres. Protein Delivery: Physical Systems. S. a. Hendren. New York, Plenum Press**:** 1-43.

Cleland, J. L. and A. J. S. Jones, (1996). Stable formulations of recombinant human growth hormone and interferon-gamma for microencapsulation in biodegradable microspheres. *Pharm. Res.* **13:** 1464-1474.

Cohen, S., T. Yoshioka and R. Langer, (1991). Controlled delivery systems for proteins based on poly(lactic/glycolic acid) microspheres. *Pharm. Res.* **8(6)**: 713-720.

Costantino, H. R., K. Griebenow, P. Mishra, R. Langer and A. M. Klibanov, (1995). Fourier-transform infrared (FTIR) spectroscopic investigation of protein stability in the lyophilized form. *Biochimica et Biophysica Acta* **1253**: 69-74.

Creighton, T. E. (1984). Proteins--Structures and Molecular Properties. New York, WH Freeman and Company.

Crotts, G. and T. G. Park, (1997). Stability and release of bovine serum albumin encapsulated within poly(D,L-lactide-co-glycolide) microparticles. *J. Cont. Rel.* **44:** 123-134.

Fagain, C. O. (1995). Understanding and increasing protein stability. *Biochimica et Biophysica Acta.* **1252:** 1-14.

Freifelder, D. (1982). Physical Biochemistry-Applications to Biochemistry and Molecular Biology. New York, WH Freeman and Company.

Gombotz, W. R. and D. K. Pettit, (1995). Biodegradable polymers for protein and peptide drug delivery. *Bioconjugate Chem.* **6**: 332-351.

Griebenow, K. and A. M. Klibanov, (1995). Lyophilization-induced changes in the secondary structure of proteins. *Proc. Natl. Acad. Sci. USA* **92**: 10969-10976.

Griebenow, K. and A. M. Klibanov, (1996). On protein denaturation in aqueous-organic mixtures but not in pure solvents. *J. Am. Chem. Soc.* **118:** 11695-11700.

Griebenow, K. and A. M. Klibanov, (1997). Can conformational changes be responsible for solvent and excipient effects on the catalytic behavior of subtilisin Carlsberg in organic solvents? *Biotechnol. Bioeng.* **53:** 351-362.

Johnson, O. L., J. L. Cleland, H. J. Lee, M. Charnis, E. Duesnas, W. Jaworowicz, D. Shepard, A. Shahzamani, A. J. Jones and S. D. Putney, (1996). A month-long effect from a single injection of microencapsulated human growth hormone. *Nat. Med.* **7(July 2)**: 795-799.

Lewis, D. H. (1990). Controlled release of bioactive agents from lactide/glycolide polymers. Drugs and the Pharmaceutical Sciences. M. Chasin and R. Langer. New York, Marcel Dekker, Inc. **45:** 1-41.

Mishra, P., K. Griebenow, and A. M. Klibanov, (1996). Structural basis for the molecular memory of imprinted proteins in anhydrous media. *Biotechnol. Bioeng.* **52:** 609-614.

Okada, H., H. Toguchi, (1995). Biodegradable microspehres in drug delivery. *Crit. Rev. Therapeutic Drug Carrier Systems* **12(1):** 1-99.

Pitt, C. G. (1990) The controlled parenteral delivery of polypeptides and proteins. *Inter. J. Pharm.* **59:** 173-196.

Prestrelski, S. J., T. Arakawa and J. F. Carpenter, (1993). Separation of freezing- and drying-induced denaturation of lyophilized proteins using stress-specific stabilization. *Arch. Biochem. Biophys.* **303(2)**: 465-473.

Prestrelski, S. J., N. Tedeschi, T. Arakawa and J. F. Carpenter, (1993). Dehydration-induced conformational transitions in proteins and their inhibition by stabilizers. *Biophys. J.* **65**: 661-671.

Sah, H, (1999). Protein behavior at the water/methylene chloride interface. *J. Pharm. Sci.* **88(12)**: 1320-1325.

Schwendeman, S. P., H. R. Costantino, R. K. Gupta, M. Tobio, A. C. Chang, M. J. Alonso, G. R. Siber and R. Langer, (1996). Strategies for stabilizing tetanus toxoids toward the development of a single-dose tetanus vaccine. *Dev. Biol. Stand.* **87**: 293-306.

Singh, B. R., D. B. DeOliveira, F. N. Fu, and M. P. Fuller, (1993). Fourier transform infrared analysis of amide III bands of proteins for the secondary structure estimation. Proc. Biomol. Spectroscopy III. Los Angeles, CA.

Surewicz, W.K. and H.H. Mantsch, (1988). New insight into protein secondary structure from resolution-enhanced infrared spectra. *Biochim. Biophys. Acta* **952**: 115-130.

Tabata, Y., S. Gutta and R. Langer, (1993). Controlled delivery systems for proteins using polyanhydride microspheres. *Pharm. Res.* **10(4)**: 487-496.

Yang, T.H., A. Dong, J. Meyer, O.L. Johnson, J.L. Cleland, J.F. Carpenter, (1999). Use of infrared spectroscopy to assess secondary structure of human growth hormone within biodegradable microspheres. *J. Pharm. Sci.* **88(2)**: 161-165.

3. Encapsulation of proteins via spontaneous emulsification

3.1. Introduction

Typical release kinetics from double emulsion (DE) microspheres exhibit an initial burst of drug upon immersion either in release medium *in vitro* or *in vivo*. The loss of drug over this initial 24 hour period can be over 50% of the total loaded drug (O'Donnell and McGinity, 1997). With certain therapeutics, this may be a distinct disadvantage in terms of efficient use of therapeutic and a desirable release profile. It is hypothesized that the immediate release of drug is due to protein either associated with the surface of the particle or situated in pockets close to the surface and easily accessible once the particle is hydrated.

Strategies to reduce the large initial burst include decreasing the drug loadings within the microspheres, decreasing the porosity of the microspheres, improving the distribution of drug within the continuous organic phase, and including excipients within the drug formulation (O'Donnell and McGinity, 1997).

In the DE process, the distribution of protein within the particles is caused by homogenization and/or sonication of the aqueous phase within the organic phase. Because the emulsion is created by physical mixing, the distribution of protein within the particles is heterogeneous. One hypothesis is that homogeneous mixing between protein and polymer will result in better encapsulated protein and lower initial burst. To study this, microspheres were made using a spontaneous emulsification (SE) solvent diffusion technique similar to that

previously reported by Niwa *et al.* for preparation of nanospheres (Niwa, Takeuchi *et al.* 1993). This process utilizes a single-phase solvent system in which both protein and polymer are soluble. It avoids the need for high energy mixing as the polymer particles form spontaneously, and it also avoids formation of a water/organic solvent interface. This may aid in improving protein stability as it is at the aqueous/organic interface that many proteins become denatured (Tabata, Gutta *et al.,* 1993; Lu and Park, 1995; Schwendeman, Costantino *et al.,* 1996; Krishnamurthy, 1997, Sah, 1999).

The SE method is a process where a single-phase solution, in which both polymer and drug are dissolved, is added to a larger volume of aqueous poly(vinyl alcohol) (PVA) solution thus forming particles instantaneously. The single-phase solvent consists of an organic solvent, water, and a co-solvent that is miscible with both the organic solvent and water. Addition of the single-phase solution of polymer and drug to a larger aqueous volume causes the co-solvent to rapidly diffuse out into the PVA solution. This decreases the surface tension at the interface between the organic solvent and water thus causing the organic solution to form fine droplets. The resultant solvent droplets contain both polymer and drug. The organic solvent is extracted into the aqueous bath and evaporates while water partitions in the polymer-rich phase resulting in phase inversion, and the spheres harden.

Currently, the published methods for fabrication of SE particles describe procedures for encapsulating small molecules, DNA, or peptides within nanospheres (Niwa, Takeuchi *et al.,* 1993; Niwa, Takeuchi *et al.,* 1994; Wehrle, Magenheim *et al.,* 1995; Quintanar-Guerrero,

Allemann *et al.,* 1998; Murakami, Kobayashi *et al.,* 1999; Mueller, Hirosue *et al.*, 2000), and one indicates conditions to achieve micron-sized particles (Murakami, Kobayashi *et al.,* 1999). Studies show the effects of processing factors such as polymer concentration, solvent choice, and drug solubilities on the size of and drug loadings within the nanoparticles. There are, however, inherent difficulties in working with nanoparticles. Because of the large surface area to volume ratio, the burst is usually high, drug loadings are often low and polymer degradation occurs more rapidly. The smaller particles are difficult to recover and tend to aggregate.

Here, the focus is to encapsulate large, hydrophilic proteins within micron-sized particles. Recombinant methionyl human Glial-cell line derived neurotrophic factor (r-met-HuGdNF), BSA, and lysozyme will be tested within this system. Bovine serum albumin (BSA) and lysozyme will serve as model proteins for r-met-HuGdNF. R-met-HuGdNF is a neurotrophic growth factor that has shown potential efficacy in treating disease states such as Parkinson's disease, amyotrophic lateral sclerosis, and retinal degeneration (Lapchak, 1996). A controlled release formulation of r-met-HuGdNF could greatly enhance the effectiveness of therapy by providing local and continuous delivery.

There are several advantages for using the SE method for encapsulation. As the protein is soluble in the same phase as the polymer, homogeneous distribution of protein within the microspheres is expected. This may lead to a minimal initial burst of protein upon hydration of the particles and release which is closely tied with polymer degradation. In scaling up for manufacturing, there should be few problems since the process is driven by thermodynamics

(Niwa, Takeuchi *et al.*, 1994; Mueller, Hirosue *et al.,* 2000). There is also the added possibility of designing a continuous manufacturing scheme as opposed to one that is a batch process.

3.2. Glial cell line–derived neurotrophic factor (GdNF)

GdNF is a member of the transforming growth factor beta superfamily, and like other members of that family it exists naturally as a disulfide-bonded dimer (30,384 MW) (Figure 3-1). In the nervous system, GdNF functions as a neurotrophic factor for both dopaminergic and motor neurons. However, GdNF is widely distributed and found in many tissues outside the nervous system including the kidney, bone, lung, and gastrointestinal organs. This suggests that GdNF functions as a multifunctional cytokine (Unsicker, 1996).

Exogenous r-met-HuGdNF, when injected into rats through the intramuscular route at a dose of 5 mg/kg/day, have shown an extremely short half-life. After 24 hours, serum levels of r-met-HuGdNF is below detection as measured by a standard immunoassay (Burke, 1998).

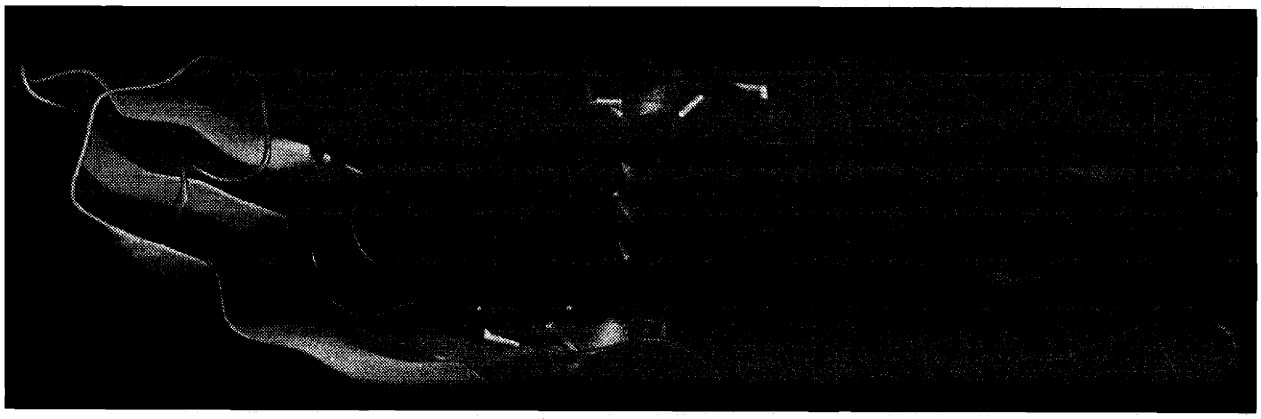

Figure 3-1. Three dimensional ribbon structure of GdNF. Protein is represented as disulfide-bonded dimer.

3.3. Protein:surfactant complexes

The area of proteins suspended in non-aqueous environments has been well studied, and many enzymes have been shown to maintain activity when suspended in organic solvents (Klibanov, 1997) . Efforts have also been made to solubilize enzymes within organic solvents. Two approaches include chemical modification and the use of surfactants either as complexing agents or reversed micelles. Chemical modification often leads to protein inactivation and the use of reversed micelles still maintains a high water content within the system. However, at low surfactant concentrations below the critical micelle concentration, proteins can be extracted from aqueous solution into organic solvents by ion pairing a surfactant with protein (Matsuura, Powers *et al.* 1993; Paradkar and Dordick, 1994). These complexes have been shown to have activity within the organic solvent (Paradkar and Dordick, 1994) and maintain secondary structure (Matsuura, Powers *et al.* 1993). Moreover protein extracted from the organic solvent back into aqueous phase maintains activity (Bromberg and Klibanov, 1994) and structure (Matsuura, Powers *et al.* 1993) similar to that of native protein.

It is thought that at low concentrations the surfactant forms a complex with the protein where the charged portion points towards the protein while the hydrophobic tail points out towards the solvent, somewhat like a micelle, which renders the complex hydrophobic (Paradkar and Dordick, 1994). Due to the hydrophobic nature of these complexes, a natural application would be for delivery of proteins across the intestinal wall as these complexes can pass through cell membranes (Lione-Bay, Ho *et al.* 1996; New and Kirby, 1997; Milstein, Leipold *et al.*,

1998). Similarly, this technique may be applied to the delivery of proteins and peptides to the brain across the blood-brain barrier.

3.4. Materials and Methods

3.4.1 Materials

Chicken egg-white lysozyme (95% purity) and BSA were purchased from Sigma (St. Louis, MO). R-met-HuGdNF was manufactured at Amgen, Inc. PLGA 50:50, RG502 and RG502H, were purchased from Boehringer Ingelheim (Montvale, NJ). PVA (88% hydrolyzed, 25,000 Da) was obtained from Polysciences (Warrington, PA). The Lowry protein assay kit was purchased from Bio-Rad Laboratories (Hercules, CA), the BCA assay kit from Pierce (Rockford, IL), and the CBQCA assay kit and Oregon green fluorescent labeling kit were from Molecular Probes (Eugene, OR). Monoclonal anti-r-met-HuGdNF antibody and biotinylated goat polyclonal anti-r-met-HuGdNF were purchased from R&D Systems (Minneapolis, MN). All other chemicals were of reagent grade.

3.4.2 Preparation of microspheres by DE

Protein microspheres were prepared by a double-emulsion technique (Cohen, Yoshioka *et al.,* 1991). To 250 μL of aqueous 1 mM r-met-HuGdNF solution was added a 7-mL solution of 29 mg/mL PLGA in methylene chloride, and the mixture was sonicated on ice for 10 s with a Vibracell (Danbury, CT) sonicator using a microtip probe with an output of 3 and 50% duty.

This primary emulsion was then added to a 100-mL aqueous solution of 1% (w/v) poly(vinyl alcohol). The second emulsion was formed by homogenization for 1 min at 3,000 rpm on a Silverson (East Longmeadow, MA) homogenizer using a 5/8" micro-mixing assembly with a general-purpose disintegrating head. The resultant water-in-oil-in-water (w/o)/w emulsion was stirred continuously for 3 h for solvent evaporation. The hardened microspheres were centrifuged, washed 3 times with water, freeze-dried, and stored under dessicant at -20°C.

3.4.3 Preparation of microspheres by SE

Protein microspheres were prepared by a technique as reported by Niwa *et al.* (Niwa, Takeuchi *et al.,* 1993) with modification. As the Niwa *et al.* procedure described preparation of nanospheres, modifications were required to fabricate larger, micron-sized particles and optimal conditions are given below. A mixture of co-solvent and organic solvent was added to the polymer and then the aqueous protein was added. This mixture was vortexed and then poured into a larger volume of a PVA solution. The resultant mixture was stirred continuously for solvent evaporation. The hardened microspheres were then centrifuged, washed 3 times with water, freeze-dried, and stored under dessicant at -20°C.

Optimal conditions for manufacturing the r-met-HuGdNF microspheres are given in the following protocol: addition of 150 μL of r-met-HuGdNF:surfactant complex (1:30 (mol:mol)) to a solution of 100 mg polymer dissolved in 2.5 mL of single-phase solvent (1:4 methylene

chloride:trifluoroethanol (TFE)). After mixing, this mixture was added directly to 100 mL of 5% chilled PVA, stirred, washed, and freeze-dried.

3.4.4 Protein loading

Ten mg of dried microspheres were dissolved in 0.1N NaOH/0.5% SDS (3 mL) overnight at 37°C. Protein content was then determined using the Lowry assay.

3.4.5 Protein release studies

Ten mg of dried microspheres were suspended, in triplicate, in round-bottom, 1.8-mL cryovials containing 1 mL of 10 mM citrate, pH 5.0. Sample tubes were incubated at 37°C with rotation on a Labquake shaker/rotator. To sample the released protein, tubes were centrifuged and the supernatant was removed and frozen at -80°C. The sample tubes were replenished with buffer, vortexed to resuspend the microspheres, and placed back in the incubator. Protein concentrations were determined using either the BCA or CBQCA assay.

3.4.6 Particle size determination

Average particle diameter was measured using a Beckman-Coulter Counter Multisizer II (Miami, FL). A 100 μm orifice was used and at least 50,000 particles were counted for each sample.

3.4.7 Protein partitioning into organic and single-phase solvent systems

Protein partitioning experiments were conducted following an approach similar to that reported by Bromberg and Klibanov (Bromberg and Klibanov, 1994). One mL of organic solvent was first added to each 18 x 100 mm glass test tube. An equal volume of protein solution or protein and surfactant mixture (final protein concentration of 1 mM) was then added to the test tube, and the tube was capped, and vortexed. The mixture was then incubated at room temperature overnight to allow partitioning to reach equilibrium. One-half mL of the organic phase was removed, placed in a clean test tube and placed under vacuum to evaporate to dryness. Two hundred fifty μL of 0.1 N HCl was added to the tube, and the tube was placed in a sonicating water bath for 30 s. BCA assay was then performed on the solution to determine protein content.

3.4.8 R-met-HuGdNF:surfactant solubility in single-phase solvent system

One hundred μL of a 1 mM r-met-HuGdNF solution or r-met-HuGdNF (1mM):surfactant complex mixture was added to 2.5 mL of the single phase solvent system (1:4 methylene chloride:TFE) and vortexed. Turbidity measurements (OD 600 nm) were then taken.

3.4.9 Scanning electron microscopy (SEM)

Scanning electron micrographs were obtained using a JEOL JSM-6320 FV microscope at 0.8 kV. Microspheres were mounted in the powder form and were not coated.

3.4.10 Confocal microscopy

Microspheres containing either FITC-BSA or r-met-HuGdNF labeled with Oregon green were imaged using a Bio-Rad MRC 1200 confocal microscope with an excitation wavelength of 488 nm and emission wavelength of 522 nm.

3.4.11 *In vivo* release

As the rat is frequently used in pharmacokinetic and drug metabolism studies as a representative of a rodent species, male Sprague-Dawley rats of age 40-60 days and approximately 230 g were selected. Fifteen rats were separated into three groups of 5 and were injected either (a) daily with soluble r-met-HuGdNF, (b) once on day 0 with r-met-HuGdNF microspheres made by DE, or (c) once on day 0 with r-met-HuGdNF microspheres made by SE. Prior to injection, 0.45 mL of blood was obtained from the tail vein and subsequently, blood samples were obtained at 1 hr, 2hr, 4 hr, 8 hr, 12 hr post day 0 injection and then daily for 13 days (prior to the daily injection). All blood samples were kept at room temperature for approximately 30 minutes following sampling. Blood samples were then centrifuged at 11,500 rpm for 10 minutes at 2-8°C. The separated plasma was stored in fresh vials at –80°C until assayed.

3.4.12 Enzyme-linked immunoassay (ELISA)

Standard sandwich ELISAs were performed. Ninety-six well plates were coated with monoclonal anti-r-met-HuGdNF antibody (3 μg/mL) and blocked with 2% BSA blocking buffer. Following sample addition, biotinylated goat polyclonal anti-r-met-HuGdNF was added. After incubation, strepavidin-horse radish peroxidase was added followed by ABTS substrate. Optical density was then measured at 405 and 490 nm for a dual wavelength kinetic reading. r-met-HuGDNF concentrations and coefficient of variation were calculated for each unknown sample from a 5-parameter curve fit of the plate standard dilutions. Standards ranged from 31.3 pg/ml to 2000 pg/ml. The monoclonal anti-r-met-HuGdNF antibody detects full-length as well as cleaved or shorter length r-met-HuGdNF.

3.5. Results and Discussion

As most of the SE methods previously described created nano-sized particles, initial experiments focussed on defining the critical parameters that would give larger, micron-sized particles. Several sets of experiments were then conducted to better understand the processing factors important for controlling the size of and the protein loading within the microspheres. The parameters that were considered are included in Table 3-1.

Table 3-1. Parameters of SE method examined

Polymer concentration	PVA concentration
Polymer	PVA solution volume
Organic solvent volume	Aqueous volume
Organic solvent	Protein concentration
Co-solvent volume	Stir rate
Co-solvent	Stir time

3.5.1 Particle size and size distribution

The factors that had the largest affect on size were the choice of organic solvent, the choice and volume of co-solvent, and the PVA concentration of the aqueous external phase. As can be seen from Figure 3-2, the trend tends towards smaller particles with increasing co-solvent volume, and this effect is independent of the type of organic solvent used. These findings agree with to those found by Wehrle *et al* (Wehrle, Magenheim *et al.*, 1995). They concluded that the mean particle size depends strongly on co-solvent volume with other factors having little effect. While the choice of co-solvent has an effect on particle size, the solubility of the protein in the single-phase system was the main criterion for selection of co-solvent. Solvent choice also affects the size of the particles. Chloroform yielded the largest particles followed by methylene chloride and then ethyl acetate.

One study showed the effects of PVA grade on nanoparticle recovery yield and nanoparticle characteristics (such as redispersibility) (Murakami, Kawashima *et al.*, 1997). In addition, they showed that increased PVA concentration yielded larger particles due to the increased viscosity of the aqueous medium. Here, the data support that finding. By increasing the PVA concentration 5-fold, average particle size doubled.

The particle size distribution for the SE microspheres were comparable to those made by DE (Figure 3-3). Unlike the DE particles, the distribution of the SE particles was slightly skewed as small nanoparticles are formed during fabrication.

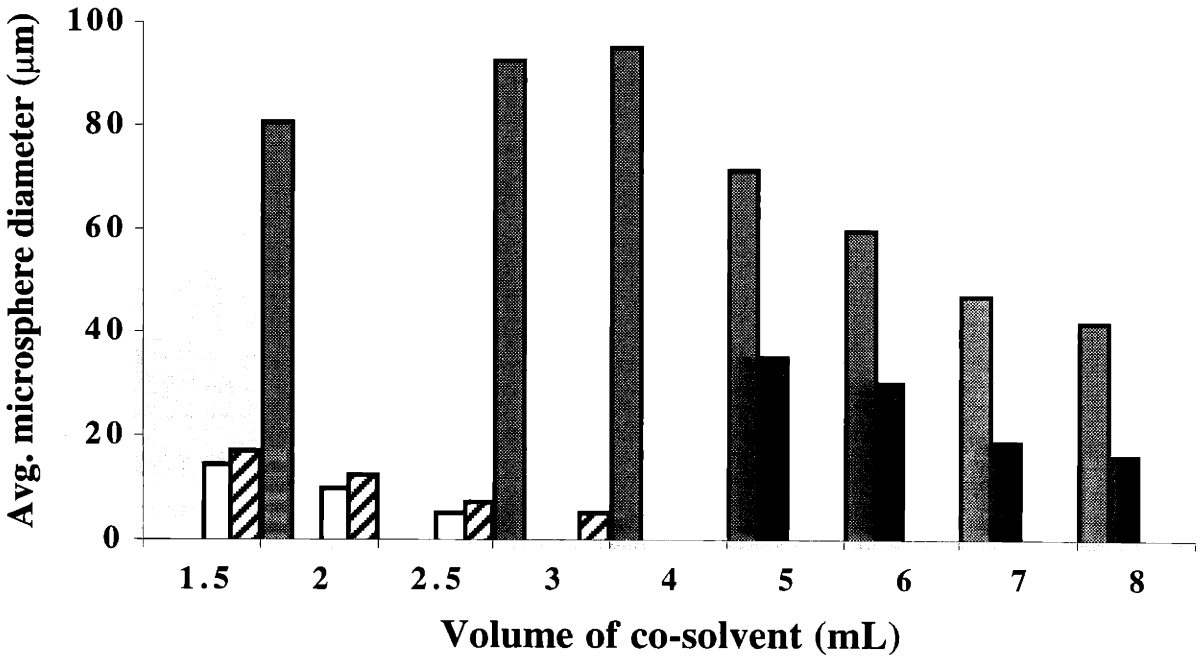

Figure 3-2. The effect of processing parameters - co-solvent and solvent volume – on microsphere diameter. ■ - methylene chloride and acetone co-solvent, ▩ - chloroform and acetone co-solvent, □ - ethyl acetate and acetone co-solvent, ▨ -methylene chloride and TFE co-solvent. All other conditions were kept constant and include: 100 mg of polymer, 0.5 mL of organic solvent, 100 μL aqueous solution, 100 mL 5% PVA external aqueous phase.

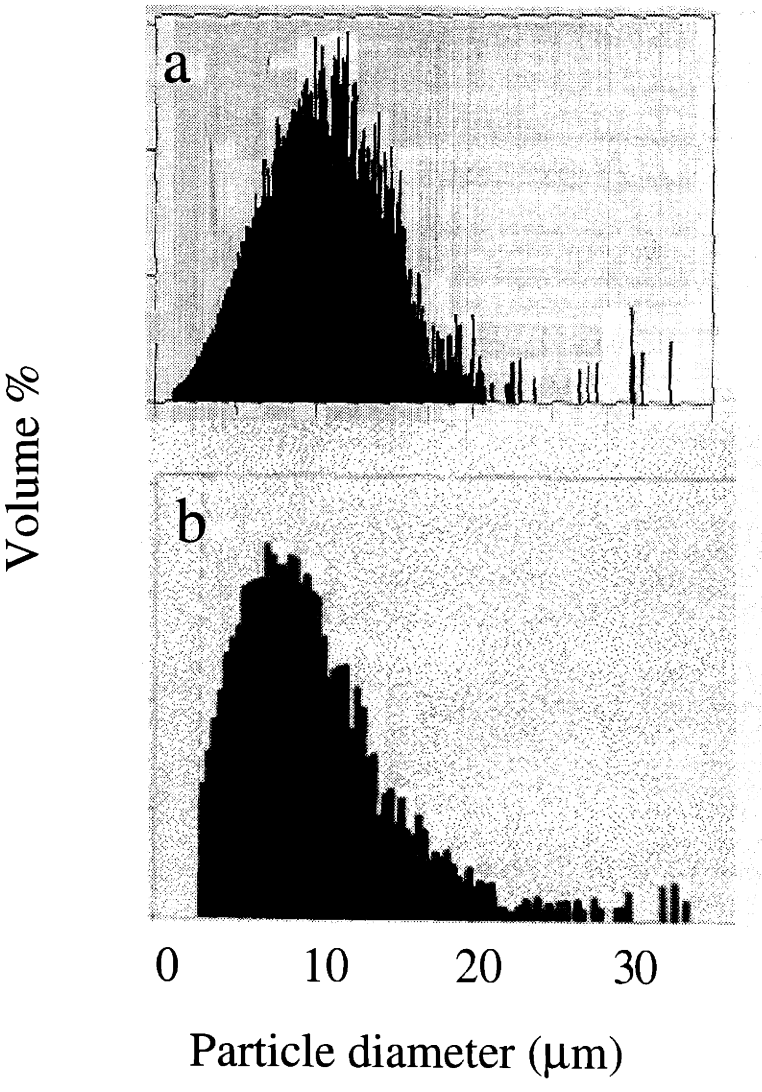

Figure 3-3. Size distribution of particles made by a) DE and b) SE. Average mean diameter of the DE microspheres is 12 μm and of the SE microspheres is 15 μm.

3.5.2 Protein loading without the presence of surfactant

Protein loading within the SE microspheres varied between proteins and varied as a function of processing parameters. The processing parameters that had the largest effect on loading included the choice of polymer and the choice of co-solvent.

Microsphere loading was higher when lysozyme was used as opposed to r-met-HuGdNF. The difference in loading was due to differences in protein solubility within the single-phase solvent system. Addition of lysozyme to the solvent mixture yielded a clear solution, but addition of an equimolar concentration of r-met-HuGdNF to the solvent mixture gave a hazy or cloudy mixture. Others have shown increased drug loading by increasing the solubility of the drug in the organic phase. For insulin, the PLGA was exposed to sodium hydroxide to enhance the ionic interaction between protein and polymer (Kawashima, Yamamoto *et al.,* 1999). For nafarelin acetate, PLGA with a free end hydroxyl was first complexed with the drug creating a hydrophobic drug/polymer complex that is more soluble in the single-phase solution (Niwa, *et al.,* 1994). By applying this approach and using PLGA with a free end hydroxyl, loading of r-met-HuGdNF was increased from 0.27 ± 0.06% to 2.6 ± 0.3%.

As solubility of protein in the singe-phase solvent system was critical, the criteria for co-solvent selection included the ability to solubilize protein and miscibility with the organic solvent. As r-met-HuGdNF was not soluble in acetone, dioxane and TFE were examined. While dioxane was able to dissolve the protein, dioxane was not miscible with the organic solvents

tested. However by switching from acetone to TFE, the protein loading was increased from 2.6 ± 0.3% to 4.7 ± 0.7%.

3.5.3 Minimization of burst

Solubility of the protein in the single-phase solution is important for maintaining high loadings, high encapsulation efficiencies, and also contributes to better distribution of protein within the polymer microspheres. To achieve the improved distribution and thus minimze the burst effect, the protein was first complexed with a charged surfactant before encapsulation. Here, solubility of lysozyme and r-met-HuGdNF into organic solvents and the single-phase system were improved upon complexation with a charged surfactant. (For other attempted strategies, see Appendix A.)

As r-met-HuGdNF, and lysozyme have high isoelectric points (10.5 and 11.0, respectively) and are positively charged in the buffer system selected, negatively charged surfactants were tested. The surfactants selected were relatively non-toxic and varied in charge group and hydrophobicity. Results of lysozyme partitioning experiments are shown in Figure 3-4. Because lysozyme has an overall charge of +10 in the selected buffer system (10 mM citrate, pH 4.5), the ratio of protein:surfactant tested was 1:10 (mol:mol). These data indicate that both the surfactant charge group and hydrophobicity and the overall charge of the protein affect the partitioning of protein. For lysozyme, a sulfonate head is more effective than a carbonate head likely due to a stronger interaction between surfactant and protein. Hydrophobicity results are

similar to those obtained by others (Bromberg and Klibanov, 1994) where a longer hydrophobic tail is more effective. Here, the data indicate that surfactants with two hydrophobic chains are more effective than surfactants with one. Overall, the solubility of lysozyme in organic solvent can be increased by a factor of 10 when it is complexed with a surfactant.

The effect of protein:surfactant complexes partitioning into different organic solvents was also explored (Figure 3-5). Interestingly, under equivalent conditions, more protein partitioned into chloroform than into methylene chloride. While a higher protein concentration in the organic phase is ideal, chloroform was not selected as the solvent due to its limitations for microsphere fabrication (Section 3.5.1). Microspheres of the desired size range could not be produced by SE with chloroform as the organic solvent. Mixtures of solvents were also tested and little to no protein was detected in methanol and mixtures of 1:1 chloroform:methanol (vol:vol), and 1:1 chloroform:ethanol (vol:vol).

While the solubility of r-met-HuGdNF in organic solvents was not significantly improved upon complexation with surfactants (data not shown), the solubility within a single-phase solvent system was affected. Figure 3-6 shows the decrease in turbidity or increase in solubility of r-met-HuGdNF in the single-phase solution upon addition of a surfactant.

Using the optimal conditions, microspheres were made with the SE method. R-met-HuGdNF was first complexed with aerosol OT (AOT) at a ratio of 1:30 (mol:mol), surfactant:protein, and encapsulated within PLGA microspheres. These particles were compared with those made without surfactant to determine which formulation yielded a lower *in vitro*

burst. Microspheres containing r-met-HuGdNF gave a 2 h burst value of 1.7% of total loaded protein while r-met-HuGdNF complexed with AOT yielded a 2 h burst of 0.4% of total protein loaded.

It is hypothesized that the differing results between lysozyme and r-met-HuGdNF arise due to inherent differences between the protein sequence. The surface hydrophobicity of the proteins may play an important role in determining the partitioning into organic solvents. However, this value was calculated and compared between r-met-HuGdNF, lysozyme, insulin, and BSA. Lysozyme, insulin, and BSA complexed with ionic surfactants have been shown to partition into methylene chloride (Bromberg and Klibanov, 1994); calculated values of surface hydrophobicity did not indicate any correlation with higher partitioning. The hypothesis for the mechanism of action of the charged surfactants is to partially unfold the protein. By this reasoning, it seems that the partition coefficient should then correlate with the total hydrophobicity of a protein sequence. Calculated in this manner, r-met-HuGdNF has fewer hydrophobic residues relative to total residues than lysozyme, insulin, and BSA.

3.5.4 Powder property and morphology

As shown with PLGA nanospheres made by SE, the powder properties of the microparticles are excellent. Microspheres reconstituted to 200 mg/mL in 10% saline passed easily through a 20.5-gauge, syringe needle. From SEM, the particles are smooth, spherical, and do not show indication of aggregation (Figure 3-7a). The internal structure of the larger

microspheres is porous (Figure 3-7b), while the smaller particles are less porous. As discussed, the porous internal architecture may be caused by phase separation between the co-solvent and solvent.

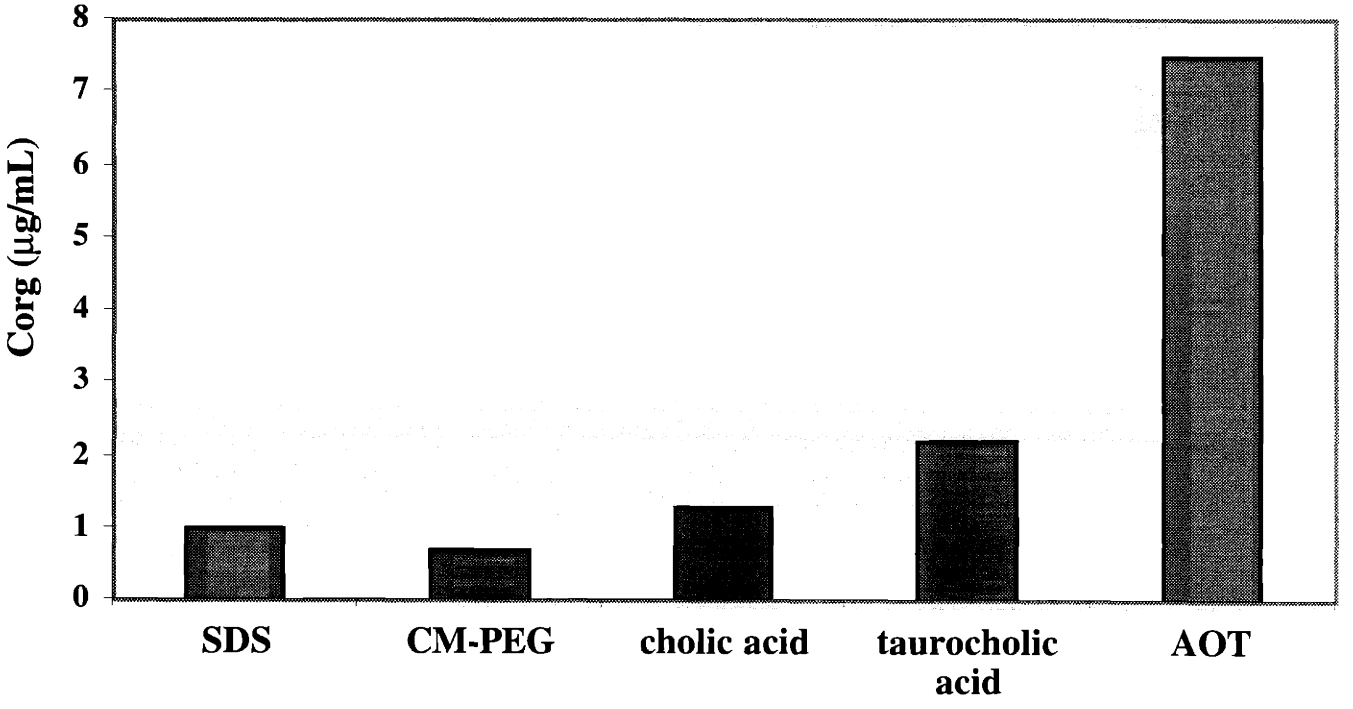

Figure 3-4. Partitioning of lysozyme:surfactant 1:10 (mol:mol) complex into methylene chloride. Surfactants tested include sodium dodecyl sulfate (SDS), carboxymethyl poly(ethylene glycol) (CM-PEG), cholic acid, taurocholic acid, and AOT. Corg represents the concentration of protein detected in the organic phase. Lysozyme concentration was 1 mM and the buffer used was 10 mM citrate, pH 4.5.

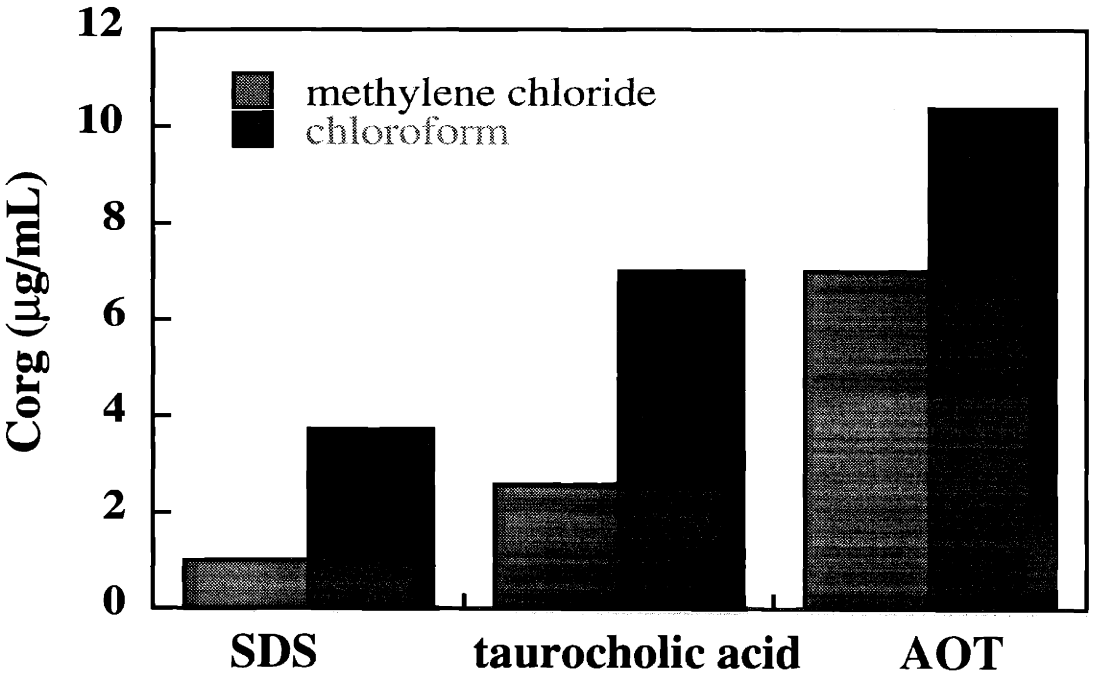

Figure 3-5. Partitioning of lysozyme:surfactant 1:10 (mol:mol) complex into organic solvents. Corg represents the concentration of protein detected in the organic phase. Lysozyme concentration was 1 mM and the buffer used was 10 mM citrate, pH 4.5.

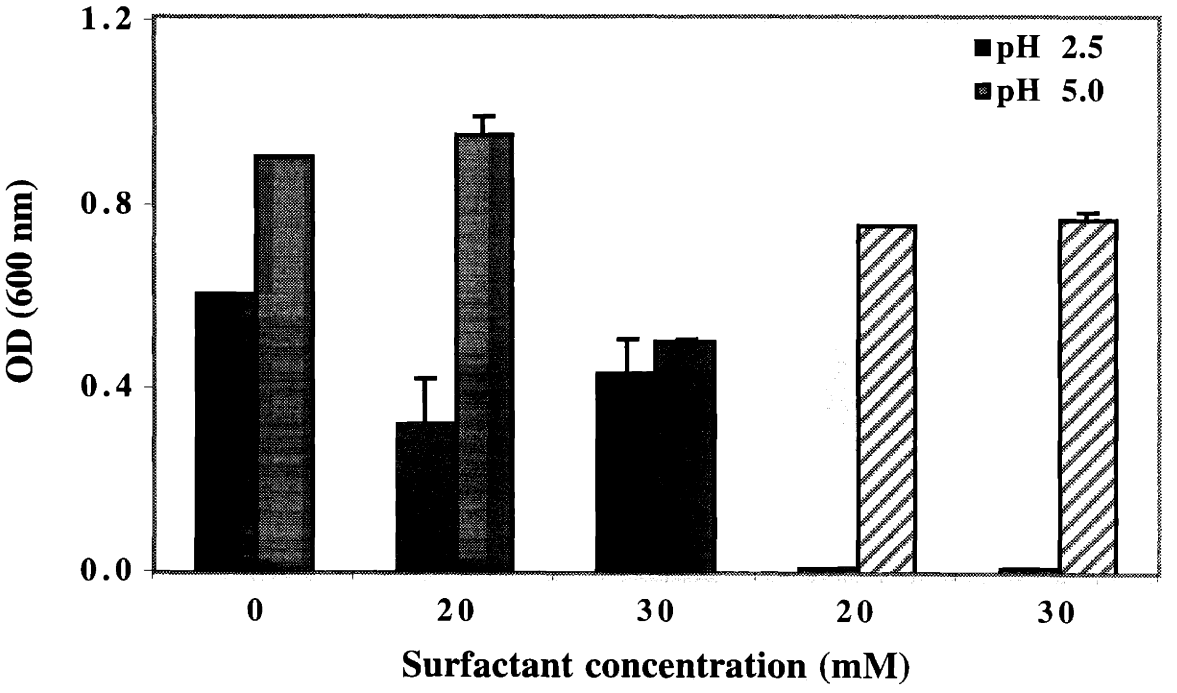

Figure 3-6. Solubility of r-met-HuGdNF:surfactant complex in single-phase solution of 0.5 mL methylene chloride and 2 mL TFE. An increase in turbidity or optical density (OD) indicates a lack of solubility. Solid bars represent r-met-HuGdNF (1 mM) complexed with SDS and hashed bars represent r-met-HuGdNF (1 mM) complexed with AOT.

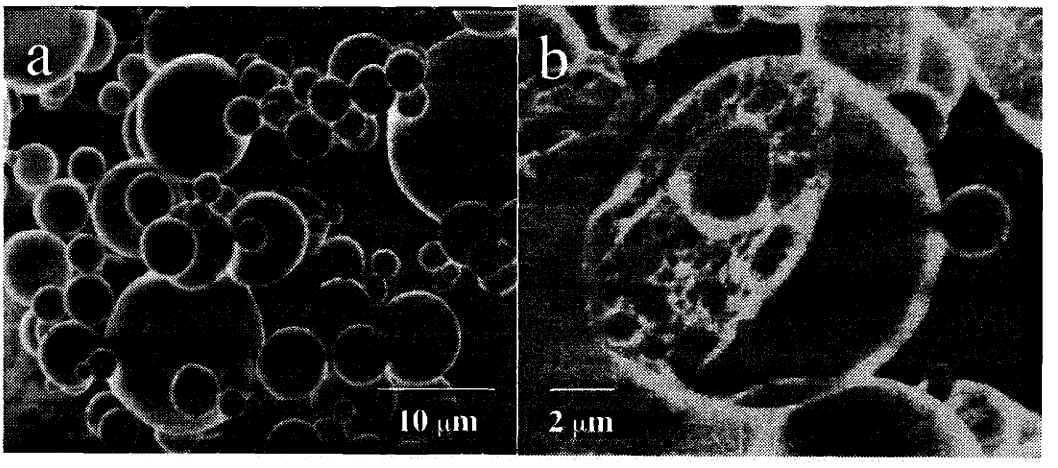

Figure 3-7. Scanning electron micrographs of microspheres made by SE. a) Distribution of microspheres - magnification 2500x, b) Fractured microsphere - magnification 6000x.

3.5.5 Process scale-up

The SE process was simple to scale. By maintaining equivalent microenvironment conditions, the microparticles formed at a scale of 40x were similar (in size and protein loading) to those formed on the 1x scale (See Table 3-2). The scalability and ease of manufacturing of this process makes it an attractive alternative to a DE technique.

3.5.6 Stability of R-met-HuGdNF at 37°C as determined by ELISA

The stability of the protein under physiologic temperatures was studied by incubating r-met-HuGdNF in 10 mM citrate, pH 5.0 at 37°C for over 40 days. A measure of stability was estimated by the recognition of r-met-HuGdNF by a monoclonal antibody. Samples were analyzed by ELISA, and results showed good relative stability (93.7 ± 9.2%) with a slight decrease at days 4 and 40 (79.6% and 86.2%, respectively). While this indicates that elevated temperature may not affect r-met-HuGdNF stability, it does not speak to r-met-HuGdNF stability in biological fluid. This may be a cause of protein inactivation or unfolding as r-met-HuGdNF is not stable in phosphate buffer systems (Burke, 1998).

Table 3-2. Scale-up of SE method of encapsulating r-met-HuGdNF within PLGA

Scale	Mass of polymer (g)	Mean diameter of sphere (μm)	Protein load (%) (w/w)
1	0.1	14.1	3.9
10	1	14.6	4.1
40	4	14.4	4.0

3.5.7 *In vitro* release

Direct comparison was made between microspheres made by a standard DE and the SE techniques. The microspheres had equal loading of 4% (w/w) and were approximately the same size; the DE microspheres had an average diameter of 17.7 ± 2.7 μm and the SE microspheres had an average diameter of 14.1 ± 2.6 μm. *In vitro* release experiments showed sustained release of r-met-HuGdNF for over 40 days (Figure 3-8). The SE spheres had a small to negligible initial burst of protein release with three phases of constant rate release. The first phase was from day 0 – 15, the second was from day 15 – 30 and the final phase from day 30 - 40. While within each phase, the release of protein was zero order, there was a burst of protein release between each phase. In addition, the rate of release within each phase differed. The DE spheres showed zero order release over the first 30 days, however, there was a large initial burst of over 25% of the r-met-HuGdNF loaded. Over 55 days of release, the DE microspheres released over 90% of the encapsulated r-met-HuGdNF and the SE microspheres released over 50%.

An initial burst of protein, which can range from 10-90% depending on the drug and carrier formulation, is commonly seen with processing techniques including DE. Nanoparticles made by SE can also result in a large initial burst (Kawashima, Yamamoto *et al.*, 1999). The small burst observed in the SE spheres is hypothesized to be due to the homogeneous mixing of polymer and protein within the single-phase solution. As opposed to the DE process where polymer and protein are mixed together physically, the SE process allows coexistence of both species in one solution. Confocal images of microspheres containing fluorescently labeled r-

met-HuGdNF or FITC-BSA indicated even distribution of protein throughout the microspheres (Figure 3-9).

An estimate of the functional protein released was determined by ELISA. This was compared to the actual amount of protein detected via a standard protein assay (Figure 3-10). In comparing the microsphere formulations, there were losses in protein function in both cases. Neither formulation was able to achieve release of fully functional protein. While the SE formulation did not release more stable protein than the DE formulation, the losses in protein function were of the same order of magnitude.

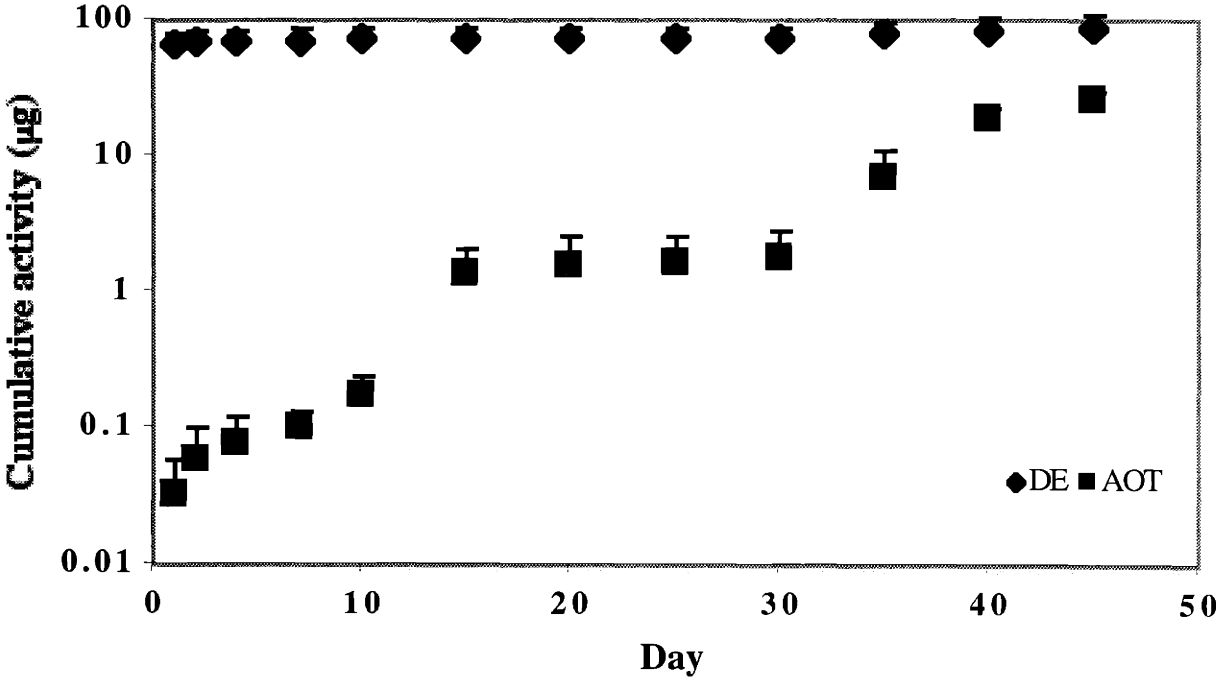

Figure 3-8. *In vitro* release of r-met-HuGdNF from the DE and SE microsphere formulations. Results are shown as cumulative release as determined by ELISA.

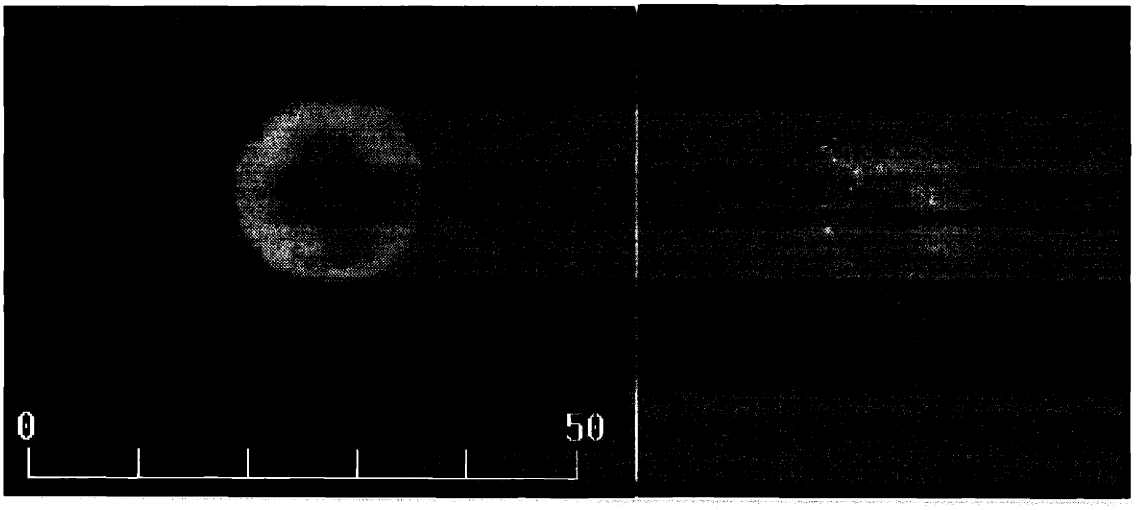

Figure 3-9. Fluorescent confocal microscopy image of SE microsphere containing a) FITC-BSA:AOT and b) Oregon green-r-met-HuGdNF:AOT. Due to inefficient modification of r-met-HuGdNF with the fluorescent tag, the distribution of protein throughout the particle does not appear as constant.

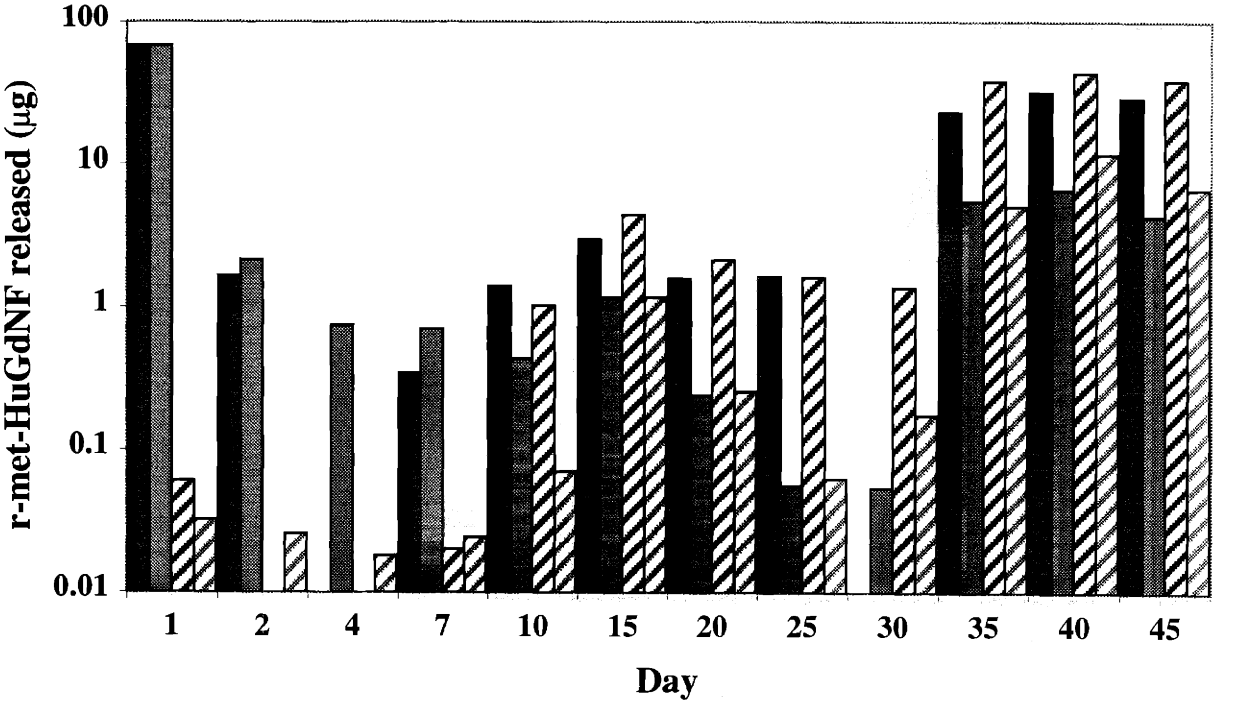

Figure 3-10. Daily release of r-met-HuGdNF from DE and SE microspheres under *in vitro* conditions. The filled bars represent r-met-HuGdNF released from DE microspheres - ■ as determined by a protein assay and ■ as determined by ELISA. The hashed bars represent r-met-HuGdNF released from SE microspheres - ▨ as determined by a protein assay and ▨ as determined by ELISA.

3.5.8 *In vivo* efficacy

Both DE and SE microspheres containing r-met-HuGdNF were tested in rats to confirm that the release profiles observed *in vitro* translated to *in vivo* conditions. Three groups of 5 animals each were tested. The first group was given daily injections of r-met-HuGdNF; this was performed to benchmark previous toxicology data and served as a positive control for the ELISA assay. A therapeutic concentration of r-met-HuGdNF has yet to be determined. The second group received one injection of r-met-HuGdNF encapsulated within PLGA microspheres made by DE, and the last group received a single injection of r-met-HuGdNF encapsulated within PLGA microspheres made by SE. The microspheres for both groups were fabricated under scaled-up conditions; the r-met-HuGdNF loading was 4% (w/w) and the average diameter of the particles were 14.6 ± 2.7 μm (DE) and 14.4 ± 1.9 μm (SE). The animals were bled daily and the samples were analyzed for r-met-HuGdNF by ELISA.

Over 14 days, r-met-HuGdNF release was detected continuously from both DE and SE microspheres (Figure 3-11). The DE microspheres exhibited a release profile of a large initial burst followed by sustained release. On the other hand, the SE microspheres had no initial burst and exhibited a sustained release over the course of the experiment. In addition, it appeared that both microsphere formulations were still releasing protein at the end of the 14-day experiment.

The SE microspheres had a significantly smaller initial burst as compared to the DE microspheres. Over the initial 24-hour period post injection, the burst from the DE microspheres

was 12-fold higher than the release from the SE microspheres. Thus, the trend observed *in vitro* was mimicked *in vivo*.

Although the microspheres were still releasing protein at 14 days, area under the curve (AUC) values were calculated as an estimate of bioavailability. Because the microspheres were not depleted of protein at day 14, it is likely the AUC calculations underestimated the true bioavailability of the formulations. As compared to daily r-met-HuGdNF injection, the AUC of the DE microspheres was 35% and the AUC of the SE microspheres was 13%.

The SE microspheres seemed to have a lag period where little to no release of protein occurred followed by release. This lapse of protein released may be explained by a lack of sufficient polymer degradation to give rise to protein release. In addition, the deviation of values in this early period of release was slightly high as the concentrations were at the limit of detection of the ELISA assay.

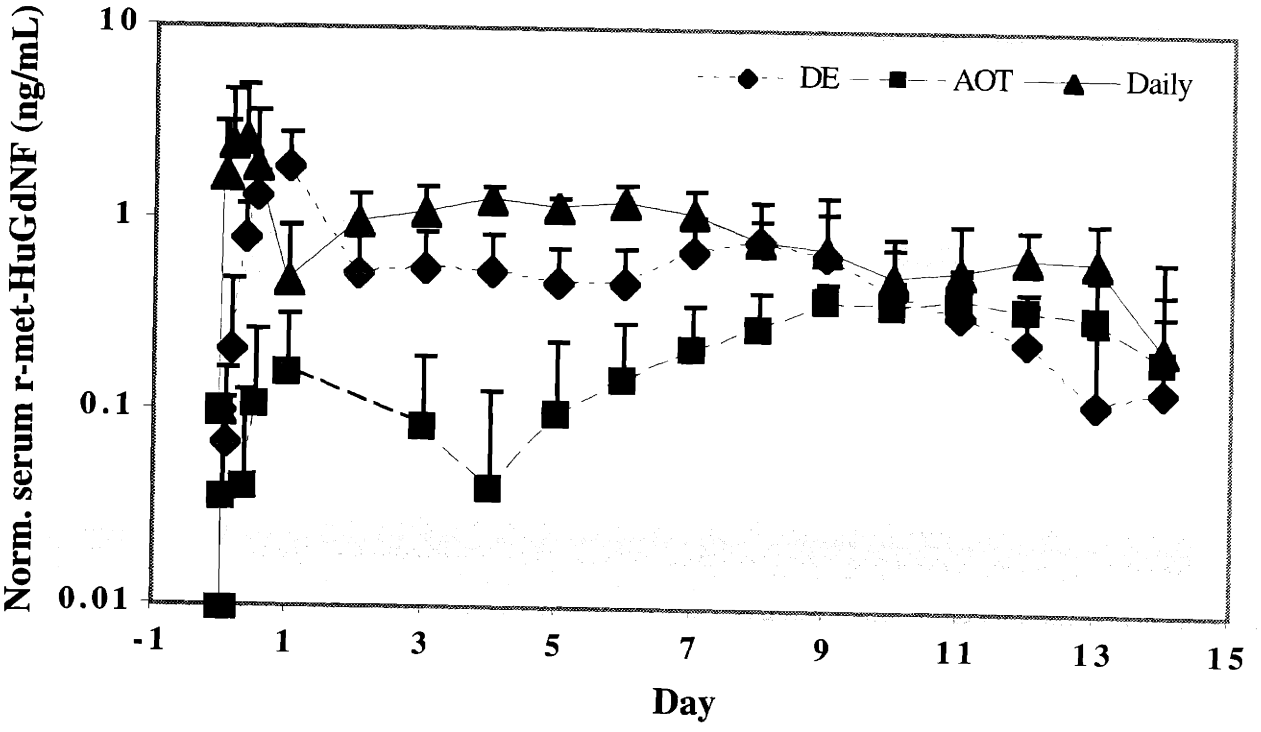

Figure 3-11. Serum r-met-HuGdNF present in rats dosed on a daily basis with r-met-HuGdNF in solution, dosed once with DE mi crospheres, or dosed once with SE microspheres.

3.6. Conclusions

PLGA microspheres containing r-met-HuGdNF were made with an optimized SE method. Several of the advantages of this method are 1) the dissolution of both polymer and drug in the same solvent system to yield a homogeneous distribution of drug within the polymer system, 2) the lack of high energy mixing in the process, and 3) the ease of process scale-up. Critical factors affecting microsphere size were identified and include the choice of organic solvent and the choice and volume of co-solvent. Drug loading, as expected, was greatly affected by the PVA concentration in the outer aqueous phase, the drug concentration in aqueous solution and the drug solubility in the single phase solvent. Enhanced drug solubility was achieved by increasing the drug hydrophobicity via complexation with charged surfactants.

The major objective was to solve the issue of the large and immediate loss of protein or burst from the microspheres upon hydration. By altering the fabrication method to obtain a more homogeneous protein distribution, the burst was eliminated as exemplified by in vitro and in vivo experiments. It is hypothesized that release of drug from the SE microspheres is closely linked with polymer degradation. Thus, there is a lag before protein is released.

Functional r-met-HuGdNF released was estimated by ELISA. While relative functionality could not be calculated for the *in vivo* results, the *in vitro* experiments indicated release of some functional protein. Although specific functionality of the protein released was not high and further improvements are required, these results represent a positive step towards solving the problem of protein loss through the initial burst.

3.7. References

Bromberg, L. E. and A. M. Klibanov, (1994). Detergent-enabled transport of proteins and nucleic acids through hydrophobic solvents. *Proc. Natl. Acad. Sci. USA* **91**: 143-147.

Burke, P. A., (1998). *Personal communication.*

Cohen, S., T. Yoshioka and R. Langer, (1991). Controlled delivery systems for proteins based on poly(lactic/glycolic acid) microspheres. *Pharm. Res.* **8(6):** 713-720.

Johnson, O. L., J. L. Cleland, H. J. Lee, M. Charnis, E. Duesnas, W. Jaworowicz, D. Shepard, A. Shahzamani, A. J. Jones and S. D. Putney, (1996). A month-long effect from a single injection of microencapsulated human growth hormone. *Nat. Med.* **2(7):** 795-799.

Kawashima, Y., H. Yamamoto, H. Takeuchi, S. Fujioka and T. Hino, (1999). Pulmonary delivery of insulin with nebulized DL-lactide/glycolide copolymer (PLGA) nanosheres to prolong hypoglycemic effect. *J. Cont. Rel.* **62**: 279-287.

Krishnamurthy, R. (1997). Denaturation of lysozyme during microencapsulation. Chemical and Biochemical Engineering. Baltimore, University of Baltimore County**:** 126.

Lapchak, P. A. (1996). Therapeutic potentials for glial cell line-derived neurotrophic factor (GdNF) based upon pharmacological activities in the CNF. *Rev. Neurosciences.* **7:** 165-176.

Lione-Bay, A., K.K. Ho, R. Agarwal, R.A. Baughman, K. Chaudhary, F. DeMorin, L. Genoble, C. McInnes, C. Lercara, S. Milstein, D. O'Toole, D. Sarubbi, B. Variano and D.R. Paton, (1996). 4-[4-[(2-Hydroxybenzoyl)amino]phenyl]butyric acid as a novel oral delivery agent for recombinant human growth hormone. *J. Med. Chem.* **39**: 2571-2578.

Lu, W. and T. G. Park (1995). Protein release from poly(lactic-co-glycolic acid) microspheres: protein stability problems. *J. Pharm. Sci. Technol.* **49**: 13-19.

Matsuura, J., M. E. Powers, M. C. Manning and E. Shefter, (1993). Structure and stability of insulin dissolved in 1-octanol. *J. Am. Chem. Soc.* **115(4)**: 1261-1264.

Milstein, S. J., H. Leipold, D. Sarubbi, A. Leone-Bay, G. M. Mlynek, J. R. Robinson, M. Kasimova and E. Freire, (1998). Partially unfolded proteins efficiently penetrate cell membranes - implications for oral drug delivery. *J. Cont. Rel.* 53: 259-267.

Mueller, B. G., S. Hirosue, T. L. Fernando, R. C. Mulligan, R. S. Langer, (2000). I. Novel solvent diffusion formulation for the formation of sub-100 nm spheres. *(in preparation).*

Murakami, H., Y. Kawashima, T. Niwa, H. Takeuchi and M. Kobayshi, (1997). Influence of the degrees of hydrolyzation and polymerization of poly(vinylalcohol) on the preparation and properties of poly(DL-lactide-co-glycolide) nanoparticle. *Int. J. Pharm.* **149**: 143-149.

Murakami, H., M. Kobayashi, H. Takeuchi and Y. Kawashima, (1999). Preparation of poly(DL-lactide-co-glycolide) nanoparticles by modified spontaneous emulsification solvent diffusion method. *Int. J. Pharm.* **187**: 143-152.

New, R. R. C. and C. J. Kirby, (1997). Solubilisation of hydrophilic drugs in oily formulations. *Adv. Drug Del. Rev.* **25**: 59-69.

Niwa, T., H. Takeuchi, T. Hino, N. Kunou and Y Kawashima, (1993). Preparations of biodegradable nanospheres of water-soluble and insoluble drugs with D,L-lactide/glycolide copolymer by a novel spontaneous emulsification solvent diffusion method, and the drug release behavior. *J. Cont. Rel.* **25**: 89-98.

Niwa, T., H. Takeuchi, T. Hino, N. Kunou and Y. Kawashima, (1994). In vitro drug release behavior of D,L-lactide/glycolide copolymer (PLGA) nanospheres with nafarelin acetate prepared by a novel spontaneous emulsification sovlent diffusion method. *J. Pharm. Sci.* **83(5):** 727-732.

O'Donnell, P. B. and J. W. McGinity, (1997). Preparation of microspheres by the solvent evaporation technique. *Adv. Drug Del. Rev.* **28**: 25-42.

Paradkar, V. M. and J. S. Dordick, (1994). Mechanism of extraction of chymotrypsin into isooctane at very low concentrations of Aerosol OT in the absence of reversed micelles. *Biotechnol. Bioeng.* **43**: 529-540.

Quintanar-Guerrero, D., E. Allemann, H. Fessi and E. Doelker, (1998). Preparation techniques and mechanisms of formation of biodegradable nanoparticles from preformed polymers. *Drug Develop. Indus. Pharm.* **24(12):** 1113-1128.

Sah, H., (1999). Protein behavior at the water/methylene chloride interface. *J. Pharm. Sci.* **88(12):** 1320-1325.

Schwendeman, S. P., H. R. Costantino, R. K. Gupta, M. Tobio, A. C. Chang, M. J. Alonso, G. R. Siber and R. Langer, (1996). Strategies for stabilizing tetanus toxoids toward the development of a single-dose tetanus vaccine. *Dev. Biol. Stand.* **87**: 293-306.

Tabata, Y., S. Gutta and R. Langer, (1993). Controlled Delivery Systems for Proteins Using Polyanhydride Microspheres. *Pharm. Res.* **10(4):** 487-496.

Unsicker, K. (1996). GdNF: a cytokine at the interface of TGF-betas and neurotrophins. *Cell Tissue Res.* **286:** 175-178.

Wehrle, P., B. Magenheim and S. Benita, (1995). The influence of process parameters on the PLA nanoparticle size distribution, evaluated by means of factorial design. *Eur. J. Pharm. Biopharm.* **41(1):** 19-26.

4. Elucidation of the environment inside the microsphere*

4.1. Introduction

Biodegradable polymer devices show great potential for a variety of therapeutic applications including controlled release of proteins and nucleic acids and polymer scaffolds for tissue engineering or cell-based therapies (Langer and Vacanti, 1993; Peppas and Langer, 1994; Langer, 1996; Mathiowitz, Jacob *et al.*, 1997). A serious obstacle, however, is the insufficient stability of the protein, nucleic acid, or cell when introduced into the environment of the polymer. Understanding the causes of this instability is crucial to successful development of these technologies and requires knowledge of the physico-chemical environment to which the entrapped therapeutic is exposed. For example, polymer degradation may result in a build-up of acidic by-products since many of the biodegradable polymers (polyesters, polyanhydrides, etc.) are made up of acidic monomers (Vert, Li *et al.*, 1991; Grizzi, Garreau *et al.*, 1995; Burke, 1996; Mader, Gallez *et al.*, 1996). As low-pH environments are known to be deleterious to some proteins and nucleic acids (Cleland, Powell *et al.*, 1993; Domb, Turovsky *et al.*, 1994; Middaugh, Evans *et al.*, 1998) and actually favorable to others (Liu, Langer *et al.*, 1991), the pH changes within these biodegradable devices are expected to be important. There has been evidence showing the influence of basic salts on the stability and release of proteins from delivery devices (Zhu and Schwendeman, 1998; Zhu and Schwendeman, 1999; Zhu, Maller, *et*

* Published in part in Fu, K., D. W. Pack, A. M. Klibanov, R. Langer, (2000). Visual evidence of acidic environment within degrading poly(lactic-co-glycolic acid) (PLGA) microspheres. *Pharm. Res.* **17(1):** 100-106.

al., 2000). Thus, quantifying the pH environment within the microspheres is critical for furthering our understanding of these delivery systems.

Several studies, using indirect methods, have shown the presence of an acidic environment within degrading polymer devices. For example, the degradation of PLGA tablets was shown to be faster on the inside of the tablet relative to the outside (Vert, Li *et al.*, 1991). Since the polymer degrades by hydrolysis and is acid-catalyzed, the conclusion was that a low-pH environment within the tablet caused the increased degradation rate. Others have used pH-sensitive dyes and confocal microscopy to measure the pH immediately surrounding degrading polyanyhydride tablets and have found it to be lower than that of the surrounding bulk media (Goepferich, 1996). Again, this was an indication of an acidic intrapolymer environment. Brange encapsulated bovine insulin, which is not stable in acidic conditions, within PLGA microspheres and released the protein under physiologic conditions (Brange, Langkjaer *et al.*, 1992). As there was little protein released from the spheres over 7 days, they concluded that there was an acidic environment within the microspheres which degraded the protein. Uchida *et al.* also analyzed insulin released from PLGA microspheres and found it to be characteristic of the protein which had been exposed to an acidic environment (Uchida, Yagi *et al.*, 1996). In addition, Shenderova *et al.* developed several methods to examine the pH within microspheres and films, and the conclusion in each case was that the microenvironment had a pH below 5 (Shenderova, Burke *et al.*, 1998; Shenderova, Burke *et al.*, 1999; Shenderova, Madou *et al.*, 1999).

There have also been efforts to use direct approaches to evaluate the pH within degrading polymer devices. In one study, microspheres incubated *in vitro* were dissolved in acetonitrile:water and the acidity of the organic phase was measured. Measurements were then correlated with the actual proton activity, and the microclimate pH was determined to be approximately 1.8 (Shenderova, Burke *et al.*, 1999). Encapsulation of fluorescein within the microsphere followed by confocal fluorescence microscopic imaging of the fluorescein emission intensity confirmed an acidic interior (Shenderova, Burke *et al.*, 1999). In another study, NMR was employed to examine PLGA microspheres incubated in sheep serum. Results showed an average pH of 6.4 within the population of the microspheres over the course of 45 days (Burke, 1996). EPR has also been used to examine PLGA tablets and microspheres. The tablets implanted subcutaneously in mice indicated an average pH of 2 to 4 after 6 days (Mader, Gallez *et al.*, 1996). Using the same technique to probe *in vitro* degradation of microspheres in phosphate buffered saline (PBS), pH 7.4, the pH dropped below 4.7 over the course of the experiment (Brunner, Maeder *et al.*, 1998; Brunner, Maeder *et al.*, 1999). The results of these studies differ from each other most likely because the systems examined were different - microspheres vs. tablets - as were the incubation conditions - *in vitro* vs. *in vivo*. However, in all these studies, the experimental techniques could only determine an average or bulk pH of a population of microspheres or throughout a device.

Although knowledge of an average pH of the system is useful, it is important to quantify the extremes of pH. A high average pH does not preclude the existence of pockets of high

acidity within the device. The range of pH environments and the amount of time in that environment which proteins can tolerate are different for every protein. Thus, to approach the problem of protein stability within a polymer system it is necessary to quantify the lowest pH environment within the device as well as the length of time that this environment exists. Herein, we observe for the first time the spatial distribution of pH changes within a population of polymeric microspheres over the course of their degradation (Fu, Pack *et al.*, 1998).

4.2. Confocal microscopy

Confocal microscopy offers advantages over conventional light and electron microscopy. First, confocal microscopy collects information from a well-defined optical section due to the shallow depth of field (0.5 – 1.5 μm). Because of this, fluorescence signal from a different focal plane is eliminated. Second, the confocal microscope optically sections specimens so that the physical sectioning artifacts are also eliminated. This sectioning can be done not only in the XY plane (perpendicular to the optical axis of the microscope) but also along the Z direction to capture information within the depth of a sample.

In confocal microscopy, the illumination of a sample is focused as a spot on one volume element of the sample at a time. Depending on the specific microscope design, this spot may be as small as 0.25 μm in diameter and 0.5 μm in depth. As the illumination beam diverges above

and below the plane of focus, volume elements away from the focal plane receive less illumination, thus reducing some of the out-of-focus information (See Figure 4-1).

Confocal imaging is based on the principle that both the illumination and detection systems are focused on the same single volume element of the sample. To achieve confocal imaging, excitation light from a laser in laser scanning confocal microscopes is directed toward the sample. The beam of light passes through a scanning system and reaches the objective, which focuses the scanning beam as a spot on the sample. Fluorescence emissions generated by the sample scatter in all directions. Fluorescence from the focal plane of the sample returns via the objective and scanning system, and is reflected off the dichroic mirror and focused on a detector. In front of the detector is a spatial filter containing an aperture (pinhole), which defines the image of the spot in the focal plane of the microscope. Most fluorescence originating from above and below the plane of focus of the sample does not pass through the aperture of the spatial filter and as a result little out-of-focus light reaches the detector.

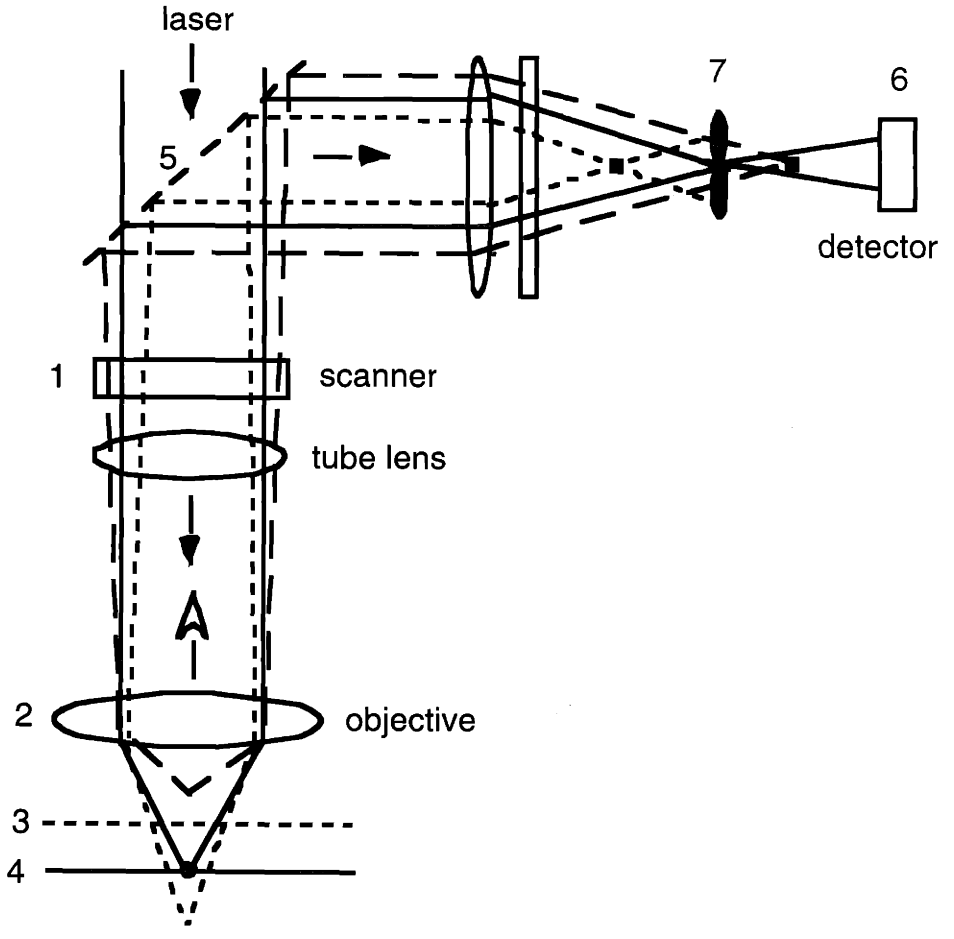

Figure 4-1. Schematic of laser confocal microscope. A laser beam is directed onto the sample by a scanning system and is focused on the sample by an objective (2). Induced fluorescent light is scattered and some of the light is collected by the objective lens and directed through the scanning system toward the beam splitter. In-focus light from the sample retraces the incident light path and is directed back through the pinhole to the detector. 1, Tube lens, 2, objective, 3, out-of-focus region, 4, focal plane, 5 dichroic reflector, 6, detector, 7, pinhole (Wright, Centonze, *et al.*, 1993)

4.3. Materials and Methods

4.3.1 Materials

PLGA 50:50 (RG503, lot 34033) was purchased from Boehringer Ingelheim (Montvale, NJ) and had a number-average molecular weight of 25,000 Da. Poly(vinyl alcohol) (PVA) (88% hydrolyzed, 25,000 Da) was obtained from Polysciences (Warrington, PA). Carboxy SNARF-1 conjugated to 10,000 Da dextran and Cl-NERF conjugated to 10,000 Da dextran were from Molecular Probes (Eugene, OR). All other chemicals were reagent grade.

4.3.2 Preparation of double emulsion and ProLease microspheres

Microspheres were prepared by two methods, double emulsion (Cohen, Yoshioka *et al.*, 1991) and a spray freeze-dry technique (Tracy, 1998). For the double emulsion microspheres, 100 μL of aqueous dye solution was added 1 mL of a solution of 200 mg/mL PLGA in methylene chloride, and the mixture was sonicated for six 0.5-second, 40-watt pulses with a Vibracell (Danbury, CT) sonicator using a microtip probe. This primary emulsion was then added to 20 mL of an aqueous solution of 2.5% (w/v) PVA. The second emulsion was formed by homogenization for 1 min at 5000 rpm on a Silverson (East Longmeadow, MA) homogenizer using a 5/8" micro-mixing assembly with a general-purpose disintegrating head. The resultant water-in-oil-in-water (w/o/w) emulsion was then poured into 80 mL of 1% PVA and stirred

continuously for 3 h to evaporate the solvent. The hardened microspheres were centrifuged, washed 3 times with water, freeze-dried, and stored under dessicant at -20°C.

To prepare microspheres by the spray freeze-dry technique, 1.5 mL of aqueous dye solution was added 30 mL of a solution of 100 mg/mL PLGA in acetone. This solution was sprayed through a sonicating nozzle with settings of 20 kHz and 60% amplitude at a flow rate of 2.0 mL/min into a bath of frozen ethanol and liquid nitrogen. The particles were cured for 24 hours at -80°C. Additional ethanol was added 3 hours into the curing process. Following curing, the particles were filtered, lyophilized, and passed through a 106 μm sieve. The particles were stored under dessicant at -80°C.

4.3.3 Loading of microspheres

Ten mg of dried microspheres were dissolved in 3 mL of 0.1 N NaOH/0.5% SDS overnight at 37°C. Samples were then diluted 1:9:9 with 1 mM HCl and PBS (at 10-fold concentration) so that all the samples were analyzed at the same pH to avoid artifacts due to the pH sensitivity of the dyes. The pH of the resulting solutions was measured using a standard glass electrode to ensure that the samples were all buffered to the same pH as the standards (pH 7.0). Standards were made by dissolving known amounts of dye in similar solutions. All samples were then measured for fluorescence intensity using a Photon Technology International

fluorimeter (Ashland, MA) using λ_{ex} = 488 nm and a ratio of λ_{em} of 535 nm (Cl-NERF) to 580 nm (SNARF). Measurements were related to the standard curve to determine dye content.

4.3.4 pH electrode measurements

pH electrode measurements were made essentially as described previously (Shenderova, Burke *et al.*, 1998). Acetonitrile was added to a sample of microspheres in PBS to a final ratio of 4:1 (v/v). This solution was mixed for 15 sec, and the pH was measured using a glass electrode pH meter. To correlate this with a concentration of hydronium ions, standards were made up with known concentrations of lactic acid in a solution of acetonitrile:water, 4:1 (v/v). pH measurements of the standards were taken 15 sec after addition of acetonitrile. Samples were run in triplicate.

4.3.5 Release from microspheres

Ten mg of dried microspheres were suspended in a round-bottom, 1.8-mL cryovial containing 1 mL of PBS, pH 7.4. Sample tubes were incubated at 37°C with continuous shaking. To sample the released dye, tubes were centrifuged and the supernatant was removed and analyzed. pH of the supernatant was measured to verify that it was at 7.4. The sample tubes were replenished with PBS, vortexed to resuspend the microspheres, and placed back in the incubator. Samples were run in triplicate.

4.3.6 Data collection

Ratio imaging was conducted on a Bio-Rad (Hercules, CA) MRC 600 laser-scanning confocal microscope. The pH was determined using two different dyes; a combination of SNARF (λ_{em} = 580 nm) and Cl-NERF (λ_{em} = 535 nm) was used at a ratio of 2:1 (w/w). Images at the two wavelengths were collected in photon-counting mode using a 63x objective. The gain was set on 8.0 and the black level was set on 5.5 for each channel. Images in the two channels were then collected by accumulating to peak. The ratio was calculated using NIH Image 1.61 (developed at the U.S. National Institutes of Health and available on the Internet at http://rsb.info.nih.gov/nih-image/). Calibration curves were generated for each dye set by placing solutions of dye at known pH on a microscope slide and focusing the microscope within the solution. Multiple ratios were taken for each pH value and then averaged to obtain the calibration curve.

4.3.7 Gel permeation chromatography

Microspheres pre-incubated in PBS were washed with water to remove buffer salts, freeze-dried, resuspended in chloroform and filtered. Samples were analyzed on two PL-Gel mixed-D columns in series (5 μm, 300 x 7.5 mm, Polymer Laboratories, Amherst, MA) and eluted with chloroform at 1 mL/min on a Perkin Elmer LC-250 with refractive index detection.

Molecular weight was determined relative to polystyrene standards. All samples were run in triplicate.

4.3.8 Scanning electron microscopy (SEM)

Scanning electron micrographs were obtained using a JEOL JSM-6320 FV microscope at 0.8 kV. Microspheres were mounted in the powder form and were not coated.

4.3.9 Dye binding to PLGA microspheres

PVA-free microspheres made using a spray/freeze-drying technique (Tracy, 1998) were used so that the dyes contacted polymer rather than PVA on the surface of the microspheres. SNARF/NERF solutions (2:1 w/w) were made in phosphate buffers (50 mM phosphate, 100 mM NaCl) at pH 2, 4 and 7.4 at concentrations of 0.5 and 0.05 μg/mL. The rationale for using 0.05 μg of dye with 10 mg of microspheres was to mimic similar loading conditions of dye within the microspheres. One mL of solution was added to 10 mg of microspheres and incubated at 37°C for 24 h with agitation. Samples were then centrifuged and the supernatant was measured for fluorescence intensity and compared with controls where dye was incubated without microspheres. Samples were run in triplicate.

4.4. Results and Discussion

The technique of imaging pH-sensitive, fluorescent dyes conjugated to dextrans within microspheres using confocal microscopy was selected herein for several reasons: 1) it would allow determination of pH values throughout a microsphere as opposed to an average pH value within a population, 2) pH distributions could be determined at different planar sections within the microsphere, 3) quantitative information that is independent of dye concentration could be obtained, and 4) the large dextran molecules conjugated to the dyes would prevent diffusion of the latter out of the microsphere during the course of the experiment.

Microspheres were incubated in aqueous solution under physiologic conditions, whereupon the microsphere becomes wetted and the PLGA undergoes hydrolysis. As the polymer chains of the microsphere degrade, either by end-chain or random-chain scission, smaller polymer chains are created. This increases the number of carboxylic groups and thus of the total hydronium ion concentration within the particle.

4.4.1 Verification of pH change within the microsphere

Prior to the microcopy measurements, we verified there was a pH change occurring within the microspheres. The bulk acidity of the microenvironment was determined by solubilizing the microspheres in aqueous acetonitrile and measuring pH with a glass electrode (see Methods). The results were compared with those of the buffered solution in which the microspheres were incubated. As seen in Figure 4-2, there is a large difference between the

buffered solution pH and that of solubilized microspheres after two weeks: the average pH within the microspheres dropped to 5.2, whereas that of the buffered solution remained at about 6.9. While the acidity of the entire system rose, the rate of increase within the microspheres was approximately double that of the external buffer, likely due to acid-catalyzed hydrolysis.

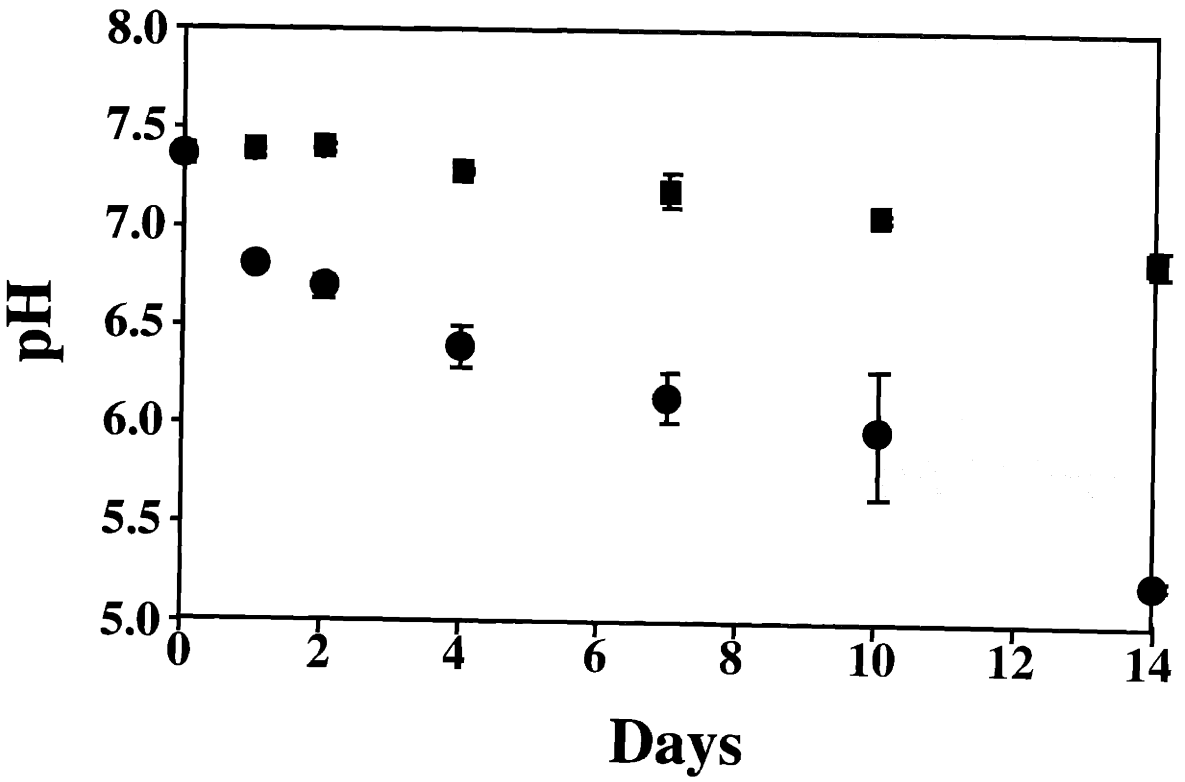

Figure 4-2. pH measurements of solubilized microspheres in 4:1 acetonitrile:water (●) corrected against standards measured in identical solutions and of PBS buffer in which the microspheres are incubated (■). Error bars represent standard error of 3 - 5 experiments.

4.4.2 Mathematical modeling of diffusion of polymer degradation products

In addition to measuring the bulk acidity of the degrading microspheres, a mathematical model was developed to predict the potential distribution of pH within a PLGA microsphere. A general diffusion equation was written in spherical coordinates (Equation 4.1); a representation of the microsphere is shown in Figure 4-3. The equation describes the transient change in monomer concentration throughout a microsphere. A constant homogeneous reaction term, b, was included to account for the generation of acid within the microsphere due to polymer degradation. In this equation, c represents the concentration of monomer or acid, t represents time, r represents the position within the microsphere, and D represents the diffusion coefficient of the acids. c_0 represents the concentration of acid in the bulk fluid in which the microsphere sits and that value is 4×10^{-8} M (equivalent to pH 7.4). Thus, the boundary equations given in equations 4.2(a,b) are given as c_0 at the edge of the sphere of radius R and c_0 at time 0. Equation 4.1 is a non-homogeneous partial differential equation and can be solved using Finite Fourier Transform (Appendix B).

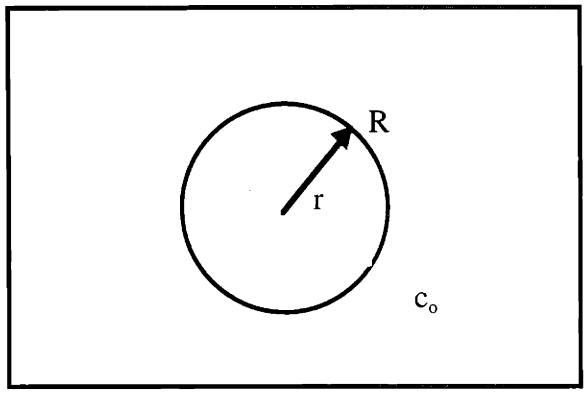

Figure 4-3. Representation of a single microsphere of radius R in spherical coordinates.

$$\frac{\partial c}{\partial t} = D\frac{1}{r^2}\frac{\partial}{\partial r}\left(r^2\frac{\partial c}{\partial r}\right) + b \qquad \text{Eq. 4.1}$$

$$c(t,R) = c_o$$
$$c(0,r) = c_o \qquad \text{Eq. 4.2(a,b)}$$

The solution is given below in equation 4.3.

$$c(r,t) = c_o\sum_{n=1}^{\infty}\sqrt{2}R\frac{\sin\left(n\pi\frac{r}{R}\right)}{r}\left[\frac{\sqrt{2}(-1)^n\left[n\pi + \frac{bR^2}{Dc_o n\pi}\right]}{(n\pi)^2} + e^{-\frac{(n\pi)^2 tD}{R^2}}\left(\frac{\sqrt{2}(-1)^n\left[\frac{bR^2}{Dc_o n\pi}\right]}{(n\pi)^3}\right)\right]$$

Eq. 4.3

Estimated values for the polymer degradation rate constant and diffusivity of small molecules from PLGA microspheres were taken from literature and used in the model. As shown in Figure 4-4, there is a steep distribution of acidity throughout the microsphere particle.

Thus, a diffusion-controlled model indicates that a pH distribution could exist within the microspheres.

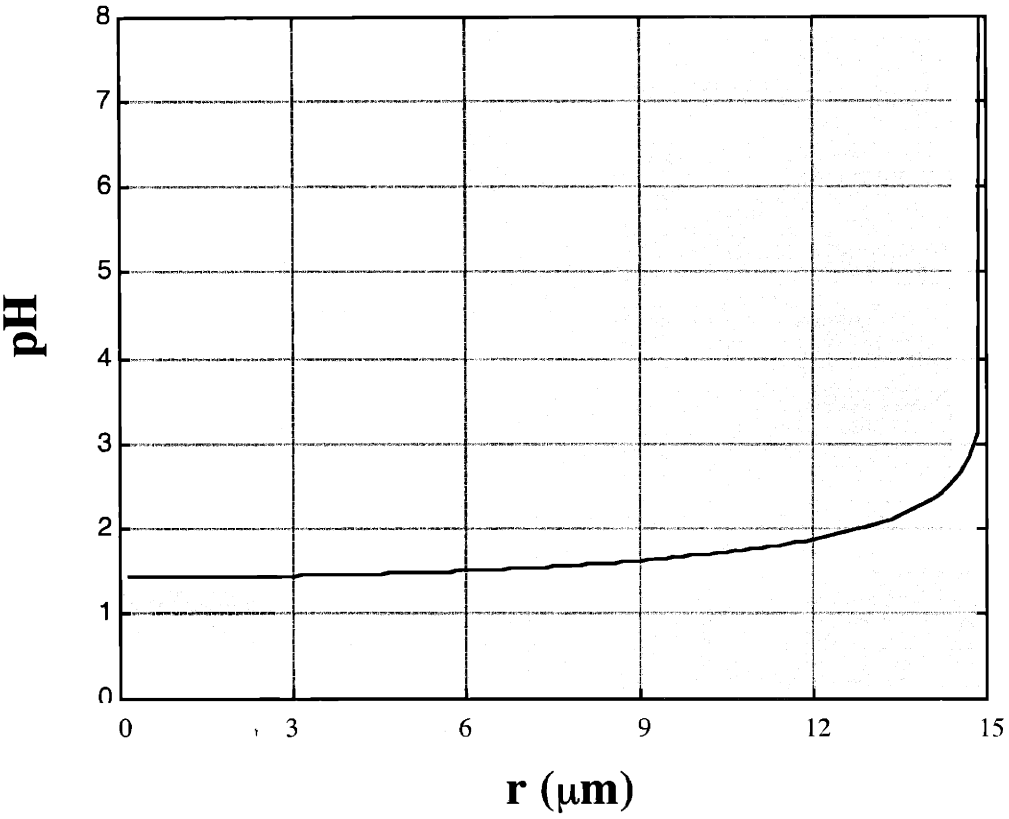

Figure 4-4. Predicted pH profile throughout PLGA microsphere. Conditions used include a particle radius of 15 mm and an incubation time of 10 days. The radius of the microsphere is represented by r.

4.4.3 Development of experimental methods

Having confirmed the existence of an acidified environment within the particles, we next established suitable conditions, such as dye concentration and SNARF:NERF ratio, for the confocal microscopy experiments. We generated a standard curve wherein a combination of the SNARF and NERF dyes (2:1, w/w) was dissolved in phosphate buffers (50 mM phosphate/100 mM NaCl) with pH, adjusted by addition of HCl, ranging from 1.5 to 7.0 and imaged with confocal microscopy. As shown in Figure 4-5a, the SNARF/NERF emission ratio linearly correlates with pH in the range from 1.5 to 3.5. (Standard curves were generated with every experiment.) A standard curve was also generated for a higher pH range (Figure 4-5b). This was accomplished using SNARF dye alone and an emission ratio of 640 nm and 580 nm. Although a linear standard curve was generated, experiments using microspheres showed interfering fluorescent signal from the polymer itself. Thus, quantifying the pH values in the higher range (> 4.0) was not further pursued.

Several controls were performed to avoid artifacts. PLGA microspheres without dye (both wetted and dry) were imaged and found to have no fluorescence (Figure 4-6a). Dry microspheres containing the dyes were imaged and again found to have no fluorescence (Figure 4-6b). Dye loading within the microspheres was determined, and a 15-day release experiment confirmed that the dye did not leach out of the microspheres over the course of the experiment: less than 10% of the dye was released from the microspheres (data not shown).

There was a concern that the dyes could bind to the polymers and undergo a change in pK, thus altering their response to pH changes. To address this issue, the following experiments were conducted. The dyes were incubated with PLGA microspheres made in the absence of PVA (to test for binding of the dyes directly to PLGA and not to the PVA which is used as an emulsion stabilizer). The dyes were prepared at two different concentrations and in phosphate buffers at three different pHs, and incubated with the microspheres for 24 hours at 37°C. Dye concentrations in solution were then determined by fluorescence spectroscopy. The difference in fluorescence intensity between the control (dye incubated at identical conditions in the absence of spheres) and the supernatant of the experiment was found to be less than 6% (i.e., within the error of the measurements). This gave a strong indication that no appreciable binding occurred between the dye and the polymer.

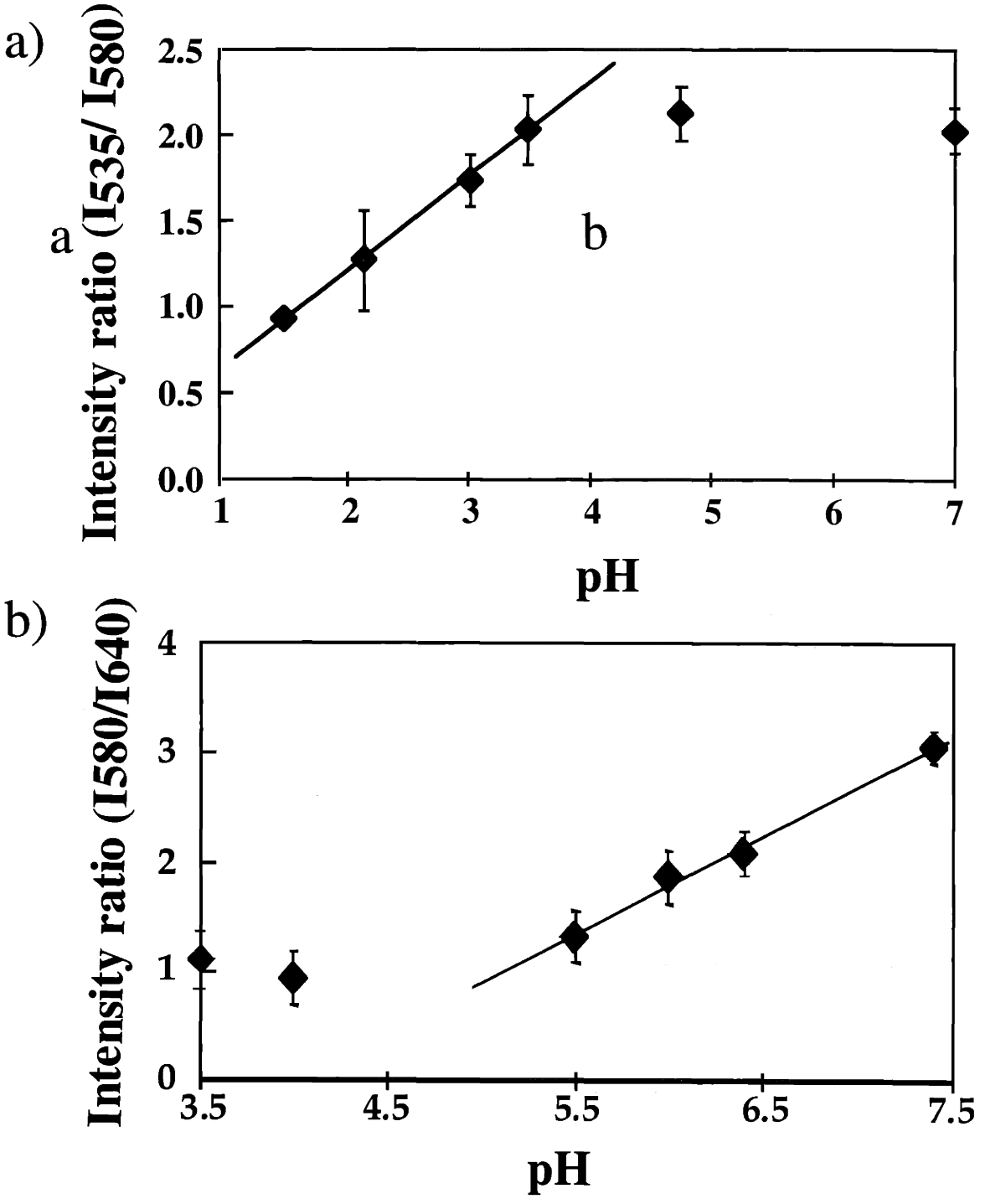

Figure 4-5. (a) Standard curve of fluorescence intensity ratios of SNARF/NERF coupled to dextran (MW of 10 kD a) (2:1 w/w) vs. pH. The equation for the fitted line is y = 0.54x + 0.13 with a r^2 value of 0.997. (b) Standard curve of fluorescence intensity ratio of SNARF coupled to dextran (MW of 10 kDa) vs. pH. Equation for the fitted line is y = .89x - 3.57 with a r^2 value of 0.99. Results are the average of at least 3 images. Error bars represent standard error.

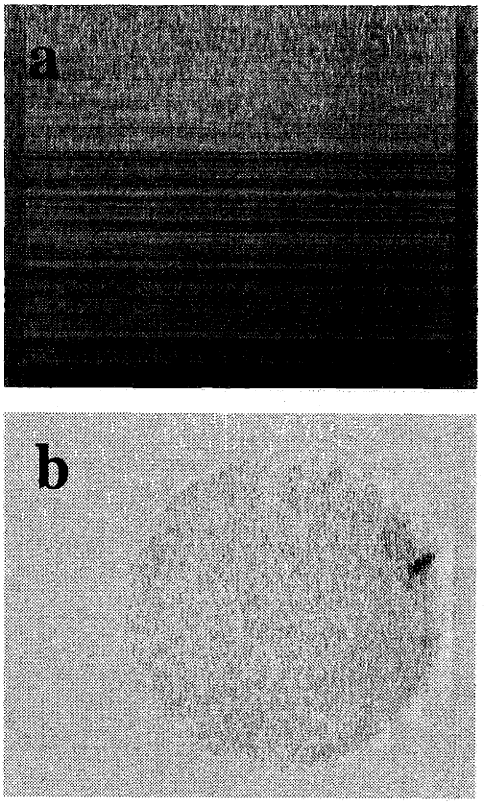

Figure 4-6. (a) Ratio image of blank PLGA microsphere (containing no dye) which had not been incubated in PBS. (b) Ratio image of dye-containing microsphere which, again, had not been wetted with PBS.

4.4.4 Kinetics of pH change within microspheres

Using our technique, we monitored the change in pH within microspheres over time. Microspheres were incubated continuously for 15 days and imaged several times over that period. A distribution of fluorescence intensity ratios (related to pH) could be seen within the microsphere particles, as exemplified in Figure 4-7, and as predicted from the mathematical modeling. Over the incubation period, the pH within the microspheres drops precipitously, down to as low as 1.5 in the center of the microsphere (Figures 4-8a - d). The pH increases from the center of the bead to the edges due to diffusion of degradation products out of, and of the outside buffer solution into, the microsphere, thus resulting in a concentration gradient of acidic by-products. Thus, a zone of higher pH exists near the surface which moves toward the center as the microsphere becomes more permeable.

The pH changes within the microspheres are dependent on the diameter of the polymer bead as well (Figures 4-8e - h). In smaller spheres, clearance of acidic by-products is faster due to shorter diffusion distances, and thus only a small proportion of the bead is at a low pH.

To ensure that the inner-particle pH was not a reflection of the outer buffer pH, the latter was measured using a standard pH probe (Figure 4-9). After 15 days of incubation, the pH of the outer medium was well above that observed within the interior of the spheres.

It was hypothesized that by daily changing the outer buffer in which the microspheres were incubated, with fresh PBS, the development of the low pH region would be retarded. Figures 4-8i - l indeed show a slower development of a low-pH region within the larger

microspheres. However, by the end of the 15-day incubation, the results were the same as those in which the buffer was not changed daily. A highly acidic core had developed within the microspheres. Clearly, in the larger spheres the diffusion distance was long enough to prevent the buffer from neutralizing the pH. However, with smaller spheres, this was not the case. There was only a small volume with an acidic intrapolymer environment (Figures 4-8m - o). Thus, one tactic to avoid an acidic microenvironment would be to use smaller spheres. In our case, for example, the spheres with a diameter of approximately 15 μm do not develop a significant volume of the low-pH region.

Our findings are summarized in Figure 4-10, which depicts three spheres incubated for 10 days. This figure shows clearly the difference in pH distributions due to the size of the microspheres. As the size of the microsphere decreases, the fraction of sphere volume at neutral pH increases. As an approximation, an average pH was calculated for each particle by assuming that the dark regions were of a pH of 7.4 and integrating the pH of the light region using NIH Image. For the largest bead, the calculated average pH was 5.4, for the medium-sized particle it was 6.2, and for the smallest particle had an average pH of 7.2. The pH of 6.2, determined for the medium-sized sphere, is similar to the average pH value found in other PLGA microsphere systems, although it is important to emphasize that the microspheres of that study (Burke, 1996) were manufactured by a different method (different processing methods give rise to microspheres with distinct structural properties, such as density or porosity). However, it is

evident from these results that a large portion of a microsphere can contain an acidic region but still maintain a high average pH.

Porosity of the microsphere structure would likely play a significant role in determining the acidity of the intraparticle environment. In more porous structures, monomers and oligomers would have a larger flux out and buffer salts could more easily diffuse in, thus mitigating acidification of the polymer interior. In contrast, more dense structures, like the microspheres shown here, retain their degradation products giving rise to microenvironments with high acidity.

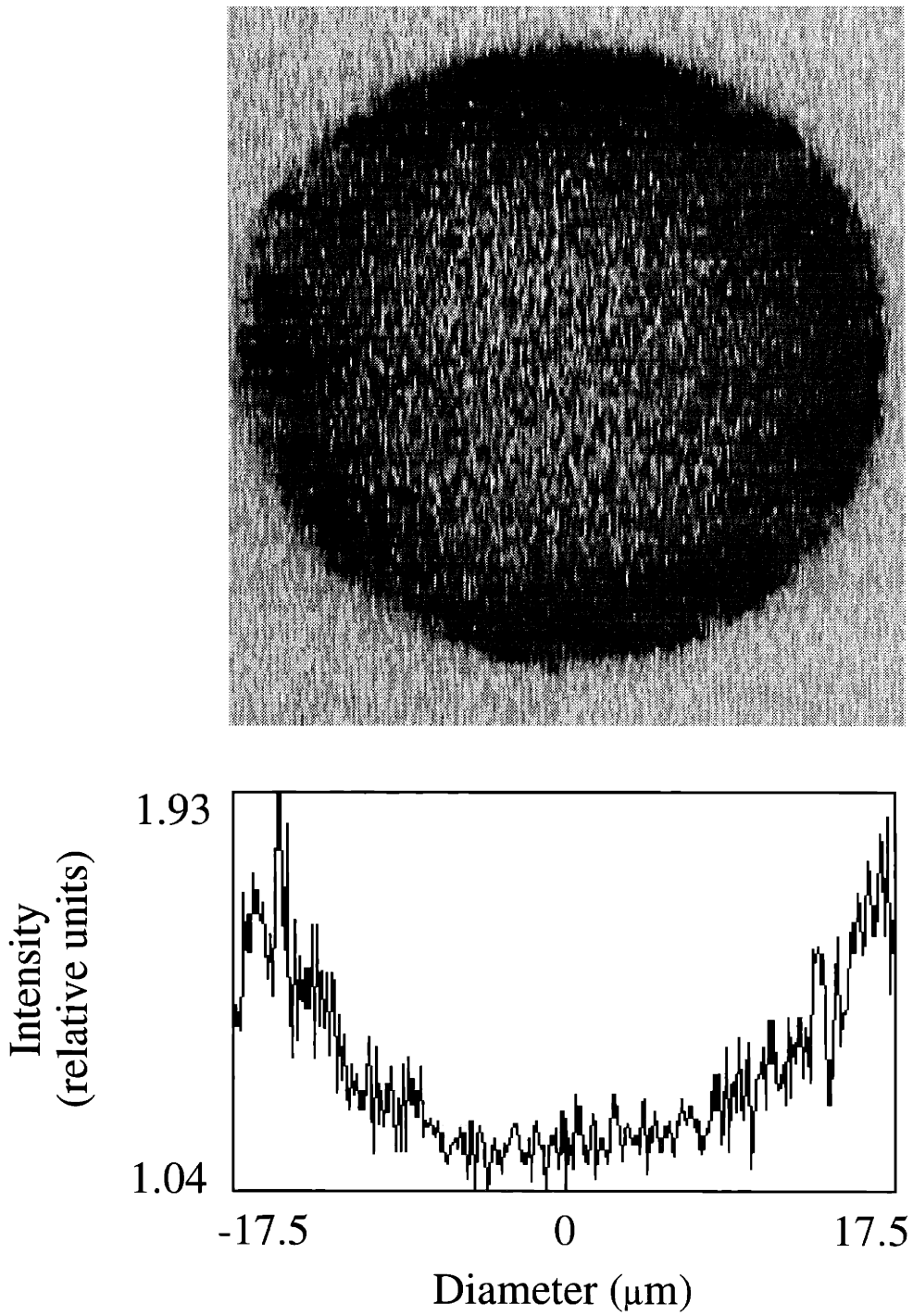

Figure 4-7. (a) Ratio image of dye-containing PLGA microsphere incubated in PBS for 8 days. (b) Fluorescence intensity profile across the diameter of the microsphere quantified using NIH Image.

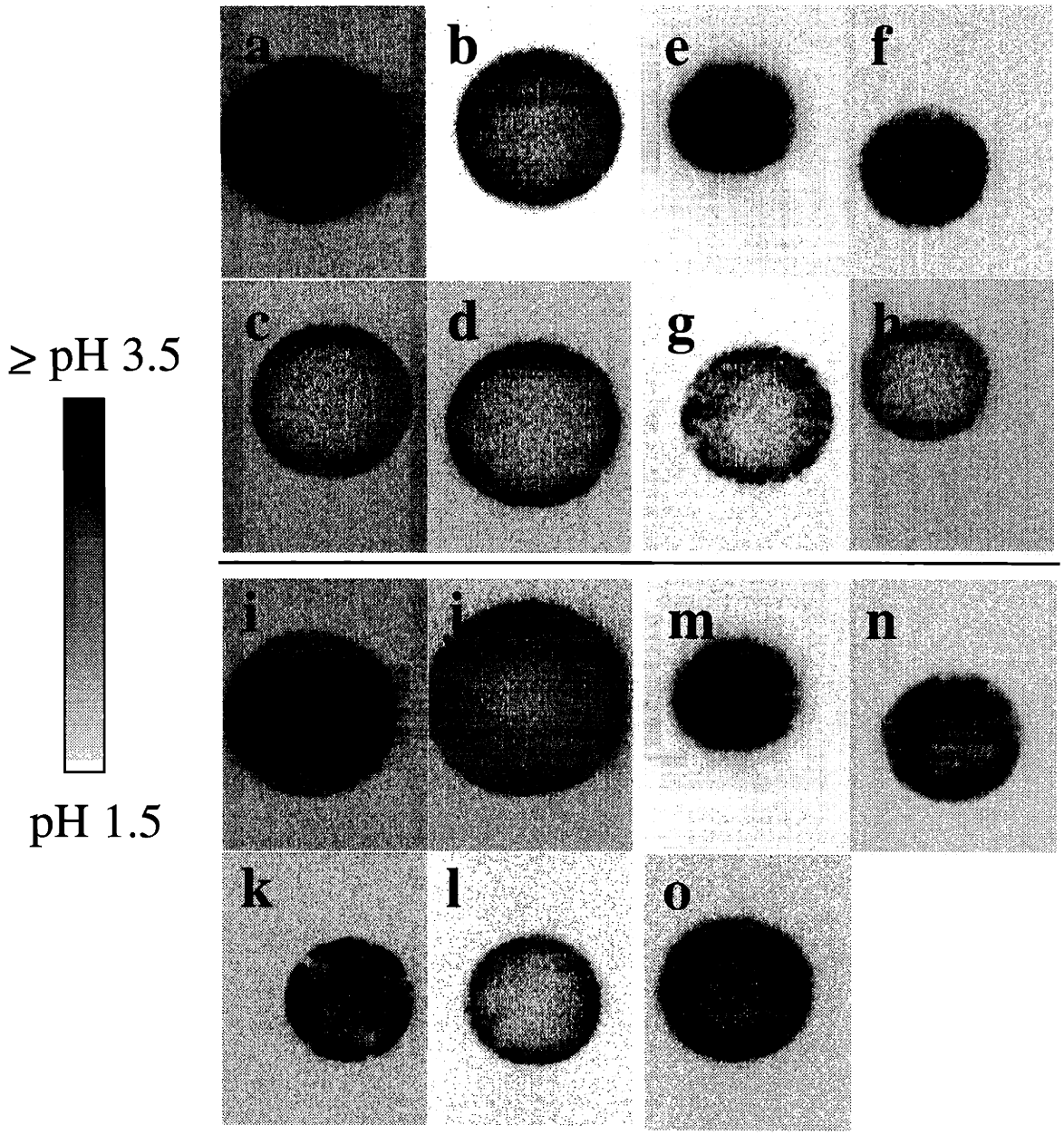

Figure 4-8. Large and small microspheres incubated either continuously for 15 days in PBS which either was not changed (a - h) or was changed daily (i - o). Images a - h were taken on day (a) 1 (d = 40 μm), (b) 2 (d = 40 μm), (c) 10 (d = 40 μm), (d) 15 (d = 46 μm), (e) 1 (d = 29 μm), (f) 2 (d = 25 μm), (g) 10 (d = 32 μm), and (h) 15 (d = 31 μm). Images i - o were taken on day (i) 1 (d = 40 μm), (j) 3 (d = 46 μm), (k) 10 (d = 40 μm), (l) 15 (d = 40 μm), (m) 1 (d = 29 μm), (n) 2 (d = 25 μm), and (o) 10 (d = 30 μm). Standard curve is represented by a grayscale curve as shown on the left.

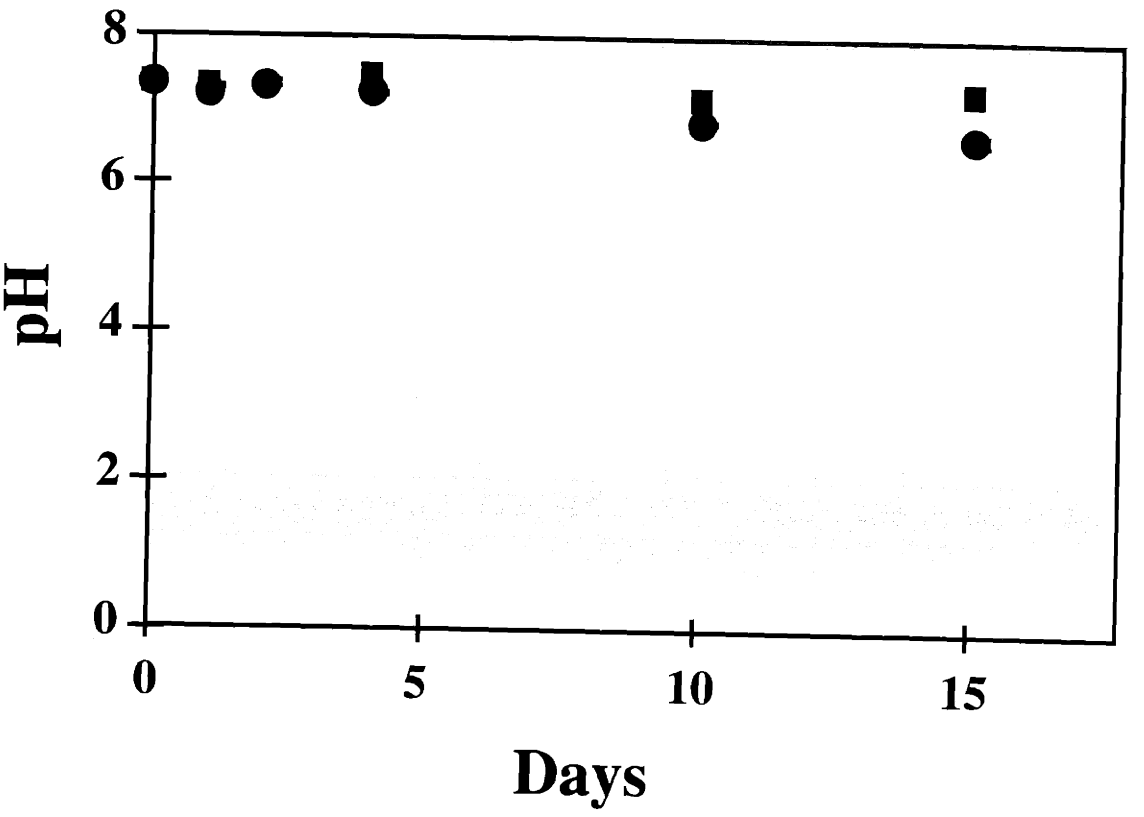

Figure 4-9. pH of bulk fluid in which the microspheres were incubated. Measurements were taken with a standard glass electrode. (■) Samples in which the buffer was changed daily. (●) Samples where the buffer was not changed throughout the course of the experiment. Results are the average of at least 3 experiments and error bars indicate standard error.

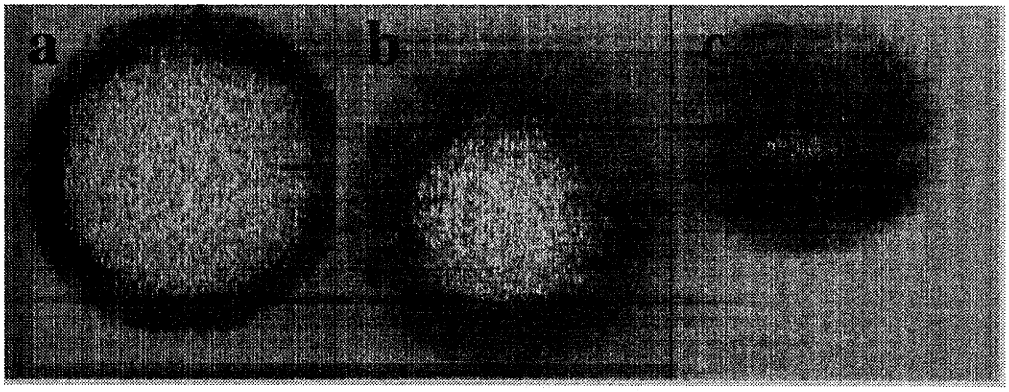

Figure 4-10. Three microspheres of different sizes imaged after 10 days of incubation in PBS without any change of buffer. (a) d = 38 μm, (b) d = 24 μm, (c) d = 14 μm.

4.4.5 Physical properties of degrading microspheres

Another way to examine the issue of low-pH environments within PLGA particles is to directly characterize polymer degradation and loss of particle mass. We observed by SEM (Figure 4-11) that the microsphere structure does not seem to be altered after incubation for 15 days. The core of the microsphere appears to remain dense with few visible pores. This implies that the polymer chains are long, on average, and that little polymer has been lost during degradation. By quantifying the molecular weight of the polymer chains of the microsphere and the dry weight of the microspheres over time, we directly examined these issues, as shown in Figure 4-12. Over the 15-day degradation, the dry weight of the microspheres remained constant, while the number- and weight-average molecular weight of the polymer chains dropped precipitously. This corresponds well with the conclusions drawn from the scanning electron micrographs.

Extension of this technique to other polymers and formulations should increase our understanding of the environment within the devices, as well as the process of polymer degradation. Models of the degradation, including accumulation of acidic by-products, could be developed to provide insight into the kinetics of polymer erosion and the patterns of drug release.

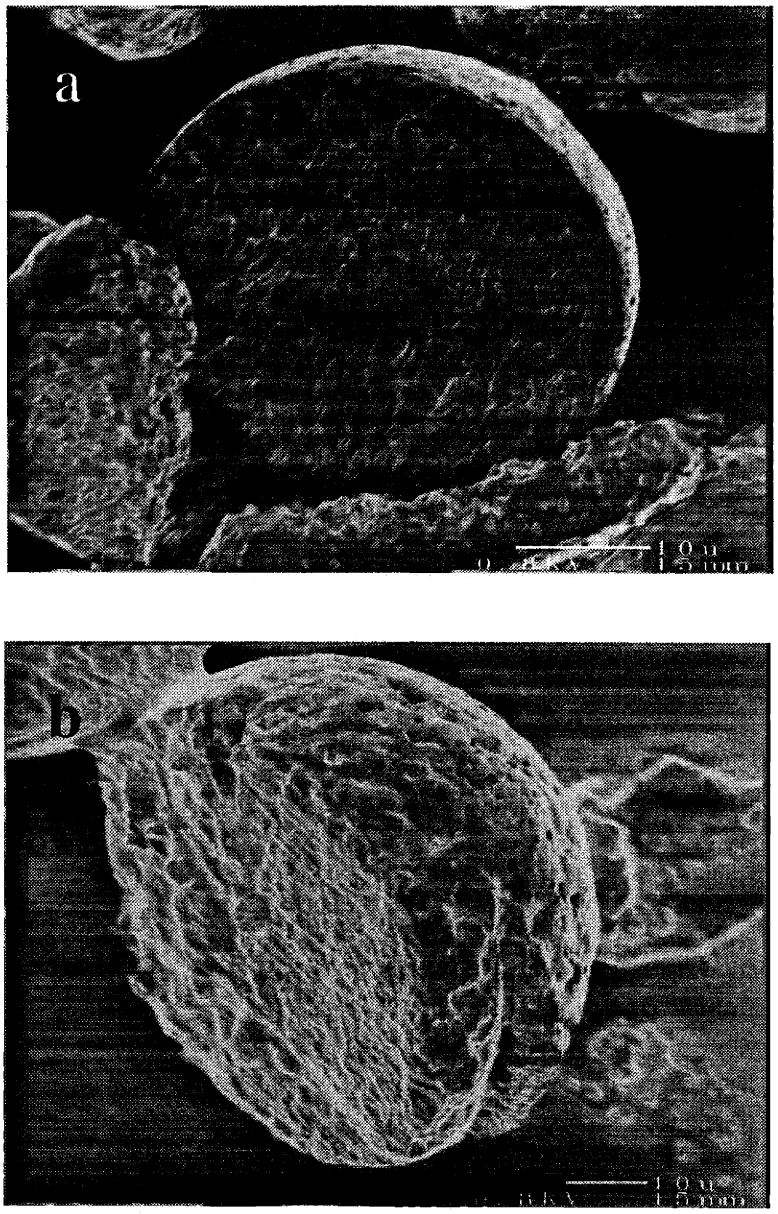

Figure 4-11. Scanning electron micrographs of fractured microspheres. Samples were mounted dry and were not coated. (a) Microsphere which had not been incubated. (b) Microsphere which had been incubated for 15 days in PBS.

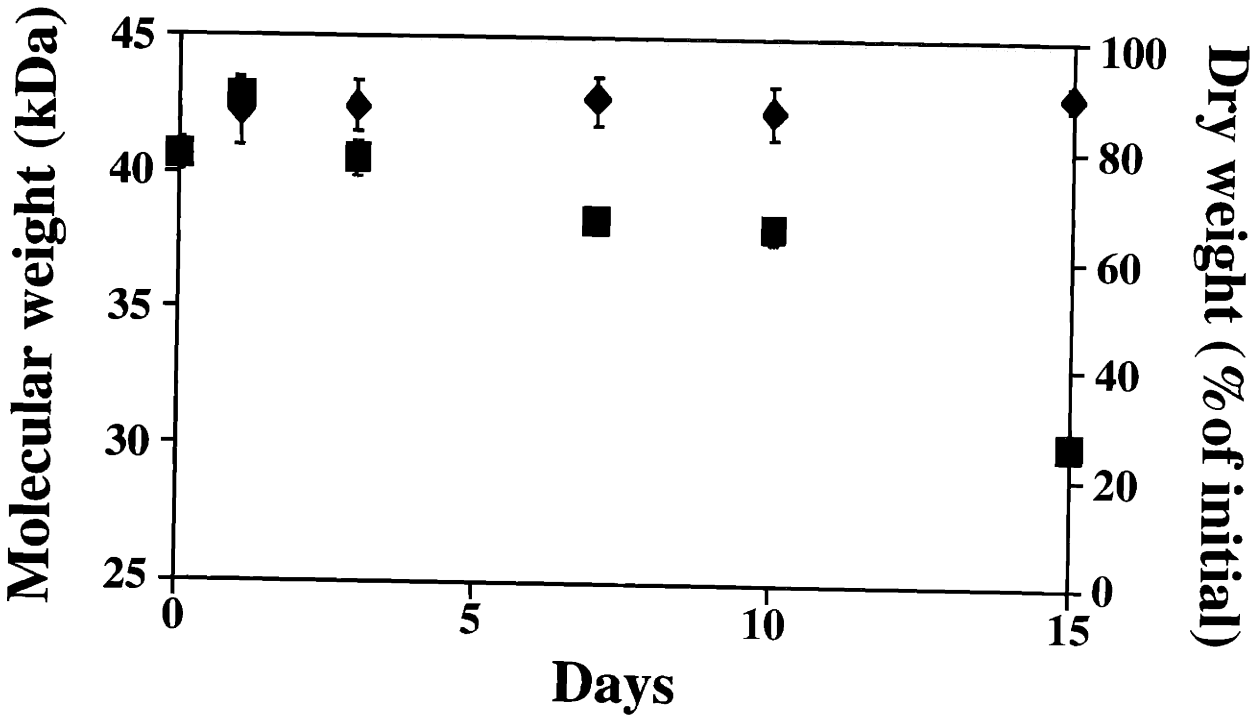

Figure 4-12. Degradation of PLGA microspheres over 15 days in PBS. (■) Dry weight of microspheres over the course of incubation. (◆) Molecular weight of polymer chains of microspheres as determined by GPC. Error bars represent standard error of three experiments.

4.4.6 Strategies to overcome the low pH environment

To examine the effect of porosity on the microacidity within the PLGA microspheres, porous particles containing the pH sensitive dyes were made using the spray-freeze dry technique (See section 4.2.2). It is hypothesized that porous structures decrease the diffusion distance of monomers and oligomers out of the particles and thus result in a higher diffusivity and ultimately lower hydronium ion concentration within the particles.

The ProLease particles containing the combination of SNARF/NERF dyes (2:1) were incubated in 5% PVA at 37°C and imaged several times with confocal microscopy over the period of 14 days. The particles were incubated in a PVA solution to prevent aggregation of the particles over the course of the experiment. To ensure the replacement of the release medium did not give rise to artifact, standard curves generated in the presence and absence of 5% PVA were compared (Figure 4-13). No difference was observed due to the addition of PVA.

The pH of the release medium was measured over the course of the experiment to ensure the environment in which the particles incubated did not change. No measurable change in pH was observed; the pH remained at 5.3 over 14 days.

As mentioned, the ProLease particles are porous and this was corroborated by confocal microscopy results. There existed, within the microspheres, pockets lacking fluorecence intensity (Figure 4-14), and these pockets were found within the particles over the course of the experiment. These regions with no intensity were interpreted as porous portions of the microspheres. An alternative explanation might be that these pockets represent regions lacking

in dye but not polymer and that the distribution of dye within the particles is heterogeneous. This explanation does not seem likely given the uniform fluorescence intensity throughout the remainder of the particle.

Over the course of 14 days, there was little evidence of a change in microenvironment pH (Figure 4-15). The majority of the particles measured did not have regions of pH below 3.5. From this, it seems clear that a strategy of using porous particles to avoid changes in intraparticle pH is viable.

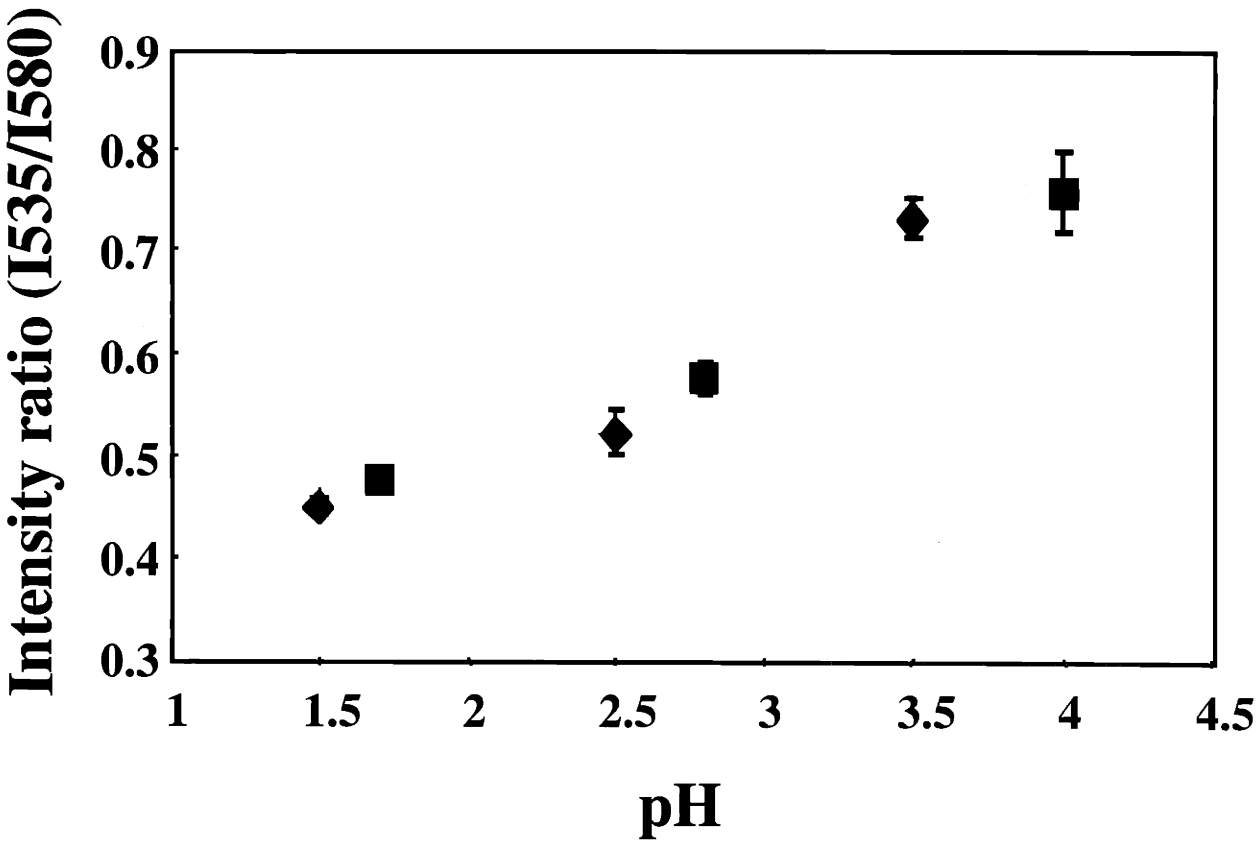

Figure 4-13. Standard curves of fluorescence intensity ratios of SNARF/NERF coupled to dextran MW of 10 kDa) (2:1 w/w) (■) in PBS and in (♦) 5% PVA vs. pH. Results are the average of at least 3 images. Error bars represent standard error.

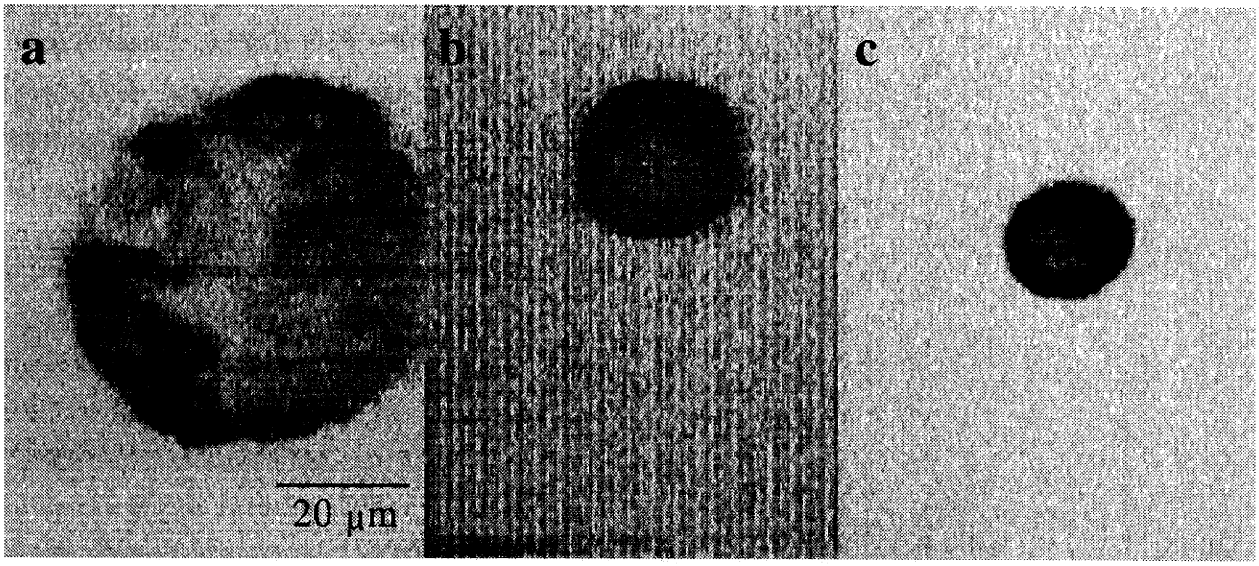

Figure 4-14. ProLease microspheres incubated in 5% PVA for (a) 1, (b) 7, and (c) 14 days. Light regions within the particles indicate porous pockets and not an intrapolymer acidity.

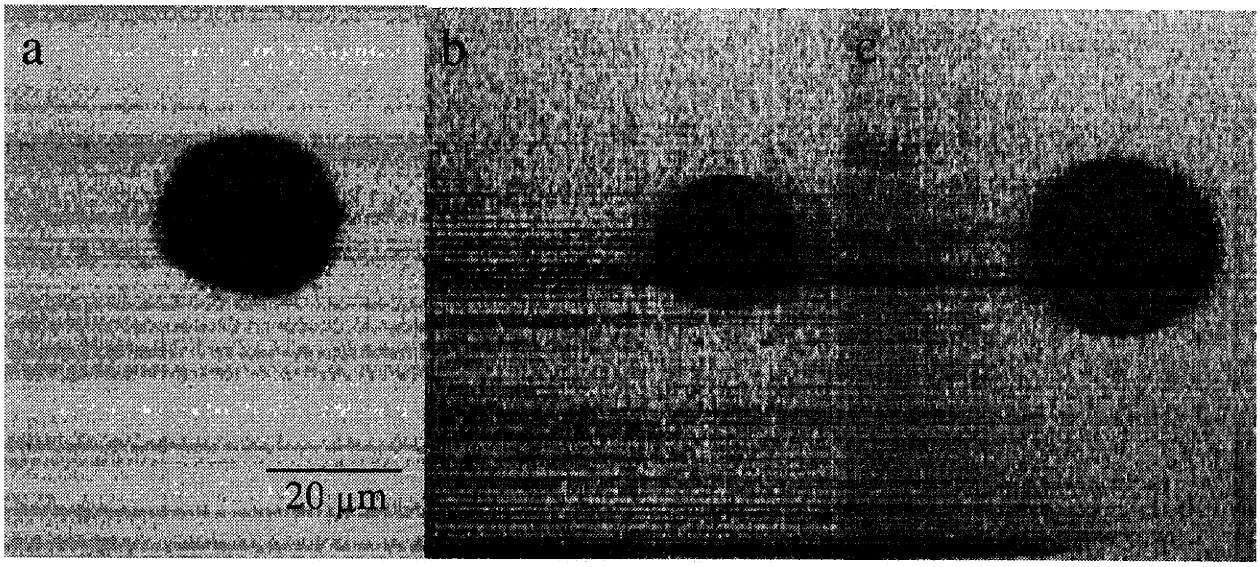

Figure 4-15. ProLease microspheres incubated in 5% PVA for (a) 1, (b) 7, and (c) 14 days showing no indication of an acidic microenvironment.

4.5. Conclusions

By encapsulating pH-sensitive, fluorescent dyes within PLGA microspheres and imaging them with confocal microscopy, we have established a method to quantitatively determine the pH distribution within a microsphere particle. This is a general method that can be applied to different polymer systems as well as other devices. After incubation for several days under physiologic conditions, an acidic region developed within the center of the microspheres. The fraction of sphere volume comprising the acidic region decreased with decreasing bead diameter. The pH within the larger (~40 μm) particles was determined to be as low as 1.5, which is sufficiently acidic to cause denaturation of, and/or deleterious reactions in, many potential protein therapeutics. However, in certain protein systems, an acidic environment may even aid in reducing aggregation (Liu, Langer *et al.*, 1991). The area of low pH diminished in size and eventually vanished with prolonged incubation (> 15 days) of the particles. These results are consistent with a diffusion-controlled mechanism in which acidic degradation products initially diffuse out of the bead slowly. As degradation proceeds, the polymer matrix becomes less dense, allowing increased diffusion and ultimately free exchange of monomers and buffer salts.

Physical parameters of the particles may be manipulated to prevent low pH environments. As demonstrated by the data shown in section 4.4.6, a low pH environment within the microspheres can be avoided by creating porous particles. With an increase in diffusivity, there is increased movement of acidic by-products of polymer degradation out of the

particles and buffering medium into the particles. In examining dense microspheres, smaller particles with a shorter diffusion distance may alleviate the problem. As shown in section 4.3.3, particles with a diameter of less than 14 μm do not have as large a volume of low pH as compared to larger particles.

Another strategy is to use excipients to buffer the low pH environment. Both laboratories of Goepferich and Schwendeman have shown efficacy by buffering the internal microenvironment with basic salts (Brunner, Maeder, *et al.*, 1999; Zhu, Maller, *et al.*, 2000).

4.6. References

Brange, J., L. Langkjaer, S. Havelund and A. Volund, (1992). Chemical stability of insulin. 1. Hydrolytic degradation during storage of pharmaceutical preparations. *Pharm. Res.* **9**: 715-726.

Brunner, A., K. Maeder and A. Goepferich, (1998). The chemical microenvironment inside biodegradable microspheres during erosion. *Proceed. Int'l. Symp. Control. Rel. Bioact. Mater.* **25**: 154-155.

Brunner, A., K. Maeder and A. Goepferich, (1999). pH and osmotic pressure inside biodegradable microspheres during erosion. *Pharm. Res.* **16(6)**: 847 - 853.

Burke, P. A., (1996). Determination of internal pH in PLGA microspheres using 31P NMR spectroscopy. *Intern. Symp. Control. Rel. Bioact. Mater.* **23**: 133-134.

Cleland, J., M. Powell and S. Shire, (1993). The development of stable protein formulations: a close look at protein aggregation, deamidation, and oxidation. *Crit. Rev. Therapeutic Drug Carrier Systems* **10(4)**: 307-377.

Cohen, S., T. Yoshioka and R. Langer, (1991). Controlled delivery systems for proteins based on poly(lactic/glycolic acid) microspheres. *Pharm. Res.* **8(6)**: 713-720.

Domb, A., L. Turovsky and R. Nudelman, (1994). Chemical interactions between drugs containing reactive amines with hydrolyzable insoluble biopolymers in aqueous solutions. *Pharm. Res.* **11(6)**: 865-868.

Fu, K., D. Pack, A. Laverdiere, S. Son and R. Langer, (1998). Visualization of pH in degrading polymer microspheres. *Proceed. Int'l. Symp. Control. Rel. Bioact. Mater.* **25**: 150-151.

Goepferich, A., (1996). Mechanisms of polymer degradation and erosion. *Biomaterials* **17**: 103-114.

Grizzi, I., H. Garreau, S. Li and M. Vert, (1995). Hydrolytic degradation of devices based on poly(DL-lactic acid) size-dependence. *Biomaterials* **16(4)**: 305 - 311.

Langer, R., (1996). Controlled release of a therapeutic protein. *Nature Medicine* **2(7)**: 742-743.

Langer, R. and J. Vacanti, (1993). Tissue engineering. *Science* **260**: 920 - 926.

Liu, R., R. Langer and A. M. Klibanov, (1991). Moisture-induced aggregation of lyophilized proteins in the solid state. *Biotechnol. Bioeng.* **37**: 177-184.

Mader, K., B. Gallez, K. J. Liu and H. M. Swartz, (1996). Non-invasive *in vivo* characterization of release processes in biodegradable polymers by low-frequency electron paramagnetic resonance spectroscopy. *Biomaterials* **17(4)**: 457 - 461.

Mathiowitz, E., J. Jacob, Y. Jong, G. Carino, D. Chickering, P. Chaturvedi, C. Santos, K. Vijayaraghavan, S. Montgomery, M. Bassett and C. Morrell, (1997). Biologically erodable microspheres as potential oral drug delivery systems. *Nature* **386**: 410-414.

Middaugh, C., R. Evans, D. Montomgery and D. Casimiro, (1998). Analysis of plasmid DNA from a pharmaceutical perspective. *J. Pharm. Sci.* **87(2)**: 130-146.

Peppas, N. and R. Langer, (1994). New Challenges in Biomaterials. *Science* **263**: 1715-1720.

Shenderova, A., T. G. Burke and S. P. Schwendeman, (1998). Evidence for an acidic microclimate in PGLA microspheres. *Proceed. Int'l. Symp. Control. Rel. Bioact. Mater.* **25**: 265-266.

Shenderova, A., T. G. Burke and S. P. Schwendeman, (1999). The acidic microclimate in poly(lactide-co-glycolide) microspheres stabilizes camptothecins. *Pharm. Res.* **16(2)**: 241-248.

Shenderova, A., M. Madou, S. Yao and S. Schwendeman, (1999). Potentiometric and impedance measurements of PLGA coated microelectrodes. *Proceed. Int'l. Symp. Control. Rel. Bioact. Mater.* **26**: #5919.

Tracy, M., (1998). Development and scale-up of a microsphere protein delivery system. *Biotechnol. Prog.* **14**: 108-115.

Uchida, T., A. Yagi, Y. Oda, Y. Nakada and S. Goto, (1996). Instability of bovine insulin in poly(lactide-co-glycolide) (PLGA) microspheres. *Chem. Pharm. Bull.* **44(1)**: 235-236.

Vert, M., S. Li and H. Garreau, (1991). More about the degradation of LA/GA-derived matrices in aqueous media. *J. Cont. Rel.* **16**: 15-26.

Wright, S.J., V.E. Centonze, S.A. Stricker, P.J. DeVries, S.W. Paddock and G. Schatten, (1993). Introduction to confocal microscopy and three-dimensional reconstruction. Methods in Cell Biology, Vol. 38. B. Matsumoto. San Diego, Academic Press, Inc.

Zhu, G. and S. P. Schwendeman, (1998). Stabilization of bovine serum albumin encapsulated in injectable poly(lactide-co-glycolide) millicylinders. *Proceed. Int'l. Symp. Rel. Bioact. Mater.* **25**: 267-268.

Zhu, G. and S. P. Schwendeman, (1999). Influence of basic salts on stability and release of proteins in injectable poly(lactide-co-glycolide) delivery devices. *Proceed. Int'l. Symp. Control. Rel. Bioact. Mater.* **26**: 6446.

Zhu, G.Z., S.R. Maller and S.P. Schwendeman, (2000). Stabilization of proteins encapsulated in injectable poly (lactide-co-glycolide). *Nat. Biotechnol.* **18**: 52-57.

5. Summary and future work

5.1. Summary of thesis

This body of work has addressed issues of protein stability during encapsulation within microspheres and also during release after administration. Two nondestructive methods were developed to address the problem of protein stability within the microspheres: 1) use of FTIR spectroscopy to evaluate the encapsulated protein, and 2) use of confocal microscopy and pH sensitive fluorescent dyes to determine the pH distribution within degrading microspheres. The loss in secondary structure was prevented by including trehalose within the formulation. As the double emulsion technique for protein encapsulation showed detrimental consequences to protein structure, a novel method of protein encapsulation was explored. Micron-sized particles were made with a spontaneous emulsification method and optimized for microsphere size, loading, and release. In addition, the environment within the microsphere during protein release was explored. The pH distributions with the degrading microspheres were determined and the results showed that the inner pH of the microspheres dropped to as low as 1.5.

5.2. Summary of controlled release*

The field of controlled drug delivery has evolved from one in which there were few products a quarter century ago to one with current annual US sales in excess of fourteen

* Published in part in Fu, K., A. M. Klibanov, R. Langer, (2000). Protein stability in controlled-release systems. *Nat. Biotech.* **18:** 24-25.

billion dollars. New treatments for cancer, heart disease, and many other afflictions are now available due to the ability to entrap drugs within, and subsequently release them from, polymers or liposomes. Despite significant advances, however, the majority of these delivery systems are still used for small molecules taken orally, transdermally, or through the nose or lung (Langer, 1998).

The ability to develop controlled release systems for proteins, rather than peptides, from polymers has been even more challenging. The biggest single issue with protein formulations intended for long-term controlled release (days to months) is the instability of the proteins themselves.

Protein stability, i.e., ability to maintain biological activity and structural intactness, is essential over the entire life of a controlled release system, including formulation, long-term storage, and finally release *in vivo*. Proteins are highly organized, complex structures which must maintain structural and chemical integrity to function properly. Many manufacturing methods jeopardize this by exposing proteins to potentially damaging conditions (Cleland and Langer, 1994; Bartus, Tracy *et al.*, 1998). Moreover, upon administration the solid protein becomes hydrated and exposed to physiological temperature within the delivery device for long periods of time. At this stage, the polymer matrix microenvironment and the products of polymer degradation can also reduce protein stability (Schwendeman, Cardamone *et al.*, 1996).

As the field of drug delivery has matured, the focus has shifted from studying the release kinetics of proteins from delivery devices, to strategies to maintain protein integrity (Liu, Langer

et al., 1991; Costantino, Langer *et al.*, 1994; Schwendeman, Cardamone *et al.*, 1996; Putney and Burke, 1998). The goal is to identify and understand the pathways of protein aggregation and the critical role of water in protein degradation (Liu, Langer *et al.*, 1991; Costantino, Langer *et al.*, 1994).

Upon administration, exposure of solid polymer-entrapped proteins to moisture and elevated temperatures promotes a variety of degradative reaction pathways (Volkin and Klibanov, 1989; Cleland and Langer, 1994). Detrimental consequences of these reactions for therapeutic proteins are many including the loss of biological activity and/or solubility and altered immunogenicity. Unfortunately, the relative impact of each pathway is usually unclear and difficult to gauge, and most stabilization strategies have been tailored for the specific protein of interest. The approaches have involved determining the causes and molecular mechanisms of inactivation and devising strategies to prevent them. Resultant formulations have included excipients (additives) or modified proteins to reduce deleterious chemical reactions, such as deamidation or thiol-catalyzed disulfide exchange (Schwendeman, Cardamone *et al.*, 1996). For encapsulation, two paradigms have emerged wherein proteins are incorporated either in aqueous solution or in the solid form. The former utilizes excipients such as carbohydrates or other proteins as stabilizing agents and achieves a moderate success rate in terms of preserving protein integrity. More promising results have been obtained through encapsulation of solid proteins in which both the conformational mobility and chemical reactivity are reduced (Putney and Burke, 1998).

Recent work has begun to explore the protein stability problem on the whole-system level. Instead of merely minimizing the degradation reactions of proteins, researchers strive to avoid underlying causes of these reactions. Excipients that act as glass formers have been shown to be effective in protecting proteins after administration, presumably by "freezing" the protein conformation thus reducing its propensity to undergo deleterious reactions (Putney and Burke, 1998). An excellent practical example of protein stabilization was when Alkermes and Genentech successfully encapsulated and continuously released functional rhGH for one month in monkeys (Johnson, Cleland *et al.*, 1996). In that approach, they first developed a technique to encapsulate the solid protein within polymer microparticles using a low-temperature process in the absence of surfactants (Herbert, Murphy *et al.*, 1998; Tracy, 1998). Secondly, they complexed rhGH with zinc, which decreased its solubility and thus susceptibility to degradative processes (Johnson, Jaworowicz *et al.*, 1997). Consequently, the decay of solid rhGH was greatly diminished, translating into a much longer life span during both encapsulation and release.

Since protein conformation reversibly changes upon dehydration (e.g. lyophilization) (Griebenow and Klibanov, 1995), the extent of this change, which should affect the solid state stability of a protein, represents an additional potentially important variable. Not only can these issues be addressed by the use of excipients but also by understanding the stability of the solid form of the therapeutics. For example, the structural state of solid, amorphous or crystalline, can affect its long-term stability.

There has been also a growing body of work indicating that the microenvironment of the encapsulated protein during *in vivo* release may become progressively harmful. For example, research has revealed a sharp rise in the acidity within delivery devices composed of poly(lactic-*co*-glycolic acid) (PLGA) caused by polymer degradation (Maeder, Bittner *et al.*, 1998; Brunner, Maeder *et al.*, 1999; Shenderova, Madou *et al.*, 1999; Fu, Pack *et al.*, 2000). Schwendeman and colleagues demonstrate the importance of this effect as well as potential remedies (Zhu, Maller *et al.*, 2000). By incorporating a base to raise the "microclimate pH" within their formulations, several acid-labile proteins, bovine serum albumin (BSA), basic fibroblast growth factor, and bone morphogenic protein-2 have been significantly stabilized in the PLGA millicylinder formulations and BSA in the PLGA microsphere injectable formulation during long-term release. The authors illustrate a successful methodology of elucidating the mechanism of instability, followed by designing a rational approach to overcome it. The concept of neutralizing the acidity developing upon polymer decomposition may have medical applications beyond protein stabilization. For example, it may be used to prevent such processes as acid-triggered localized inflammation caused by a degradable implantable material (Gresser, Trantolo *et al.*, 1998), DNA depurination (Middaugh, Evans *et al.*, 1998) caused by encapsulation of DNA within a biodegradable polymer, or cellular damage caused by a degrading polymer scaffold (Kim and Mooney, 1998).

Interestingly, Schwendeman and co-workers were able to stabilize BSA within PLGA microspheres where the protein was entrapped from aqueous solution. While the applicability of

this approach across a broad range of proteins remains to be seen, this solution may put into perspective the relative importance of maintaining protein stability during encapsulation *vs.* during release. In addition, the above-described approach may help explain the stabilization of rhGH in PLGA microspheres. It is possible that the polymer-incorporated zinc carbonate serves a dual purpose as both a depot for complexation with rhGH and a basic salt. Supporting this hypothesis, the pH within rhGH-containing microspheres changes little throughout degradation. (Cleland, 1997).

5.3. Future research

Application of the methods developed within this thesis can be used to better understand different formulations and microsphere preparations. Direct comparisons can be made to evaluate proteins within different microsphere systems using FTIR spectroscopy. These systems may vary by the type of polymer employed, the method of encapsulation, and the types of stabilizing excipients. In addition, pH measurements of the intrapolymer environment of these different systems can be quantified and compared.

The SE microspheres containing r-met-HuGdNF should be further explored. Released protein should be tested with cell proliferation assays to assess protein function. Detailed analysis of the released protein, including SDS-PAGE and reverse phase HPLC, will also help elucidate the pathways by which the protein becomes denatured or unfolded. Once the

degradative pathways are better understood, mechanisms by which to avoid those reactions can be established.

As the issues of protein stability in biodegradable polymers begin to be identified, future research could potentially focus on the rational design of new polymers to overcome these problems, such as those made up of monomers which would not alter microclimate pH or would completely prevent water uptake. For example, pH sensitive polymers are designed and synthesized for gene delivery (Pack, Putnam, *et al.*, 2000). Specifically, the polymer solubility changes with pH thus allowing either continued entrapment or release of DNA depending upon the surrounding environment. The glycosylated poly(histidine) could also be used to encapsulate protein within microspheres.

Because protein stability is the central issue, strategies that maintain the most stable conditions or environment for the protein should be pursued. One method is to maintain the protein in an anhydrous state. By using different polymer systems such as the poly(anhydrides) and poly(orthoesters), devices have been developed which degrade via surface erosion. Unlike the PLGA microspheres that degrade by bulk erosion, these devices erode much like a bar of soap. Proteins entrapped within these microspheres have less exposure to an aqueous environment before release from the device. There is also research focussed on the development of hollow microspheres with a shell of polymer and hollow core. These fabrication processes can form uniform, mono-dispersed particles. Proteins entrapped within poly(anhydride) or poly(orthoester) microspheres made in such a fashion may have improved stability as the protein

is not exposed to an aqueous environment prior to release and protein exposure to the polymer surface is minimized.

A developing area is the design of new methods to form the microspheres. As we begin to better understand the harsh effects of the double emulsion technique and also understand the materials in hand, new processes such as the freeze-atomization technique of Alkermes or the spray-drying technique of Acusphere come into play.

Stabilization of the protein itself is another strategy to pursue. For example, vaccines such as tetanus toxoid have improved stability due to chemical cross-linking, and proteins have prolonged half-lives *in vivo* due to addition of disulfide bonds, PEG moieties and glycosylation sites. As these approaches are developed for biotechnology, they can be applied to controlled delivery as well to prolong the lifespan of proteins.

Ultimately, as the information becomes integrated, we are able to model these systems and predict effects such as protein release kinetics (Batycky, Hanes, *et al.*, 1997). As the field of protein folding develops, the processes of protein denaturation and degradation will be better understood and incorporated within models.

Yet other areas of future research in the field of protein delivery include non-invasive delivery approaches *via* transdermal, pulmonary, mucosal, and oral routes. New devices for protein delivery that encompass emerging areas such as microfabrication, microelectronics, and nanotechnology; "smart" systems that can control the pattern of drug release; and those designed

to target specific cells or tissues represent other important areas of future research (Langer, 1998).

5.4. References

Bartus, R., M. Tracy, D.F. Emerich, and S.E. Zale, (1998). Sustained delivery of proteins for novel therapeutic products. *Science* **281**: 1161-1162.

Batycky, R.P., J. Hanes, R. Langer, D.A. Edwards, (1997). A theoretical model of erosion and macromolecular drug release from biodegrading microspheres. *J. Pharm. Sci.* **86**: 1464-1477.

Brunner, A.,K. Maeder, A. Goepferich, (1999). pH and osmotic pressure inside biodegradable microspheres during erosion. *Pharm. Res.* **16**: 847-853.

Cleland, J.L. and R. Langer, (1994). Formulation and delivery of proteins and peptides: design and development strategies. Formulation and delivery of proteins and peptides. J. Cleland and R. Langer. Washington, DC, American Chemical Society. **567:** 1-19.

Cleland, J.L., A. Mac, B. Boyd, J. Yang, E.T. Duenas, D. Yeung, D. Brooks, C. Hsu, H. Chu, V. Mukku, and A.J.S. Jones, (1997). The stability of recombinant human growth hormone in poly(lactic-co-glycolic acid) (PLGA) microspheres. *Pharm. Res.* **14:**420-425..

Costantino, H.R., R. Langer, and A.M. Klibanov, (1994). Solid-phase aggregation of proteins under pharmaceutically relevant conditions. *J. Pharm. Sci.* **83**: 1662-1669.

Fu, K., D. Pack, A.M. Klibanov, and R. Langer, (2000). Visual evidence of acidic environment within degrading poly(lactic-co-glycolic acid) (PLGA) microspheres. *Pharm. Res.* **17**: 100-106.

Gresser, J., D.J., Trantolo, R. Langer, A.M., Klibanov, D.L. Wise, (1998). Material for buffered resorbable internal fixation devices and method for making same. U.S. Patent No. 5,817,328.

Griebenow, K. and A.M. Klibanov (1995). Lyophilization-induced changes in the secondary structure of proteins. *Proc. Natl. Acad. Sci. USA* **92**: 10969-10976.

Herbert, P., K. Murphy, O. Johnson, N. Dong, W. Jaworowicz, M.A. Tracy, J.L. Cleland, and S.D. Putney, (1998). A large-scale process to produce microencapsulated proteins. *Pharm. Res.* **15**(2): 357-361.

Johnson, O.L., J.L. Cleland, H.J. Lee, M. Charnis, E. Duenas, W. Jaworowicz, D. Shepard, A. Shahzamani, A.J.S. Jones, and S.D. Putney, (1996). A month-long effect from a single injection of microencapsulated human growth hormone. *Nat. Med.* **2**(7): 795-799.

Johnson, O.L., W. Jaworowicz, J.L. Cleland, E. Duenas, C. Wu, D. Shepard, S. Magil, T. Last, A.J.S. Jones, S.D. Putney, (1997). The stabilization and encapsulation of human growth hormone into biodegradable microspheres. *Pharm. Res.* **14**(6): 730-735.

Kim, B.S. and D.J. Mooney (1998). Development of biocompatible synthetic extracellular matrices for tissue engineering. *Trends in Biotechnology* **16**: 224-230.

Langer, R. (1998). Drug delivery and targeting - The design of degradable materials and the development of intelligent delivery systems have had an enormous impact on drug-based therapies. *Nature* **392**: 5-10.

Liu, W.R., R. Langer, and A.M. Klibanov, (1991). Moisture-induced aggregation of lyophilized proteins in the solid state. *Biotechnol. Bioeng.* **37**: 177-184.

Maeder, K., B. Bittner, Y.X. Li, W. Wohlauf, T. Kissel, (1998). Monitoring microviscosity and microacidity of the albumin microenvironment inside degrading microparticles from poly(lactide-co-glycolide) (PLG) or ABA-triblock polymers containing hydrophobic poly(lactide-co-glycolide) A blocks and hydrophilic poly(ethyleneoxide) B blocks. *Pharm. Res.* **15**: 787-793.

Middaugh, C.R, R.K. Evans, D.L. Montgomery and D.R. Casimiro, (1998). Analysis of plasmid DNA from a pharmaceutical perspective. *J. Pharm. Sci.* **87**: 130-146.

Pack, D.W., D. Putnam, R. Langer, (2000). Design of imidazole-containing endosomolytic biopolymers for gene delivery. *Biotechnol. Bioeng.* **67**: 217-223.

Putney, S.D. and P.A. Burke, (1998). Improving protein therapeutics with sustained-release formulations. *Nat. Biotechnol.* **16**: 153-157.

Schwendeman, S.P., M. Cardamone, M.R. Brandon, A.M. Klibanov and R. Langer, (1996). Stability of proteins and their delivery from biodegradable polymer microspheres. Microparticulate systems for the delivery of proteins and vaccines. S. Cohen and H. Bernstein. New York, Marcel Dekker, Inc.: 1-49.

Shenderova, A., T.G. Burke and S.P. Schwendeman, (1999). The acidic microclimate in poly(lactide-co-glycolide) microspheres stabilizes camptothecins. *Pharm. Res.* **16**: 241-248.

Tracy, M.A. (1998). Development and scale-up of a microsphere protein delivery system. *Biotecnol. Prog.* **14**(1): 108-115.

Uhrich, K. E., S. M. Cannizzaro, R. S. Langer and K. M. Shakesheff, (1999). Polymeric systems for controlled drug release. *Chem. Rev.* **99:** 3181-3198.

Volkin, D.B. and A.M. Klibanov (1989). Minimizing protein inactivation. Protein function: a practical approach. T.E. Creighton. New York, IRL Press: 1-24.

Zhu, G.Z., S.R. Maller and S.P. Schwendeman, (2000). Stabilization of proteins encapsulated in injectable poly (lactide-co-glycolide). *Nat. Biotechnol.* **18**: 52-57.

Appendix A. Solubilization of r-met-HuGdNF using polymeric mediators

A.1 Introduction

To incorporate r-met-HuGdNF within microparticles using the spontaneous emulsification technique, appropriate procedures were developed to solubilize the protein in the single-phase solvent system. A variety of low molecular weight detergents were screened as mediators to aid in the solubilization of the protein.

This approach relies on the assumption that a multi-molecular complex is formed between the detergents and the highly hydrophilic r-met-HuGdNF. For such a complex the hydrophobic/hydrophilic balance is shifted toward a higher hydrophobicity thus solubilizing the complex within the single-phase solvent.

Results using the protein/surfactant complex concept indicated that, although the partitioning coefficient of the protein increased upon complexation with a surfactant, the effective concentration of the complexes in the organic solvents considered was still below the desired level.

These results were interpreted to indicate that the hydrophobic/hydrophilic balance of the complexes produced was indeed shifted towards higher hydrophobicity, but the shift achieved was not sufficiently large so as to promote the level of solubility sought.

A.2 Rationale

To further improve the hydrophobic/hydrophilic balance of the protein/detergent complexes, detergent-type compounds with the following characteristics are needed: 1) the hydrophobic section must be more dominant than that of the low molecular weight surfactants previously tested, and 2) the detergent must interact with the protein in a multi-contact mode where one molecule of detergent interacts with more than one site on the protein molecule and, hence, a higher effective association constant is reached.

These requirements lead to the concept of polymeric mediators. These molecules are built of a polymeric core, soluble in the organic solvents of interest and attached with functional moieties (capable of interacting with the protein). These functional moieties should not alter the solubility characteristics of the polymeric core.

A.3 Approaches

Implementation of the polymeric mediator concept was carried out on two avenues: 1) preparation of polymeric mediators by attachment of sulfonic acid containing moieties to ready made neutral polymers, and 2) preparation of polymeric hybrids containing PLGA and heparin. R-met-HuGdNF is purified by affinity chromatography on a heparin-Sepharose column. Thus with the latter method, r-met-HuGdNF can not only interact with the sulfonic acid moieties of heparin but perhaps also with specific interactions with other moieties of heparin.

A.4 Preparation of polymeric mediators

A.4.1 Preparation of sulfonated PLGA

This compound was prepared by reacting non-endcapped PLGA with bromoethanesulfonic acid sodium salt (BESA) in the presence of dimethylamino pyridine (DMAP). The reaction is written as follows:

$$\text{PLGA----OH} + \text{Br-CH}_2\text{-CH}_2\text{-SO}_3\text{Na} \longrightarrow \text{PLGA-O-CH}_2\text{-CH}_2\text{- SO}_3\text{Na}$$

Forty μmol PLGA was dissolved in 15 mL of methyl sulfoxide (DMSO). To this solution, 400 μmol of BESA was added followed by 400 μmol of DMAP. The reaction ran for 3 d at room temperature and the product was precipitated by addition of water and washed 5 times.

The product was further purified by dissolving it in 40 mL dioxane and precipitating it with the addition of ether.

A.4.2 Preparation of the polymeric hybrid PLGA-heparin

Following the approach delineated in the section A.3, this compound was prepared in a three-stage process:

Stage 1: Preparation of amino-terminated PLGA (PLGA-NH_2) by aminolytic cleavage (partial) of PLGA with ethylene diamine (EDA):

PLGA + H_2N-CH_2-CH_2-NH_2 ----------> PLGA-CO-NH-CH_2-CH_2-NH_2 + PLGA fragment

To 67 μmol of PLGA (30,000 Da) and 268 μmol EDA was added 20 mL chloroform. The reaction was allowed to proceed at room temperature for 24 h. A crude product was then precipitated using 200 mL ether and separated by centrifugation. This was repeated 3 times and the purified product was recovered and dried.

As a result of this reaction, the molecular weight of PLGA-NH_2 and of the corresponding PLGA fragment produced were lower than the molecular weight of the starting PLGA polymer. The average molecular weight was found to be 7,000 Da).

Stage 2: Activation of the carboxyl groups of heparin with ethyl-dimethylaminopropyl carbodiimide (EDC):

Heparin - COOH + EDC ----------> Heparin - COOX

(Carboxyl-activated Heparin)

Porcine heparin (12,000 Da) was used and 16 μmol was dissolved in 2 mL of 25 mM MES buffer, pH 4.75. To this solution was added 10 mL of a 32 μM solution of EDC dissolved in dimethylformamide (DMF). The reaction was allowed to proceed at room temperature for 24 h. As a result of this reaction, one or a few carboxyl groups were activated on each heparin molecule.

Stage 3: Coupling of carboxyl-activated heparin to amino-terminated PLGA:

Heparin - COOX + PLGA-NH_2 --------> Heparin-CO-NH-PLGA

160 μmol of PLGA-NH_2 was dissolved in 16 mL DMF. This solution was then added to the activated heparin mixture described in Stage 2. The resulting solution was stirred at room temperature for 24 h, and the final product was precipitated by addition of 2 M NaCl followed by several washed with water. As a result of this reaction, one or a few PLGA chains were attached to every heparin molecule.

A.5 Results and Conclusions

Several generations of polymers from each category were made and tested with r-met-HuGdNF. The partitioning of r-met-HuGdNF into organic solvent with these polymeric mediators was low in all cases. However, it is possible that the ratio of the charged moiety (be it heparin or sulfonic acid) to the polymer needs to be optimized. Increasing the ratio of the hydrophilic group to the hydrophobic group may achieve a higher reaction efficiency and thus produce a polymeric mediator which can induce the partitioning of r-met-HuGdNF into organic solvent.

Appendix B. FFT solution

To model the distribution of pH within a PLGA microsphere, a general diffusion equation is written in spherical coordinates. A reaction term, b, is included to account for the generation of acid within the microsphere (equation B1.1). In this equation, c represents the concentration of hydronium ions or acid, t represents time, r represents the position within the microsphere, and D represents the diffusion coefficient of the acids. The boundary equations are given in B1.2 where at the edge of the sphere of radius R, the concentration of acid in the buffer is c_0 and at time 0, the concentration within the sphere is 0. Equation B1.1 is a non-homogeneous partial differential equation and can be solved using Finite Fourier Transform.

$$\frac{\partial c}{\partial t} = D\frac{1}{r^2}\frac{\partial}{\partial r}\left(r^2\frac{\partial c}{\partial r}\right) + b \qquad \text{B1.1}$$

$$c(t,R) = c_o$$
$$c(0,r) = c_o \qquad \text{B1.2a,b}$$

Equations A1.1 and A1.2a,b are first non-dimensionalized using the following equalities:

$$\Theta = \frac{c}{c_o}, \eta = \frac{r}{R}, \tau = \frac{tD}{R^2} \qquad \text{B1.3a,b,c}$$

to give equation B1.4 with boundary conditions B1.5a,b.

$$\frac{\partial \Theta}{\partial \tau} = \frac{1}{\eta^2}\frac{\partial}{\partial \eta}\left(\eta^2\frac{\partial \Theta}{\partial \eta}\right) + \frac{bR^2}{Dc_o} \qquad \text{B1.4}$$

$$\Theta(\tau,1)=1$$
$$\Theta(0,\eta)=1 \qquad \text{B1.5a,b}$$

The required basis functions is given below with l = 1:

$$\Phi_n(\eta)=\sqrt{\frac{2}{l}}\frac{\sin(\frac{n\pi\eta}{l})}{\eta} \text{ where} \qquad \text{B1.6}$$
$$\lambda_n l = n\pi, n=1,2,...$$

The expansion and the transformed concentration are written as

$$\Theta(\eta,\tau)=\sum_{n=1}^{\infty}\Theta_n(\tau)\Phi_n(\eta) \qquad \text{B1.7}$$

$$\Theta_n(\tau)=\int_0^1\Phi_n(\eta)\Theta(\eta,\tau)\eta^2 d\eta \qquad \text{B1.8}$$

Transforming the η-derivative term in equation B1.4 gives

$$\int_0^1\Phi_n\left[\frac{1}{\eta^2}\frac{\partial}{\partial\eta}\left(\eta^2\frac{\partial\Theta}{\partial\eta}\right)\right]\eta^2 d\eta=\eta^2\left(\Phi_n\frac{\partial\Theta}{\partial\eta}-\Theta\frac{d\Phi_n}{d\eta}\right)_{\eta=0}^{\eta=1}+\int_0^1\Theta\left[\frac{1}{\eta^2}\frac{d}{d\eta}\left(\eta^2\frac{d\Phi_n}{d\eta}\right)\right]\eta^2 d\eta= \qquad \text{B1.9}$$

$$-\frac{d\Phi_n}{d\eta}_{\eta=1}-\lambda_n^2\Theta_n=-\sqrt{2}(n\pi)(-1)^n-(n\pi)^2\Theta_n$$

Transforming the generation term gives

$$A = \frac{bR^2}{Dc_o}$$

$$\int_0^1 \Phi_n A\eta^2 d\eta = A\int_0^1 \sqrt{\frac{2}{l}} \frac{\sin\left(\frac{n\pi\eta}{l}\right)}{\eta}\eta^2 d\eta = \frac{-A\sqrt{2}(-1)^n}{n\pi} \qquad \text{B1.10}$$

Transforming the boundary condition in time gives

$$\Theta_n(0) = \frac{-\sqrt{2}(-1)^n}{n\pi}$$

The resulting problem for θ_n

$$\frac{d\Theta_n}{d\tau} + (n\pi)^2\Theta_n = -\sqrt{2}(-1)^n\left[n\pi + \frac{A}{n\pi}\right] \qquad \text{B1.11}$$

$$\Theta_n(0) = \frac{-\sqrt{2}(-1)^n}{n\pi}$$

The solution for Θ_n is then

$$\Theta_n = \frac{-\sqrt{2}(-1)^n\left(n\pi + \frac{A}{n\pi}\right)}{(n\pi)^2}\left[1 - e^{-(n\pi)^2\tau}\right] - \frac{\sqrt{2}(-1)^n}{n\pi}e^{-(n\pi)^2\tau} \qquad \text{B1.12}$$

And the solution for Θ is

$$\Theta(\eta,\tau) = \sum_{n=1}^{\infty}\sqrt{2}\frac{\sin(n\pi\eta)}{\eta}\left(\frac{-\sqrt{2}(-1)^n\left(n\pi + \frac{A}{n\pi}\right)}{(n\pi)^2} + e^{-(n\pi)^2\tau}\left(\frac{A\sqrt{2}(-1)^n}{(n\pi)^3}\right)\right) \qquad \text{B1.13}$$

Rewriting the solution in dimensionalized coordinates gives

$$c(r,t) = c_o \sum_{n=1}^{\infty} \sqrt{2} R \frac{\sin\left(n\pi \frac{r}{R}\right)}{r} \left[\frac{\sqrt{2}(-1)^n \left[n\pi + \frac{bR^2}{Dc_o n\pi} \right]}{(n\pi)^2} + e^{-\frac{(n\pi)^2 tD}{R^2}} \left(\frac{\sqrt{2}(-1)^n \left[\frac{bR^2}{Dc_o n\pi} \right]}{(n\pi)^3} \right) \right]$$

B1.18

Equation B1.18 was then graphed using matlab. The following program was used:

```
C = [ ];
R = 15;
alpha = 100000;
beta = 3;
g = 4e-8;
t = 0;
spacing = 100;

for r = R/spacing:R/spacing:R;
  n = 1:1000;
  z = 2^(0.5)*R*sin(n.*pi*r/R)/r;
  y = exp(-(pi*pi.*n.*n)*t*alpha/R/R);
  x = (beta*R*R/alpha/g./n/pi)*2^(0.5)*(-1).^n./n./n./n/pi/pi/pi;
  c = z.*(v-x+y.*x);
  C = [C; sum(c)];
  f= g.*C;
  pH = -log10(f);
end;
```